# SPECTRAL ANALYSIS OF PHOSPHORUS CHEMILUMINESCENCE

Dissertation for the Degree of Ph. D.
MICHIGAN STATE UNIVERSITY
RICHARD JERRY VAN ZEE
1975





#### This is to certify that the

thesis entitled

SPECTRAL ANALYSIS OF
PHOSPHORUS CHEMILUMINESCENCE

presented by

RICHARD JERRY VAN ZEE

has been accepted towards fulfillment of the requirements for

PH.D. degree in CHEMISTRY

Date 1/20/76

0-7639

APR 2 52002

-

.

.

हुव वह १४

#### **ABSTRACT**

#### SPECTRAL ANALYSIS OF PHOSPHORUS CHEMILUMINESCENCE

Ву

# Richard Jerry Van Zee

The chemiluminescence of phosphorus oxidation under natural conditions is one of the oldest and best known chemiluminescing systems but one for which a definitive spectroscopic study has been lacking. In this thesis are reported the results of such a study for the reaction of  $P_4$  vapor with air and added  $H_2$ 0 or  $D_2$ 0 vapor under normal atmospheric conditions. In addition some results have been obtained under high temperature conditions and some under low pressure conditions.

The gas phase emission spectrum of phosphorus chemiluminescence under ambient conditions is found to consist of (i) a discrete emission system in the ultraviolet 228.8-272.1 nm region, (ii) a discrete weak emission system in the 450-650 nm region superimposed upon a continuum, (iii) a continuum which extends from 335 nm into the near-infrared region, and (iv) discrete band emission upon a continuum in the near-infrared region, from 0.7 to 1.2  $\mu$ .

In spectral studies of small horizontal rectangular cross-sections of the phosphorus flame, the relative ratios of emission from the transient species remained the same regardless of the cross-section chosen, which permits accurate spectral analysis of the chemiluminescence.

Under ambient conditions the emitter HPO has been identified in phosphorus chemiluminescence for the first time by a mass effect on the spectral features in the 450-650 nm range arising from the substitution of  $D_2^0$  vapor for  $H_2^0$  vapor in the reaction. The transition of HPO is  $A(^1A'') \rightarrow X(^1A')$ . The fact that DPO emission intensity is much more intense than HPO emission intensity under corresponding conditions is explained by a predissociative process or an isotopic dependent tunneling process. Mechanisms for the formation of HPO\* from PO dimer and PO excimer are presented.

Discrete band emissions at room temperature and under atmospheric pressure in the ultraviolet region at 228.8-272.1 nm are due to a PO  $(A^2 \Sigma^+ \to X^2 \pi_r)$  transition and at elevated temperatures or low pressures an emission at 320-337 nm is due to a PO $(B^2 \Sigma^+ \to X^2 \pi_r)$  transition. Explanations for the emission intensity distributions from vibrational levels of these electronic states are given in terms of perturbations and predissociations induced by nearby electronic states of PO. The extreme temperature-pressure emission intensity sensitivity of the PO $(B^2 \Sigma^+ \to X^2 \pi_r)$  transition is explained in terms of dissociation of a PO excimer.

The emission from an excimer is responsible for the existence of the continuum. The continuum, extending from 335 nm into the near-infrared, displays the kinetic and spectroscopic characteristics of excimer emission. A quenched monomer emission,  $PO(B^2\Sigma^+ \to X^2\pi_r)$ , adjacent to a red-shifted, diffuse emission system is indicative of excimer formation. Four diagnostic experiments which identify the PO excimer are as follows:

- (1) Thermal dissociation of the excimer results in a concommittant increased  $PO(B^2\Sigma^+ \to \chi^2\pi_r)$  monomer emission intensity increase.
- (2) The dynamics of the excimer equilibrium are affected by dilution with inert gas. Upon dilution there is a marked dramatic increase in  $PO(B^2 \Sigma^+ \to X^2 \pi_r)$  monomer emission.
- (3) From the work of others it is seen that the dynamics of the excimer equilibrium with the monomer are effected by changes in pressure. At atmospheric pressure the  $PO(B^2\Sigma^+ \to X^2\pi_r)$  monomer system is entirely quenched. At lower pressures  $PO(B^2\Sigma^+ \to X^2\pi_r)$  monomer emission becomes strong.
- (4) There is an absence of direct absorption by the excimer, since the ground state of an excimer is dissociative. The formation of the excimer occurs upon collision of a ground state  $^2\pi$  PO molecule with a B $^2\Sigma^+$  or  $^4\pi_1$  excited state PO molecule. The formation of the excimer and its dissociation with subsequent monomer emission are illustrated by the equation

$$(PO-PO*) \stackrel{?}{\leftarrow} PO(^{4}\pi_{i}) + PO(X^{2}\pi_{r}) \stackrel{?}{\leftarrow} PO(B^{2}\Sigma^{+}) + PO(X^{2}\pi_{r}).$$

From thermal studies the dissociation energies of the excimer and dimer have been determined to be  $846 \pm 200 \text{ cm}^{-1}$  and  $109 \pm 200 \text{ cm}^{-1}$  respectively. Approximate potential energy diagrams have been constructed from this information. In addition the investigation has eliminated the possibility that the continuum is due to  $PO_2$  or HOPO emission.

The near-infrared is found to consist of a continuation of the visible emission continuum upon which are superimposed band heads corresponding to transitions from very high energy ultraviolet and vacuum-ultraviolet states to lower states of PO.

Under low pressure, oxygen deficient conditions an additional emitter, P<sub>2</sub>, is observed in the ultraviolet. It is because of

(i) the necessity for traces of water for the reaction to occur,

(ii) the difference in photo-emitter depending on the oxygen concentration, and (iii) the dominance of PO in the emission process that a new proton initiated, photon propagated mechanism is proposed to account for deficiencies of previous reaction mechanisms.

The total result of this investigation is that all the major emitters in naturally occurring phosphorus chemiluminescence have been identified. The methods used in this identification can serve as a model for identification of emitting species in other chemiluminescent systems. Results of this study can serve to stimulate investigations in the general study of the chemical production of excited electronic states.

# SPECTRAL ANALYSIS OF PHOSPHORUS CHEMILUMINESCENCE

Ву

Richard Jerry Van Zee

# A DISSERTATION

Submitted to
Michigan State University
on partial fulfillment of the requirements
for the degree

DOCTOR OF PHILOSOPHY

Department of Chemistry

### **ACKNOWLEDGEMENTS**

The author would like to express sincere appreciation to Professor A. U. Khan for his guidance, encouragement, and friendship during the course of this investigation.

I would also like to express special thanks to Professor

R. H. Schwendeman for his efforts in serving as second reader. I

also thank Professors D. G. Farnum and B. Rosenberg for serving

on my committee.

Finally, special gratitude is extended toward Dr. R. D. Kenner for his help and discussions in numerous experiments.

# TABLE OF CONTENTS

				Page
LIST OF	TABI	LES		vii
LIST OF	FIGU	JRES		viii
CHAPTER	I.	INTR	ODUCTION	1
CHAPTER	II.	CHE	MILUMINESCENCE AND PHOSPHORUS CHEMILUMINESCENCE	5
Α.	Α (	Criti	que on Chemiluminescence	5
	1.	Des	cription	5
	2.	Pre	requisites	5
	3.		mples Divided According to the Requirement Molecular Oxygen	6
		а.	Reactions which do not Require Molecular Oxygen	n 6
			(i) Atom-transfer Chemiluminescent Reactions	6
			(ii) Electron-transfer Chemiluminescent Reactions	7
		b.	Reactions Requiring Free or Bound Oxygen Molecules	8
			(i) Those Involving Bound Oxygen Molecules	8
			(ii) Those Involving Free Oxygen Molecules	8
	4.		mples of Chemiluminescence Divided According Complexity of Description	9
		а.	Radiative Recombination of Atoms on a Single Repulsive Curve	9
		ь.	Radiative Recombination of Atoms through Curve Crossing	10
		с.	Three-body Systems	10
		d.	Many-body Polyatomic Systems	11

# Table of Contents Continued

	5.	Applications of Chemiluminescence	11
		a. Study of Excited States	11
		b. Illumination or Lighting	12
		c. Analytical	12
В.	His	torical Perspective	13
С.	Con	temporaneous Work on Phosphorus Chemiluminescence	20
CHAPTER	III.	A SELECTION OF ATOMS AND MOLECULES INVOLVED IN	
		PHOSPHORUS CHEMILUMINESCENCE	26
Α.	P <sub>4</sub>		26
В.	P <sub>3</sub>		30
C.	$P_2$		30
D.	P		32
E.	PO		32
F.	PO <sub>2</sub>		38
G.	нро		40
н.	OH,	но <sub>2</sub> , н <sub>2</sub> 0 <sup>+</sup>	43
CHAPTER	IV.	IDENTIFICATION OF THE EMITTING SPECIES IN PHOSPHORUS	
		CHEMILUMINESCENCE	45
Α.	Ехр	erimental Descriptions	45
	1.	Chemicals	45
	2.	Equipment	45
		a. Room Temperature Emission Spectra	47
		b. Temperature Dependent Emission Spectra	49
		c. Concentration Dependent Emission Spectra	50

# Table of Contents Continued

		d.	Dehydrated Phosphorus Emission Spectra	54
		e.	Cross-section of the Chemiluminescent Flame	54
		f.	Oxygen Deficient Chemiluminescent Studies	57
В.	The	Coo	l Phosphorus Flame	57
c.	The	Emi	ssion Spectra	61
	1.	Gen	eral Characteristics	61
	2.	The	PO γ System	61
		а.	Assignment	61
		ъ.	Interpretation of Temperature, Pressure, and Isotopic Substitution on the PO $\beta$ Emission Intensity	71
	3.	The	PO β System	78
		а.	Assignment	78
		b.	Effect of Temperature on PO $\beta$ Emission	82
		c.	Dilution Experiment	86
	4.	нро	(DPO) Emission	86
		а.	Assignment	86
		b.	Temperature Dependence of HPO(DPO) Emission	93
		c.	Attempt at Rotational Analysis	95
	5.	The	Continuum	95
		a.	General Characteristics	95
		ъ.	Two Cases Resulting in Continuous Emission	101
		c.	The PO Excimer	105
			(i) Determination of the PO Excimer	106

# Table of Contents Continued

	<pre>(ii) Necessary Characteristics of the PO     Excimer</pre>	110
	(iii) Excimer Theory	118
	6. Cross-section of the Flame	123
	7. Oxygen Deficient Phosphorus Chemiluminescence	124
	8. Weak Near-Vacuum Ultraviolet Emission	127
	9. Near-Infrared Emission	130
CHAPTER		132
Α.	General Considerations	132
В.	The Role of PO	133
С.	Production of PO* from $P_4$ , $O_2$ , and $H_2O$	135
D.	Proposed Reaction Mechanism Scheme	136
Е.	Major Energy Decay Modes in Phosphorus Chemiluminescence	138
F.	Correlation of States for the Formation of HPO	140
G.	Breakdown of the Analogy Between $PO_2$ and $NO_2$ in the System	141
н.	Suggested Further Experiments	142
CHAPTER	VI. SUMMARY	143
REFERENC	EES	145
APPENDIC	CES	
Appen	dix	
Α.	TRANSIENT EMITTING SPECIES IN PHOSPHORUS CHEMILUMINESCENCE	154
В.	THE ELECTRONIC ORIGIN OF THE COOL GREEN PHOSPHORUS FLAME	162
С.	A STRIKING DEUTERIUM EFFECT IN PHOSPHORUS CHEMILUMINESCENCE. IDENTIFICATION OF THE EMITTING SPECIES	196

# LIST OF TABLES

Table		Page
1.	Wavelengths of Band Heads of PO $\gamma$ Emission	
	System	63
2.	Wavelengths of Band Heads of PO $\beta$	
	Emission System	80
3.	Medium Resolution HPO Emission Bands and Assignments	91
4.	Medium Resolution DPO Emission Bands and Assignments	92
5.	Wave Numbers of Rotational Heads for	
	${}^{1}A''(000) \rightarrow {}^{1}A'(000)$ of HPO	98
6.	Wave Numbers of Rotational Heads for $^{1}A''(000)$	
	<sup>1</sup> A'(000) of DPO	100
7.	Wavelengths of Band Heads of	
	$PO(A,F,G^2\Sigma^+ \rightarrow A,B^2\Sigma^+)$ Emission in Near-Infrared	103
8.	Wavelengths of Band Heads of	
	$P_2(C^1\Sigma_u^+ \to X^1\Sigma_g^+ \text{ and } A^1\pi_g \to X^1\Sigma_g^+)$ Emission	126
9.	Wavelengths of Band Heads of	
	$PO(C^2\Sigma^- \rightarrow \chi^2\pi_r \text{ and } C^1\Delta \rightarrow \chi^2\pi_r)$ Emission	129

# LIST OF FIGURES

F	'igur	e	Page
	1.	A calculated valence-shell electron density	
		distribution map in three dimensions for the P <sub>4</sub> molecule	28
	2.	Potential energy diagram for the PO molecule	34
	3.	Diagram of the arrangement used for obtaining room	
		temperature phosphorus chemiluminescence emission spectra	48
	4.	Diagram of the first arrangement used for obtaining	
		temperature dependent phosphorus chemiluminescence	
		emission spectra	51
	5.	Diagram of the second arrangement used for obtaining	
		temperature dependent phosphorus chemiluminescence	
		emission spectra	52
	6.	Diagram of the arrangement used for obtaining dilution	
		(concentration dependent) emission spectra from	
		phosphorus chemiluminescence	55
	7.	Diagram of the arrangement used for distilling dried	
		phosphorus and obtaining dehydrated phosphorus	
		chemiluminescence emission spectra	56
	8.	Diagram of the arrangement used for obtaining low	
		pressure, oxygen deficient chemiluminescence emission	
		spectra	59

9.	Ultraviolet and visible chemiluminescent emission	
	spectrum of the gas phase reaction of $P_4$ , $O_2$ , and	
	a trace of H <sub>2</sub> O	62
10.	Medium resolution phosphorus chemiluminescent	
	emission spectrum of the PO $\gamma$ system in the region	
	228.8-272.1 nm	66
11.	Energy level diagram for lines of a $^2\Sigma^+$ $\rightarrow$ $^2\pi(a)$ band	
	showing spin-doublet splitting and $\Lambda$ doublet splitting	
	in the lower state and spin-doublet splitting in the	
	upper state	69
12.	A series of temperature dependent chemiluminescence	
	emission spectra for the ultraviolet and visible regions	
	from the gas phase reaction of $P_4$ , $O_2$ , and $D_2$ vapors	73
13.	An ultraviolet and visible room temperature	
	chemiluminescence emission spectrum for the gas phase	
	reaction of $P_4$ , $O_2$ , and $D_2^0$ vapors	77
14.	A medium resolution phosphorus chemiluminescence	
	emission spectrum of the PO $\beta$ system in the region	
	320-344 nm	79
15.	A room temperature phosphorus chemiluminescence	
	emission spectrum of the PO $\beta$ system showing an	
	anomolously intense $(7,7)R_{12}$ transition at 336.5 nm	83
16.	A series of temperature dependent chemiluminescence	
	emission spectra for the ultraviolet and visible	
	regions from the gas phase reaction of $P_4$ , $O_2$ , and	
	H O vapors	85

17.	Two emission spectra illustrating the effect of gas	
	phase dilution of the reaction of $P_4$ , $O_2$ , and $H_2O$	
	with additional N <sub>2</sub> buffer gas	87
18.	A spectrum of medium resolution showing visible HPO	
	emission produced by the chemiluminescent gas phase	
	reaction of $P_4$ , $O_2$ , and $H_2O$ vapors at room temperature	89
19.	A spectrum of medium resolution showing visible DPO	
	emission produced by the chemiluminescent gas phase	
	reaction of $P_4$ , $O_2$ , and $D_2O$ vapors at room temperature	90
20.	Plots of log(intensity) versus 1/T for a) POB system	
	(0,0) emission; b) PO $\gamma$ system emission; and	
	c) HPO(DPO) $^{1}A'' \rightarrow ^{1}A'$ emission	94
21.	A spectrum of the partially resolved $^{1}A''(0,0,0) \rightarrow ^{1}A'(0,0,0)$	0)
	transition of HPO	96
22.	• •	
	${}^{1}A''(0,0,0) \rightarrow {}^{1}A'(0,0,0)$ transition of DPO	97
23.	A low resolution chemiluminescence emission spectrum	
	of the near-infrared 0.7 to 1.3 $\mu$ region	102
24.	Potential energy diagram for the (PO)*2 excimer	107
25.	A generalized potential energy diagram for an excimer	
	illustrating the origins of various energies	115
26.	Dehydrated phosphorus chemiluminescence spectrum	
	of the room temperature reaction of $P_4$ and $O_2$ vapor	117
27.	Spectrum showing ultraviolet $P_2(A^1\pi_g \to X^1\Sigma_g^+)$	
	emission from an oxygen deficient, low pressure system	125

# List of Figures Continued

28.	Gas phase room temperature phosphorus chemiluminescence	
	showing weak high energy emission from the $C^2\Sigma^-$ and	
	$C^{2}$ electronic states of PO	128
29.	Potential energy diagram of PO showing all the electronic	
	transitions which have been observed in this work	134
30.	Potential energy diagram showing simultaneously a	
	number of electronic states of the species P4, P2,	
	PO, O <sub>2</sub> , and HPO	139

#### CHAPTER I

#### INTRODUCTION

#### A. Rationale Behind Selecting this Topic for Investigation

The phenomenon of chemiluminescence has intrigued the human mind The mechanism of the conversion of chemical energy into visible photon energy remains elusive and continues to be fascinating. The oldest and best known chemiluminescent system, the oxidation of phosphorus, is one which has been the object of much study but which has defied understanding. This mysterious glow resulting from the reaction of  $P_{4(g)} + O_{2(g)}$ , which is greenish in color and cool to the touch, has resisted attempts at comprehension over the last three hundred years. It is the phenomenon, in fact, for which the element was named - the word phosphorus comes from two Greek words phos, meaning light, and phore, meaning bearer or carrier. It was expected for a system this old that many good emission spectra would exist in the literature but in fact, none could be found. The few emission spectra of phosphorus chemiluminescence that were found are of very poor quality. The fact that a definitive spectroscopic study of this classic system does not exist provided motivation for choosing this problem.

The determination of the mechanism of phosphorus chemiluminescence at the atomic-molecular level was a primary goal in this study. Much

new information related to the actual photon emitters and intermediates has been obtained. All the major emitters under ambient conditions have been identified. In addition to an understanding of the mechanism, another goal of this study has been to add to the knowledge in the field of chemiluminescence.

Secondly, a reason for selecting this topic was because the early work was done without the use of modern technology. Most of the work on phosphorus chemiluminescence was done before 1940.

A third reason for this study involved the relation of phosphorusoxygen chemistry to biology. It was expected that a detailed understanding of this chemical reaction could be utilized in understanding the
role of phosphorus oxides in other fields such as the importance of the
P-O bond in a number of bioenergetic processes.

Finally, energy conversion is not only important in biology but in all of our society. Since the major use of electrical energy is for the production of light and since the efficiencies involved in the overall electrical processes from the generation by burning fossil fuels, by hydroelectric methods, and by nuclear methods to the production of visible photons from photo-emissive devices are quite low, often much less than 1%, the direct conversion of chemical energy into light is worthy of study. Even though most chemiluminescent reactions have efficiencies of less than 1%, some bioluminescent reactions approach efficiencies of 90%. This illustrates the potential of chemiluminescence.

## B. Preview of Contents

Chapter one of this thesis is an introduction to the problem of phosphorus chemiluminescence. Chapter two is concerned with the

historical aspect of phosphorus chemiluminescence. Many great scientists of the past were involved with this phenomenon. Phosphorus was discovered in the 1600's by Henning Brand and shortly thereafter investigated by Robert Boyle and later by DeFourcroy and others. Coming into the nineteenth and twentieth centuries such luminaries as Emeleus, Backstrom, Bowen, Semenoff, and others persevered in determining the mechanism of the light emission. Semenoff, in particular, developed the chain theory of chemical kinetics to account for the observed properties of phosphorus chemiluminescence. Ghosh and Ball were the first to make a correct identification of an emitter in this system, PO. As a consequence of this identification most investigations since that time have been carried out under gas discharge type conditions. Also contained in this chapter are a few contemporaneous investigators such as Dainton, Walsh, and Thrush. Dainton investigated mainly the kinetics of this luminescent reaction. Walsh and Thrush came to conflicting conclusions as to an emitter in the system. Walsh on one hand, from spectral considerations, suggested that PO be the only source of emission. Thrush on the other hand, insisted from stoichiometric data that the visible continuum was due to PO2.

Chapter three is a compilation of the known physical, chemical, and spectroscopic properties of the reactants, suspected and known intermediates, and products of the reaction.

Chapter four describes the experiments, procedures, and apparatus and the results obtained. The main thrust of the experiments was to obtain emission spectra. These spectra were taken under varying conditions of reactants, detectors, and resolution. Calculations and

other manipulations on the data were performed to extract information regarding the species responsible for chemiluminescence and also to obtain activation energies essential for the construction of potential energy diagrams. The most important results in the investigations of emitting species are the identification of excimer emission and HPO emission in the chemiluminescent system.

Chapter five is concerned with the mechanism of production of electronic excited states in this reaction. Correlation diagrams have been constructed between the electronic states of a number of transient species. Spin and symmetry arguments employed in the construction of such state correlation diagrams are useful in reducing the number of choices in a mechanism.

Chapter six is a summary of this work.

#### CHAPTER II

#### CHEMILUMINESCENCE AND PHOSPHORUS CHEMILUMINESCENCE

### A. A Critique on Chemiluminescence

### 1. Description

Chemiluminescence arises from the generation of excited electronic states in exothermic chemical reactions. During the lifetime of the excited states, usually  $\sim 10^{-9}$  sec, many non-luminous pathways exist to compete with the luminescent transition to the ground state (1). These include energy transfer to non-emitting acceptors, interaction with other molecules to form non-radiative excimers and exciplexes, and intra-molecular radiationless deactivation. It is because there is such a multiplicity of deactivation mechanisms that a large number of exothermic chemical reactions are not luminescent. Because of the short lifetime of excited electronic states, they are less susceptible to deactivation than excited vibrational states and for this reason chemiluminescence is seen in gas and condensed phases of matter (2).

#### 2. Prerequisites

There are three requirements that must be simultaneously satisfied in order to achieve significant luminescence (3). These are:

(i) The negative of the free energy change for the reaction must be at least equal to Planck's constant multiplied by the lowest frequency of the radiation that will excite the emitting species.

- (ii) There must exist an efficient mechanism for the production of electronic excited states. This means that the reaction coordinate should favor excited state formation over ground state formation (4).
- (iii) The emitting species must have a high quantum yield for emission. For direct chemiluminescence the overall chemiluminescent quantum yield is the product of the excitation and emission efficiencies. But for indirect chemiluminescence, such as when the emitting species is excited by energy transfer from a non-emitting product molecule, the overall quantum yield is the product of the efficiencies of each individual step (3). These requirements can be circumvented somewhat in schemes which involve energy doubling (5) and energy pooling (6), but these are not especially noted for their efficiencies.

There exist different schools of thought regarding the classification of chemiluminescent reactions. There is a group which classifies the reactions according to whether oxygen is required and a group which classifies reactions according to whether the reaction is a two body or many body problem. The following survey of some typical chemiluminescent reactions is not exhaustive but illustrates by analogy possible chemiluminescent reactions in phosphorus oxidation.

- Reactions Classified According to their Requirement for Molecular Oxygen
  - a. Reactions which do not Require Molecular Oxygen
- (i) Atom-transfer Chemiluminescent Reactions

$$C1(^{2}P_{u}) + Na_{2}(^{1}\Sigma_{g}^{+}) \rightarrow NaC1(^{1}\Sigma_{g}^{+}) + Na*(^{2}P_{u}) \rightarrow Na(^{2}S) + hv$$
 (7)

This type of atom-transfer is relatively rare because not many transfer reactions are exothermic enough to give electronically excited products (8).

#### (ii) Electron-transfer Chemiluminescent Reactions

In electron-transfer, or electrochemically generated chemiluminescence, cation and anion radicals are generated alternately at electrodes by an alternating current in a solution of a compound such as an aromatic hydrocarbon (9). A large number of reactions involving cation and anion radicals produce light as a result of fluorescence, triplet-triplet annihilation, or excimer emission. Equations which show the formation and reactions of anthracene radicals are as follows:

$$A + e^{-} + A^{-}$$
 $A + A^{+} + e^{-}$ 
 $A^{+} + A^{-} + {}^{1}A^{*} + A$ 
 ${}^{1}A^{*} + {}^{1}A + h\nu_{f}$ 
 $A^{+} + A^{-} + {}^{3}A^{*} + A$ 
 ${}^{3}A^{*} + {}^{3}A^{*} + {}^{1}A^{*} + A$ 
 $A^{+} + A^{-} + {}^{1}A^{*}_{2}$ 
 ${}^{1}A^{*}_{2} + {}^{2}A + h\nu_{e}$ 

An explanation of the production of electronic excited states by the electron-transfer process can be illustrated in HMO (Huckel Molecular Orbital) terms. In simple HMO terms the radical cation is produced by removing an electron from the highest filled  $\pi$  orbital while the anion is produced by adding an electron to the lowest empty  $\pi^*$  molecular orbital.

Electron transfer is envisioned as a transfer from the  $\pi^*$  orbital of the anion to the  $\pi^*$  orbital of the cation, which results in the excited singlet or triplet state of the molecule.

- b. Reactions Requiring Free or Bound Oxygen Molecules
  - (i) Those Involving Bound Oxygen Molecules

The number of chemiluminescent reactions requiring oxygen molecules far exceeds those that do not. The oxygen may be molecular oxygen, a peroxide, or a superoxide. A recent example is the reaction of hypochlorite ion and hydrogen peroxide (10).

$$H_2O_2 + OC1^- + O_2 + C1^- + hv$$

An extensive study of this system has resulted in breakthroughs in many other systems as well.

(ii) Those Involving Free Oxygen Molecules

An example of a chemiluminescent system involving free molecular oxygen is that which this work is concerned with, the gas phase reaction of molecular oxygen and molecular phosphorus.

$$P_4 + O_2 \xrightarrow{\text{trace}} ----- \rightarrow PO^* + (PO)^*_2 + HPO^* \rightarrow 3PO + HPO +$$

vacuum uv, uv, visible, and near-infrared photons

At least four different excited electronic states of three different molecules are directly involved in light emission, as this work shows. The reaction is not stoichiometrically balanced as shown because the amounts of each product can be varied by temperature, pressure and dilution of inert gas. The dotted line represents the gap in our knowledge.

4. Examples of Chemiluminescence According to Complexity of
Description

In addition to the classification of chemiluminescent reactions according to whether or not oxygen is necessary, there is the more rigorous scheme of classification according to the concept of electronic state and complexity of description in mathematical terms (11).

a. Radiative Recombination of Atoms on a Single Repulsive Curve

For the least complex two-body radiative recombination case the electronic state is well defined at all distances of interest. This may be the case of two atoms approaching each other and interacting repulsively. At some moment during the collision a photon is emitted. A transition to the ground state occurs and a stable diatomic molecule forms (12). This is the inverse of photodissociation. repulsive interaction may take place along a completely repulsive potential, or above the dissociation limit of a stable electronic state. This two-body radiative process is to be distinguished from the three-body association in which stabilization is the result of excess energy being carried away by a third body, which is not a photon. The period of time during which the excess energy can be radiated is that of a period of vibration,  $\sim 10^{-13}$  sec. The radiative lifetime of a typical electronic state with an allowed transition is  $\sim 10^{-9}$  sec and as a result recombination is rare; only about one in  $10^4$  to  $10^5$  collisions result in recombination. Because of the range over which the kinetic energy of the colliding atoms may have values,

a continuous emission spectrum results. Two-body radiative recombination takes precedence over three-body association only at very low pressure such as in the upper atmosphere and interstellar space, where it occurs exclusively (13).

b. Radiative Recombination of Atoms through Curve Crossing

A more complex situation than two-body radiative recombination is that of curve crossing. Whereas the two-body radiative recombination of atoms on a single curve is the inverse of photodissociation, a radiative recombination of atoms through potential curve crossing is the inverse of predissociation. For chemiluminescence resulting from curve crossing, there is ambiguity in the concept of electronic states near the crossing of potential curves. The two atoms approach each other and during a collision a radiationless transition from the repulsive state to a discrete state may occur. The molecule immediately formed may predissociate or chemiluminesce. The probability of formation of a stable molecule is about the same as that for the simpler two-body radiative recombination (13). A difference is that here the Born-Oppenheimer description fails in the region of the intersection. A known example is (14):

$$N(^{4}S) + O(^{3}P) \rightarrow NO(a^{4}\pi) \rightarrow NO(C^{2}\pi) \rightarrow NO(X^{2}\pi) + h\nu$$

It is possible that  $P(^{4}S)$  and  $O(^{3}P)$  react similarly.

c. Three-body Systems

Because of the large increase in complexity in going from a two-body to a three-body problem, the three-body system dynamic treatment is extremely difficult. There is hardly any experimental information on excited state potential surfaces except in the region

of the equilibrium conformation. There are, however, some extensive theoretical calculations of adiabatic surfaces for molecules of interest, such as  $NO_2$  (15). An example might be that proposed by Walsh for the production of excited state PO (16).

$$P(^{4}S) + O(^{3}P) + M \rightarrow PO(A^{2}\Sigma^{+} \text{ or } B^{2}\Sigma^{+}) + M \rightarrow PO(X^{2}\pi) + h\nu$$

d. Many-body Polyatomic Systems

Next in complexity after the three-body problem are those of two and three body polyatomic systems. The best that can be done here is to average over possible collisions, determine the symmetry and energy of the transition state, and finish with thermodynamics. There is no necessary symmetry element which carries through and spin may be the only good quantum number. An example of a chemiluminescent system of this type is (17):

$$o_3^{(1)}A_1 + NO(X^2\pi) \rightarrow o_2^{(3)}E_g + NO_2^{(2)}B_2^{(2)}$$

5. Applications of Chemiluminescence

It is fair to ask what use chemiluminescence has besides being a chemical curiosity. The answer is that it has a wide range of applicability, much of which has not been fully exploited. It is a method for the study of electronic excited states and of the kinetics of reactions. It has potential for illumination, and it is used for analytical purposes in biology and chemistry.

a. Study of Excited States and Kinetics of Reactions

Chemical production of electronic excited states has some
advantages over photo-excitation. In chemical production excitation
is uniform and population of some normally inaccessible states is

possible (3). It is also possible to study energy transfer in some systems which could not be studied by any other means. For example, the mechanism of energy transfer from a weakly luminescent ketone donor to an anthracene acceptor has been examined (18). This could not have been studied by photo-excitation because the anthracene molecules would also have been excited.

# b. Illumination or Lighting

Chemiluminescent reactions have potential for use as illumination sources. Some processes are used commercially as temporary light (19) and if higher efficiencies can be achieved, they may well compete with conventional sources of light.

### c. Analytical

Chemiluminescence is used for the detection of specific reactants. Any reaction where photon emission is proportional to the concentration of one of the reactants has uses for qualitative and quantitative analytical purposes. In biology the firefly activated enzyme-subtrate complex is used for specific detection of ATP (20). In this respect it can be used for determination of bacterial contamination, microbial biomass, and extra-terrestrial life. The calcium ion specificity of Aequorea bioluminescence can be used for detection of as little as 10<sup>-7</sup> M Ca<sup>2+</sup> (21). Chemiluminescent detection of ozone, nitrogen oxides, and sulfur dioxide has sensitivity in the parts per billion range (22,23). The intense HPO emission in flames is used for analytical detection of phosphorus compounds. Because the ions of several transition metals catalyze the oxidation of luminol by hydrogen peroxide in basic solution, the reaction has

capability for trace metal analysis. In the presence of excess reagents the light intensity is proportional to metal ion concentration over a certain range. Some typical detection limits are as follows:  $\text{Co}^{2+}$ ,  $10^{-11}$  M;  $\text{Cu}^{2+}$ ,  $10^{-9}$  M; and  $\text{Cr}^{3+}$ ,  $10^{-9}$  M (24).

It can be seen that chemiluminescent techniques are more sensitive than most other analytical methods. In addition, they do not require expensive instrumentation. In this discussion of the applications of chemiluminescence the use of the ultrasensitive photodetection devices currently available implied. The use of single photon counting techniques allows the observation of a single molecule or atom chemiluminescent reaction.

#### B. Historical Perspective

It is generally agreed that phosphorus chemiluminescence was first seen by Henning Brand, a Hamburg physician, in 1669. He obtained phosphorus by a reduction of phosphates which were the products of a dry distillation of the solids of urine (25). News of the mysterious glowing material spread through Europe quickly. One of the earlier and more famous investigators to work on phosphorus chemiluminescence in the seventeenth century was Robert Boyle (25). He published two books on the subject and among many other things showed that air was necessary for the reaction to occur. DeFourcroy in 1788 extended this observation and determined the upper and lower bounds of oxygen pressure for chemiluminescence to occur (25). Many prominent scientists worked on the problem of elucidating the mechanism of the light emission. Most of their conclusions are correct.

Of the most carefully done of the early experiments that have been confirmed is one that concerned the relation of water vapor to phosphorus chemiluminescence. Because earlier experiments had shown that a trace of moisture was necessary for the oxidation of carbon monoxide, H. B. Baker, in collaboration with H. B. Dixon, in the years 1885-1888 performed a series of experiments which involved the use of very carefully dried oxygen to oxidize several combustibles, including phosphorus (26). After washing commercial phosphorus with potassium bichromate and dilute sulfuric acid, they distilled a small portion of the phosphorus over phosphorus trichloride and diphosphorus pentoxide in a sealed tube. This distillation took three weeks. The part of the tube which contained the purified phosphorus was sealed off and dried in the presence of  $P_2O_5$  for eleven more days. Oxygen which had been dried for eleven days over  $P_2O_5$  was admitted and no glow resulted. Even when the phosphorus was heated to its boiling point (230°C), there was no glow. Thus, Baker concluded that phosphorus does not chemiluminesce in dried oxygen.

In their attempts to determine the emitter in phosphorus chemiluminescence, T. E. Thorpe and A. E. Tutton in 1890-1891 produced an oxide of phosphorus corresponding closely to  $P_4O_6$  (27). Because of a slight contamination with elemental white phosphorus, they wrongly concluded that it was the oxidation of this oxide that produced the phosphorus glow. After the work of Thorpe and Tutton, there was renewed interest in the work of Baker.

In 1903 E. J. Russell investigated an apparent exception to the law of mass action - that the rate of phosphorus oxidation increased

as the pressure of oxygen was decreased within a certain range

(28). Although Russell could offer no satisfactory explanation for the apparent exception, he found that a small quantity of water was necessary for the reaction to occur confirming the results of Baker.

Although many investigators had studied the effects of pressure and added chemicals on the emission properties of phosphorus chemiluminescence, the first to spectrally analyze the emission were P. Geuter in 1907 (29) and M. Centnerszwer et al. in 1912 (30). Their photographs of the spectrum in the ultraviolet and visible regions showed a number of bands superimposed on an emission continuum. No attempts were made at identifying the emitters, which are now known to belong to PO, and the weak bands in the visible, which this work has identified as belonging to HPO, and the continuum, which this work has identified as originating from (PO)<sub>2</sub>\* excimer. Evidence that the reaction emits in the vacuum ultraviolet was left to be demonstrated by W. E. Downey (31).

Downer performed some ingeneous experiments to determine whether the ozone which is formed in phosphorus chemiluminescence is produced chemically or photo-chemically. By detecting ozone chemically on the opposite side of a fluorite window from the phosphorus glow, Downey was able to show that the reaction emits radiation in the wavelength region 120 to 180 nm, which is energetic enough to generate ozone from oxygen molecules. Wrongly, like Downey, Emeleus also attributed chemiluminescence to the slow oxidation of diphosphorus trioxide.

By comparing the cool and hot flame emission spectrograms, Emeleus et al. concluded that the flame emits the same bands, whether cool or hot (32). (There are important differences according to this work.) Attempts were also made to determine the nature of the emitting species. The ultraviolet spectrum of the phosphorescence of  $P_2O_5$ was photographed, but it exhibited none of the bands occurring in the spectrum of the glow of phosphorus. The spectrum which results from an electric discharge through the vapor of  $P_2O_5$ , however, very closely resembles the ultraviolet spectrum which results from the glow of phosphorus. From the spectral correspondence it was concluded that the ultraviolet spectrum of the glow of phosphorus has its origin in a lower oxide than  $P_2O_5$  (33). Similar emission spectra were obtained from the chemiluminescence of phosphine and diphosphorus trioxide (34), but as Miller discovered, the glow of the latter was due only to the fact that a trace of elemental phosphorus remained mixed with the oxide.

C. C. Miller in 1928, by a recrystallization from carbon disulfide of diphosphorus trioxide prepared by the method of Thorpe and Tutton, showed that pure diphosphorus trioxide neither glows nor oxidizes in oxygen or air at ordinary temperatures (35). It, in fact, exerts an inhibitory effect on the glow of phosphorus. Diphosphorus trioxide, prepared by repeated exposure of a mixture of phosphorus and diphosphorus trioxide to light and subsequent volatilisation from the red amorphous phosphorus produced, behaved in the same manner as that purified by recrystallization from carbon disulfide. The inhibitory effect of diphosphorus trioxide was removed with water

and ozone, both of which react with the trioxide. That a product of the reaction can have an accelerating effect on the reaction was shown by H. L. J. Backstrom (36).

H. L. J. Backstrom in 1927 (36) found that the rate at which oxygen was consumed was greatly increased by illumination with a mercury lamp of a quartz tube containing phosphorus dissolved in heptane which has been saturated with oxygen. Furthermore, he showed that it was the ultraviolet emission from the lamp which caused the enhanced oxidation. He correlated this enhanced oxidation with the ultraviolet absorption spectrum of phosphorus. The light sensitivity observed corresponded to a quantum efficiency of reaction of about thirty. He concluded that the oxidation of phosphorus was a chain reaction. In contrast to this quantum yield of the reaction, the photon quantum yield which measures the efficiency of the reaction in terms of light production is very low.

E. Q. Adams in 1924 measured by visual comparison the intensity of a standard lamp to the intensity of the green phosphorus flame and in terms of photon flux at 556 nm obtained a value of  $10^{-6}$  photon quantum yield (37). By measuring photographically the quanta of light emitted in comparison to a standard tungsten lamp, E. J. Bowen and E. G. Pells determined the ratio of the number of visible photons emitted to the number of phosphorus molecules being oxidized (38). This ratio they determined to be 1 in 2000. In terms of green light this gives a photon quantum efficiency of 3 X  $10^{-5}$ , which is more than a factor of ten greater than that obtained by Adams. The number

of molecules emitting ultraviolet light is not considered in this type of experiment, and consequently it is expected that the efficiency is greater than that proposed by these investigators.

E. J. Bowen and A. C. Cavell also tested the effect of temperature on the reaction and the effects of trace amounts of ozone, chlorine, sulfur dioxide, and ether (39). It was found that above certain low levels of ozone the intensity of light emitted increased linearly with the concentration of ozone. Chlorine and sulfur dioxide, on the other hand, diminished the glow intensity. Ether had no effect. They found that within the temperature range 60-380°C, there was no appreciable change in the intensity of the glow, which is in agreement with the isothermal branched chain mechanism of oxidation introduced by Semenoff (40).

From the facts (i) that some trace amounts of foreign molecules effect the intensity of the light production in a significant manner, depending on the nature and concentration of the species, (ii) that above certain oxygen pressures phosphorus does not glow, (iii) that below certain oxygen pressures phosphorus does not glow, (iv) that the size of the vessel containing the phosphorus determines the lower oxygen limit, and (v) that additions of helium, argon or nitrogen accelerate the reaction, Semenoff derived the theory of chain reactions (40). According to this theory the propagating steps of a chain reaction involve the production of active centers. If one active center produces only one other active center, this is a straight chain reaction. If one active center produces more than one active center, this is a branched chain reaction. The reaction of

phosphorus and oxygen is a branched chain reaction according to Semenoff, and the active centers are oxygen atoms. He proposed the following mechanism to explain the observed kinetics of the reaction:

$$0 + P_4 = P_40$$
  
 $P_40 + O_2 = P_4O_2 + O_4$   
 $0 + P_4 = P_40$  etc.

The theory accounts for the two limiting cases of oxygen pressure, and the dependence on the size of the container and the presence of an inert gas (chains stopped exclusively on the walls of the container or exclusively in the gas phase). The theory also accounts for the presence and effects of trace amounts of foreign molecules, but does not specify the photo-emitter.

The first correct assignment of a photo-emitter in the phosphorus glow was due to P. N. Ghosh and G. N. Ball in 1931 (41). From an electrical discharge tube containing  $P_2O_5$  they obtained ultraviolet spectra which matched the ultraviolet spectra of the cold phosphorus glow, an experiment similar to that of Emeleus and Purcell. From the theories of band spectra published by Hund (42) and Mulliken (43) a few years earlier, Ghosh and Ball were able to correctly assign the ultraviolet emitting species to PO. They performed a vibrational analysis on what is now known as the  $\gamma$  system of PO and correctly designated the system as a  $^2\Sigma \rightarrow ^2\pi$  transition.

K. Rumpf in 1938 concurred with Ghosh and Ball's assignment of the ultraviolet emission in naturally occurring phosphorus chemiluminescence and assigned the visible bands superimposed upon the continuum to the same species, PO (44). Rumpf also observed another strong band around 327 nm which he could not fit into any of the known or postulated PO band systems. This band is now known to belong to the PO  $\beta$  system. In addition, Rumpf postulated the mechanism

$$P_2 + O_2 = (P_2O_2) = P0* + PO = 2PO + hv$$

to explain the formation of electronically excited PO. He estimated from the known dissociation energies of  $P_2$  and  $O_2$  and the energy of hv that the dissociation energy of ground state PO was at least 6.2 ev. As this work shows, the band system in the visible attributed by Rumpf to PO is actually due to HPO. After Rumpf's work most spectroscopists concentrated on electric discharge emission studies of phosphorus oxidation rather than studies of the reaction under naturally occurring conditions. Some kineticists continued to study the chemiluminescent reaction at or near ambient conditions however, which brings this review into contemporary times.

### C. Contemporaneous Work on Phosphorus Chemiluminescence

From available thermodynamic and spectroscopic data F. S. Dainton has calculated bond energies for some phosphorus-oxide molecules and used these energies to predict a mechanism for the chemiluminescent reaction (45). He concluded that the apical PO bond energy in  $P_4O_{10}$  is 156 kcal/mole, the bond energy in PO is 138 kcal/mole, and the bridge PO bond energy in  $P_4O_{10}$  or  $P_4O_6$  is 80 kcal/mole. Like Semenoff, Dainton et al. proposed a mechanism to fit the experimental observations (46). This mechanism is:

$$P_4 + O_2 \rightarrow P_4O + O$$
 Initiation, slightly endothermic  $P_4 + O + M \rightarrow P_4O + M$  Propagation, quite exothermic  $P_4O_n + O_2 \rightarrow P_4O_{n+1} + O$  Propagation, exothermic for  $9 > n > 5$   $O + X$  (= poison)  $\rightarrow$  stable products Termination  $O + wall$  Termination

In addition, Dainton et al. worked out empirical relations for luminescence as a function of temperature at the lower and upper limits of oxygen pressures in this luminescent reaction (47). They suggested that the glow is an exothermic degenerate explosion reaction (isothermal branched chain reaction). Thus the glow changes into a hot flame only when it attains a critical rate. It is noteworthy that all the theories of the kinetics of the process lack explicit consideration of the modes of formation and electronic excitation of the emitting species.

After the studies of the kinetics by Dainton et al., the next to do extensive spectroscopic work was Dressler (48). By using a Geissler discharge tube for an emission source, he carried out a new vibrational analysis on the  $\beta$  bands of PO. A rotational analysis by Singh of this system in 1959 correctly assigned the  $\beta$  system to a  $^2\Sigma^+ \rightarrow ^2\pi$  transition (49). In addition to the work on the  $\beta$  system, Dressler discovered and vibrationally analyzed the  $(\text{C-X}^2\pi)$ ,  $(\text{D-X}^2\pi)$ , and  $(\text{E-X}^2\pi)$  systems of PO. Part of the  $(\text{C-X}^2\pi)$  system is seen weakly in the chemiluminescence of naturally occurring phosphorus near the vacuum ultraviolet. In addition to PO, he discovered new band systems for PO $^+$  and P $_2$ .

The next spectroscopist after Dressler to work on phosphorus chemiluminescence was Walsh (16). He attributed all the emission from the glow of phosphorus to transitions from three different electronic excited states of PO to the ground state. These were the  $A^2\Sigma^+$  and  $B^2\Sigma^+$  states and an unknown electronic state which he suggested was a  $^{2}\Sigma^{+}$  state and which he proposed emitted the well known greenish glow in the visible region. According to the work reported in this thesis, he has correctly assigned the  $A^2\Sigma^+$  and  $B^2\Sigma^+$  states in the phosphorus glow. In addition, Walsh found that PO emitted from vibrational levels no higher than v' = 2 of the  $A^2\Sigma^+$  state and v' = 10 of the  $B^2\Sigma^+$  state. These levels are known to be almost coincident in energy, and the coincidence suggested to him that there is a common upper limit and that the limit is the dissociation energy of the ground state of PO (5.4 ev). We find no description of the experimental conditions under which Walsh obtained his spectra, but it is suspected that his experiment involved the reaction  $P(^{4}S) + O(^{3}P)$ , under low pressure, discharge type conditions. Under the conditions of the reported work in this thesis PO emission is seen from up to v' = 5 of the  $A^2 \Sigma^+$  state in addition to emission from the even higher electronic states C, C', F, and G.

Cordes and Witschel (50) in 1965 assigned the visible bands obtained by Rumpf (44) from a cold phosphorus flame and the visible bands obtained by Ludlam (51) in 1935 from phosphorus burning in a hot hydrogen flame both to  $PO_2$ . Cordes and Witschel made this assignment by a comparison of the frequencies they obtained from both Rumpf's and Ludlam's bands to literature values of the frequencies emitted by excited  $PO_4$  one and to theoretically derived  $PO_2$  vibrational

frequencies. However, the present work shows that both Rumpf's and Ludlam's bands are due to HPO. Ludlam had assigned his bands to PH but the work of Lam Thanh and Peyron from gas discharge experiments demonstrated that Ludlam's bands were due to HPO (52). The assignment of Rumpf's bands remained ambiguous because the bands were both very weak and few in number. The results of isotopic substitution in this work show conclusively that Rumpf's bands are also due to HPO.

Following Cordes and Witschel's suggestion of the importance of emission from  $PO_2$ , Davies and Thrush in 1968 further postulated that the continuum in phosphorus chemiluminescence was due to  ${\rm PO}_2$  emission (53). By allowing atomic oxygen to react with molecular phosphorus under low pressure conditions, they determined the stoichiometry to be correct for PO2. Under these conditions they observed weak emission from the v' = 0 level of the  $A^2\Sigma^+$  state of PO and a stronger emission from the  $B^2\Sigma^+$  electronic state of PO. They also observed a molecular oxygen effect on the (7,7) transition of the PO ß system ( $B^2\Sigma^+ \rightarrow \chi^2\pi$ ). In the presence of  $0_2$  this transition becomes at times as strong as the (0,1) transition of the same system. (It is worthwhile to note that this effect may be interpreted in terms of a singlet molecular oxygen feedback mechanism (6).) Davies and Thrush substituted phosphine for phosphorus in their chemiluminescent studies because of their similar chemiluminescent properties. In addition, by analogy to HONO, they assigned HOPO as a continuum emitter in the near ultraviolet emission from the phosphine glow. It was decided that PO and P play only minor roles in the P + P reaction. They concurred with Dainton et al. (46) that most of the oxidation of phosphorus involves stepwise direct insertion of oxygen atoms into the  $P_{\Lambda}$  molecule to eventually form higher oxides. How this fits into their PO2 stoichiometry conclusion is not clear.

Beginning in 1966, before the work of Davies and Thrush, and extending to the present, high resolution experimental work has been done on electronic states of PO by a group in Reims, France. There is no one single author's name that appears on all the papers from this group but the list includes Guenebaut, Couet, Coquart, Larzilliere, Ngo, Prudhomme, and Da Paz (54-62). Their emission spectra were obtained from a high frequency discharge in  $P_2O_5$ ,  $P_2O_3$ , or  $POCl_3$  and include oxygen isotopic substitution (58-62). In addition, they have also performed a detailed analysis of the vibrational and rotational structure of the  $B^2\Sigma^+$  state of PO and have positively established that it is a  $^2\Sigma^+$  state (56). Also, they have reassigned the C' state from  $^2\Sigma^-$  to  $^2\Delta$  and derived molecular constants for the  $C^2\Sigma^-$ ,  $C^{\prime}^2\Delta$ ,  $D^{\prime}^2\pi_-$ , and  $E^2\Delta$ states (57,58,60,61). First and second order deperturbations were carried out on transitions from the  $A^2\Sigma^+$ ,  $F^2\Sigma^+$ ,  $G^2\Sigma^+$ ,  $H^2\Sigma^+$ , and  $I^2\Sigma^+$  to  $B^2\Sigma^+$ ,  $A^2\Sigma^+$  and  $X^2\pi$  states. The results yielded molecular constants of some of these states (59). A vibrational assignment of the  $b^4\Sigma^-$  state, whose existence was first postulated by Verma et al., was also attempted (62).

Another group which has been working on PO, often concurrently with but independent of the French group, is that of Verma et al. (63-71). In addition to improving molecular constants for the  $D^2\pi_r$  and  $D^{*2}\pi_r$  states of PO (63), this group discovered and analyzed a new  $B^{*2}\pi_1 \to X^2\pi_r$  transition (64). A preferential population in the  $B^2\Sigma^+$  (v' = 7) level at low pressures suggested to these authors that there existed a heterogeneous perturbation of this state (65). It was later decided that this perturbation was caused by the  $B^{*2}\pi_1$ 

state and another new state, the  $b^4\Sigma^-$  electronic state (69). Molecular constants for PO in this later state were then evaluated. In addition, a number of instances of predissociation were observed along with perturbations in a number of new  $^2\Sigma^+$  states (F, G, H, and I) and were attributed to the presence of  $^4\pi_1$  and  $A^{*2}\Sigma^+$  states, which dissociate to ground state atoms (67). From this the upper limit of the dissociation energy of ground state PO is set at 49,536 cm $^{-1}$ . Finally, the  $A^2\Sigma^+$   $B^2\Sigma^+$ ,  $F^2\Sigma^+$   $A^2\Sigma^+$ ,  $G^2\Sigma^+$   $A^2\Sigma^+$ ,  $F^2\Sigma^+$   $B^2\Sigma^+$  transitions were observed in the region 700-1200 nm and several perturbations noted and assigned (69). The existence of a  $^4\pi_1$  state is particularly interesting with respect to excimer formation for the following reasons:

- 1. It is the lowest excited state of PO.
- 2. The  $^4\pi_i \rightarrow X^2\pi_r$  transition is spin forbidden; hence the lifetime of the  $^4\pi_i$  electronic state should be fairly long.

  Thus electronic energy finally degrades to the lowest metastable  $^4\pi$

state and is trapped long enough to be ideal for excimer formation. The  $b^4\Sigma$  state is also fairly well suited for excimer formation and could explain the anomolous population observed in the  $B^2\Sigma^+$  (v' = 7) level at low pressures by Verma et al. (65).

With Verma et al. (65) the previous work on phosphorus chemiluminescence is brought up to date. The atomic, molecular, and spectroscopic properties of some of the molecules and atoms known or suspected to be involved in phosphorus chemiluminescence will be presented next.

### CHAPTER III

# A SELECTION OF ATOMS AND MOLECULES INVOLVED IN PHOSPHORUS CHEMILUMINESCENCE

### A. P

Phosphorus chemiluminescence is the gas phase oxidation of molecular phosphorus,  $P_4$ , by molecular oxygen,  $O_2$ , in the presence of trace amounts of H<sub>2</sub>O. It is therefore appropriate that a critical compilation begin with the electronic structure of the phosphorus molecule itself. In 1935 Maxwell, Hendricks, and Mosely determined by electron diffraction that the structure of a molecule of gaseous white phosphorus has the form of a regular tetrahedron and that the P-P distance is 2.21  $\pm$  0.02 % (72). Solid phosphorus exists in a number of allotropic forms; for example, white phosphorus consists of monomeric  $\mathbf{P}_{L}$  molecules whereas red phosphorus is a polymer of phosphorus. White phosphorus has  $P_{\Lambda}$  molecules in equilibrium in the gaseous phase and is the form commonly associated with phosphorus chemiluminescence. White phosphorus has a melting point of 44.1°C and a boiling point of  $280^{\circ}\text{C}$  (73). The trivalent phosphorus atom shows all the oxidation states from -3 to +5 inclusive, and has a  $1s^2 2s^2 2p^6 3s^2 sp^3 3d^0$  configuration. The three half-filled p orbitals are at 90° to one another and in a regular tetrahedral array there are angles of only  $60^{\circ}$  between the lines joining the centers. As a result, if the atomic orbitals are taken

as 3p, then the molecule must contain strongly bent bonds and have considerable strain energy.

In order to reduce this strain energy mixtures of higher s and d orbitals with the 3p orbital have been proposed to obtain the  $60^{\circ}$ angles necessary for zero strain energy (74,75). By contrast Pauling and Simonetta have calculated that the promotion energies for the higher s and d atomic configurations are too high to relieve the strain (76). They deduce 22.8 kcal/mole as the strain energy in  $P_{A}$ from thermodynamic data under the assumption of an angle of  $101^{\circ}$ for no strain. By assuming unstrained angles of  $90^{\circ}$  and from similar calculations of the strain energy of cyclopropane, Moffit calculated a strain energy of 42.4 kcal/mole for  $P_{L}$  (77). Another approach has been that of Hart, Robin, and Kuebler, who with an SCF-CI (self-consistent field with configuration interaction) calculation using a 3p atomic orbital basis, came to semiquantitative agreement with the observed absorption spectrum in the region 4-9 ev (78). Their calculation further predicts a strong pi resonance which invalidates the concepts of bent bonds and strain energy in the molecule P/. Figure 1, taken from Hart et al. (78), shows the calculated valence-shell electron density distribution in three dimensions. The valence-shell electron density map shows that the regions of highest density are situated symmetrically above each triangular face of the tetrahedron, that is, in corners of the cube not occupied by phosphorus cores. The authors conclude that because the results are in agreement with the absorption spectrum, which is also included in their paper, hybridization with s, p, and d orbitals is not necessary.

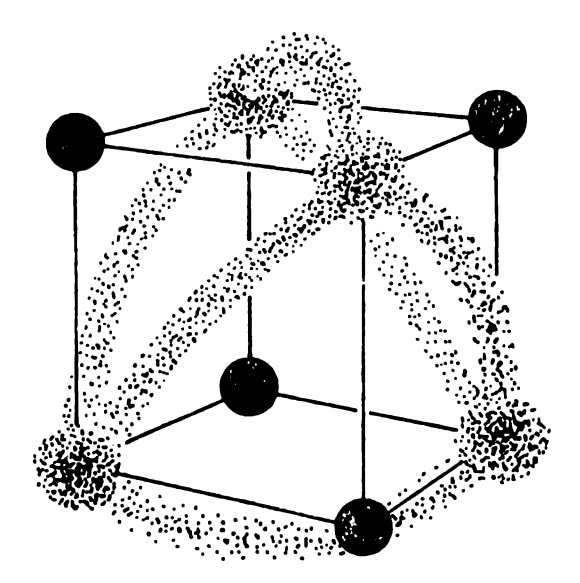


Figure 1. A calculated valence-shell electron density distribution map  $\text{in three dimensions for the P}_{\Delta} \text{ molecule}$ 

Disagreeing with this conclusion are calculations by Archibald and Perkins (79). By using a valence-electron SCF method, they found considerable contribution from d orbitals. They claim that the d orbital participation is responsible in the main for the stability of  $P_4$  over that of  $P_2$ .

Directly disagreeing with Archibald and Perkins, but somewhat agreeing with Hart et al., (78) is the work of Hillier and Saunders (80). An all-electron SCF-MO calculation shows that inclusion of phosphorus 3d orbitals is not necessary to account for the stability of  $P_4$  relative to  $P_2$ . Their calculated stability of  $P_4$  over  $P_2$  of 35 kcal/mole is less than the experimental value of 55 kcal/mole,

but the stability is in the correct direction. With inclusion of d orbitals the stabilization is expected to improve somewhat.

Thus far the discussion has centered around the electronic structure of ground state  $P_4$ . Very little has been said about the excited electronic states of P, nor is there an abundance of information on this topic in the literature (78). From use of the <u>aufbau</u> principle (the building-up of molecules from atoms) as outlined in Herzberg, (81) there are a large number of possible electronic states that result from the construction of  $P_4$  from four P atoms. From  $4P(^4S_u) \rightarrow P_4$  the possible states are given by the direct product  $^4S_u \times ^4S_u \times ^4S_u \times ^4S_u \times ^4S_u$  as follows:

$$^{1}A_{1}$$
,  $^{1}A_{2}$ ,  $^{1}E$ 
 $^{3}T_{1}^{(2)}$ 
 $^{5}A_{2}$ ,  $^{5}E(2)$ ,  $^{5}T_{1}$ ,  $^{5}T_{2}$ 
 $^{7}A_{2}$ ,  $^{7}T_{1}^{(2)}$ ,  $^{7}T_{2}$ 
 $^{9}A_{2}$ ,  $^{9}E$ ,  $^{9}T_{1}$ 
 $^{11}T_{1}$ 
 $^{13}A_{2}$ 

The ground state of  $P_2$  is  ${}^1\Sigma^+_g$  and  $P_4$  can be built-up from  $P_2$ ,  $2P_2({}^1\Sigma^+_g) \rightarrow P_4$ . The only possible molecular state from this correlation is  ${}^1A_1$ . Magnetic susceptibility measurements show that  $P_4$  is diamagnetic. Such measurements indicate that the  ${}^1A_1$  state is actually the ground state of  $P_4$ .

B. P3

 $P_3$  is a very rare species. The only conditions under which it has been seen are those present in a mass spectrometer, and it has been seen there in only very small amounts (82). The following results were obtained:

$$D(P_4 \rightarrow P_3 + P) = 3ev$$
 $I(P_2) = 12 ev$ 
 $I(P_3) = 11.5 ev$ 

 $C.P_2$ 

Because of its close analogy with the diatomic nitrogen molecule, diatomic phosphorus  $P_2$  has been the object of considerable research in terms of its absorption and emission properties. At least thirteen different electronic states of  $P_2$  have been found and characterized. These electronic states have been summarized by Carroll and Michell (83) and by Brion, Malicet, and Guenebaut (84). Electron configurations for the lowest electronic state and some of the low-lying excited electronic states are as indicated:

Of these  $X^1\Sigma_g^+$  is the ground state and  $b^{*3}\Sigma_u^-$ ,  $A^1\pi_g$ , and  $C^1\Sigma_u^+$  appear next, in increasing order of energy. The emission from these lower states is in the visible and ultraviolet and because of rather large differences in internuclear distances from the ground state, these and some even higher states have been seen only in emission and never in absorption. The emission is to rather high vibrational levels of the ground electronic state. Rotational analyses of the  $C^1\Sigma_u^+ \to X^1\Sigma_g^+$  transition have been carried out by Herzberg (85), Marais (86), and others some time ago, but the  $A^1\pi_g$  and  $b^{*3}\Sigma_u^-$  states have only recently been discovered (87,88). Although all of these states are analogous to states in diatomic nitrogen (N<sub>2</sub>), P<sub>2</sub> does not exist under ordinary conditions.

The vapor phase of phosphorus, as has been stated before, consists almost entirely of  $P_4$  molecules at ordinary temperatures and only at temperatures higher than  $800^{\circ}\text{C}$  does  $P_2$  exist in appreciable quantities. In the past, absorption and emission studies were done at temperatures near  $900^{\circ}\text{C}$ , but the high population of higher vibrational and rotational levels at these temperatures leads to very complex spectra. In order to circumvent this problem most of the modern work is done by using a microwave discharge to produce  $P_2$  from  $P_4$  (89). Verma and Broida have seen some  $P_2$  emission in the spontaneous reaction of atomic oxygen with phosphorus (65). In this work  $P_2$  emission was seen in the spontaneous reaction of molecular oxygen and molecular phosphorus, but only in oxygen deficient, low pressure conditions. (Classification of phosphorus chemiluminescence as oxygen sufficient and oxygen deficient will be discussed later.)

Although there have been many experimental studies on  $P_2$ , there have been very few theoretical studies and these are fairly recent. An accurate SCF calculation which used multi-centered basis sets of Slater orbitals has been performed for the ground state of P2 by Boyd and Lipscomb (90). To obtain the experimental dissociation and zero-point energies to within 99% they found the use of 3d orbitals to be important. Population analysis indicates that nearly all the bonding in  $P_2$  occurs through pi orbitals. This is interesting in comparison with the calculation by Hart et al. (78), who found substancial pi bonding in  $P_{\lambda}$ . A similar calculation by Mulliken and Liu (91) on P<sub>2</sub> approximately confirms the work of Boyd and Lipscomb.

D. P

Atomic phosphorus is easier to obtain than  $P_3$ , but more difficult to prepare than  $P_2$ . The ground state of P is  ${}^4S_{u}$  and the first two excited states are  ${}^{2}D_{5/2,3/2}$  and  ${}^{2}P_{5/2,3/2}$ , in increasing order of energy. The atomic energy levels and related spectra have been experimentally determined for neutral and singly ionized phosphorus atoms (92). The phosphorus atom has been studied with a mass spectrometer (82), and the rate constants for the reactions of  $P(^{2}D_{5/2,3/2})$  and  $P(^{2}P_{5/2,3/2})$  with  $H_{2}$ ,  $O_{2}$ ,  $PC1_{3}$ , Ar, Kr, Xe,  $N_{2}$ ,  ${\rm CO,\ CO_2,\ N_2O,\ CH_3,\ and\ C_{2}H_4}$  have been determined (93). The dissociation energy of  $P_2$  to give P is 5 ev according to Herzberg (13).

### E. PO

Because PO is a pivotal species in phosphorus chemiluminescence it is required that its electronic states and energies be known very well. To this end, it is fortunate that recently considerable research, both experimental and theoretical, has been devoted to this molecule.

Some of the electronic states of PO are shown in Figure 2. This potential energy diagram is copied from Verma et al. (67) and modified to include the more-recently discovered  $b^4\Sigma^-$  electronic state (69), but is lacking the  $A^{2}\Sigma^{+}$ ,  $D^{2}\pi_{r}$ ,  $D^{2}\pi_{r}$ ,  $E^{2}\Delta$ ,  $G^{2}\Sigma^{+}$ , and  $\mathrm{H}^2\Sigma^+$  states because their presence would only unnecessarily complicate the figure. A comprehensive energy diagram will, however, be presented later. The lowest spin allowed electronic transition in PO is the  $B^2\Sigma^+ \to \chi^2\pi_r$  transition, known as the  $\beta$  system. This transition is strong under low pressure gas discharge conditions. The fact that in this work this emission system was seen only very weakly in phosphorus chemiluminescence at room temperature under atmospheric pressure but strongly at moderately high temperatures suggested that the  $B^2\Sigma^+$  state was possibly being intermolecularly quenched by another PO molecule resulting in an energy transfer to the nearby  $4\pi_{i}$  state. This  $4\pi_{i}$ state is the lowest excited electronic state in PO. The  $A^2\Sigma^+ \to X^2\pi_$ transition is termed the  $\gamma$  emission. In this work under ambient conditions (room temperature under atmospheric pressure) the  $\gamma$  system is much stronger than the  $\beta$  system; the  $\beta$  system is almost completely quenched. Increasing the temperature increases the relative intensity of the β system. Dilution of the reactant gases with inert gas at elevated temperatures also increases the relative intensity of the β system. However, it should be pointed out that there is no relationship of reciprocity between the intensities of the  $\beta$  and  $\gamma$  systems in emission. This  $A^{2}\Sigma^{+}$  state is higher in energy than the  $B^{2}\Sigma^{+}$  state, as can be seen from figure 2, and its transition to the ground state with stronger intensity was puzzling at first. Our suggestion of the

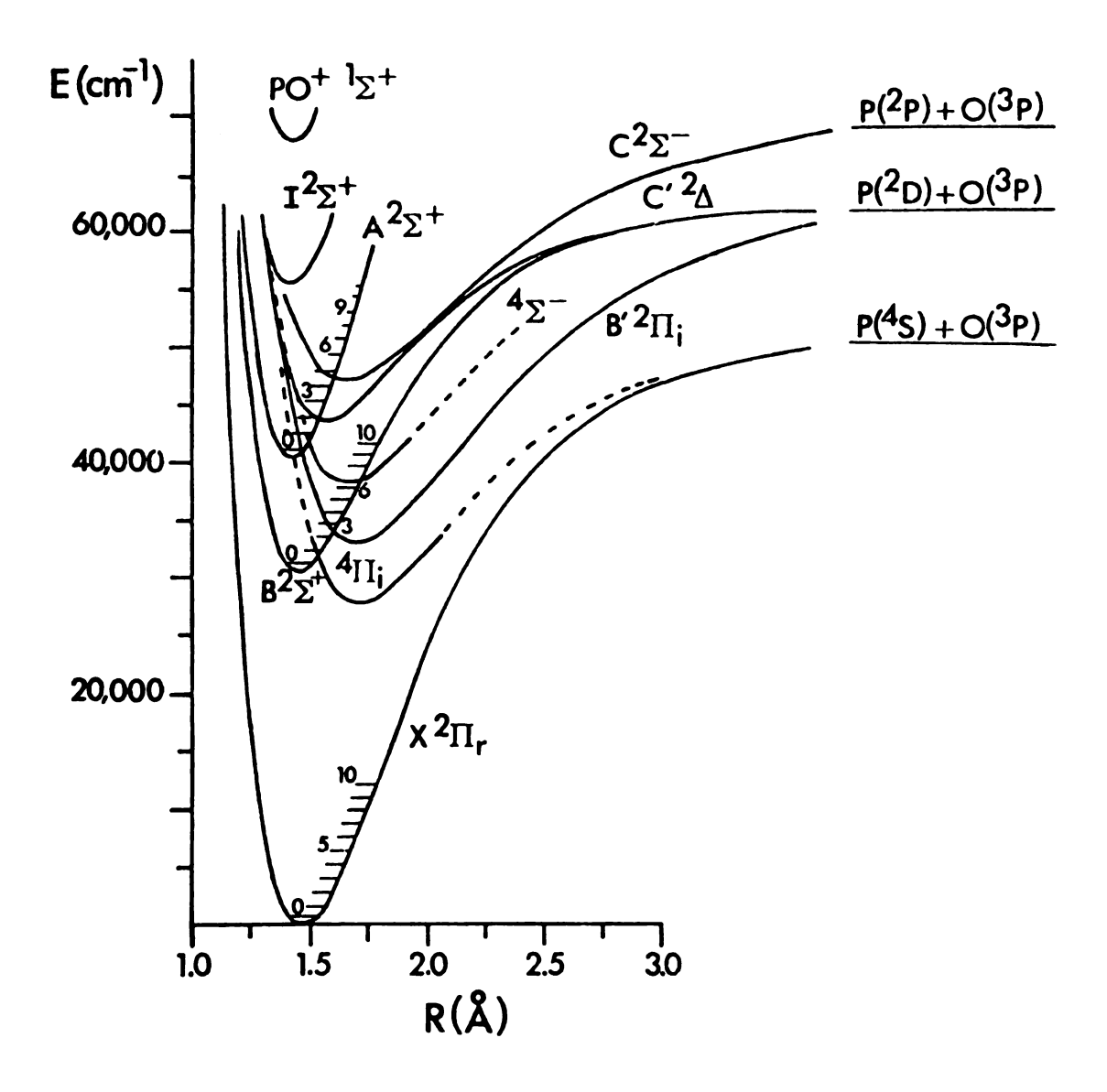


Figure 2. Potential energy diagram for the PO molecule

existence of a PO excimer, as will be explained later, suffices to explain this seeming paradox in intensities.

The two band systems of PO,  $\gamma$  and  $\beta$ , have been known for many years. The  $\beta$  system was first vibrationally analyzed by Curry et al. (94) and the  $\gamma$  system by Ghosh and Ball (41). Rotational analyses of the  $\beta$  system have been carried out by Singh (49), Couet et al. (56), and Mohanty et al. (95). Rotational analyses of the  $\gamma$  system have been carried out by Rao (96), and Coquart et al. (55). The D and D' states of PO, initially and wrongly designated as  $^2\Delta$  states, were found by Durga and Rao (97). The incorrect designation occurred because the transitions observed were D  $\rightarrow$  B and D'  $\rightarrow$  B and the B state at this time was still incorrectly designated  $^2\pi$ . Mrozowski and Santaram first identified the  $F^2\Sigma^+$  and  $G^2\Sigma^+$  states of PO (98). These authors noticed a band at 526 nm, and assigned it to a transition to one of the repulsive states of PO. By deuterium substitution and a resulting frequency shift, the results of this work show that this band belongs to HPO, as will be seen later. The latest assignments and molecular constants associated with these states of PO and others of higher energy are given by the French group (54-62) and the Canadian group (63-71). The Canadian group, Verma et al., (67,69) was the first to postulate the existence of the low lying  $^4\pi$ , and  $^4\Sigma^-$  states of PO from perturbations in the A, F, G, H, and  $I^2\Sigma^+$  states. As stated earlier, there is particular interest in these two quartet states in relation to this work. The electron configurations which give rise to these states of PO are:

(1) . . . 
$$(z\sigma)^2(y\sigma)^2(w\pi)^4(x\sigma)^2(v\pi)*$$
  $\chi^2\pi$ 

(2) . . . 
$$(z\sigma)^2 (y\sigma)^2 (w\pi)^4 (x\sigma)^2 (u\sigma)^*$$
  $B^2 \Sigma^+$ 

(3) . . . 
$$(z\sigma)^2(y\sigma)^2(w\pi)^4(x\sigma)(v\pi)^{*2}$$
  $F^2\Sigma^+$ ,  $A^{*2}\Sigma^+$ ,  $b^4\Sigma^-$ ,  $C^{*2}\Delta$ ,  $C^2\Sigma^-$ 

(4) ... 
$$(z\sigma)^2 (y\sigma)^2 (w\pi)^3 (x\sigma)^2 (v\pi)^{*2}$$
  $D'^2 \pi_r, B'^2 \pi_i, {}^4 \pi_i$ 

These are the valence states of PO. The ground state has been assigned by analogy to NO (67). From Figure 2 it can be noticed that the excited states fall into two groups, those with  $r_e > r_e (X^2 \pi_r)$  and those with  $r_e \approx r_e (^1\Sigma^+)$  of PO $^+$ . From these observations and the fact that the vm\* orbital is strongly anti-bonding, it suggests that the states with  $r_e > r_e (X^2\pi_r)$  are valence states and that to obtain the more tightly bound states with  $r_e < r_e (X^2\pi)$  the strongly antibonding electron is promoted to a bonding Rydberg orbital. That is how the tentative configuration-state assignments have been made. This means that A, D, E, G, H, and I are Rydberg states, and B, F, A', b, C, C', D', B', and  $^4\pi_1$  states are valence states of PO according to this analysis.

The  $B^2\Sigma^+$  state has the  $v\pi^*$  antibonding electron assigned to  $u\sigma^*$ , which is an even more antibonding orbital according to Verma et al. (67), but which is a weakly antibonding orbital according to Ackermann et al. (99). The  $B^2\Sigma^+$  state has partial Rydberg character according to both Ackermann et al. and Tseng and Grein (100).

The  $F^2\Sigma^+$ ,  $b^4\Sigma^-$ , and  $C^{*2}\Delta$  states have rather large internuclear distances and relatively looser bonds. This is interpreted as being the result of a transfer of an electron from the slightly bonding

xo orbital to the vm\* antibonding orbital, compared to the ground state. The doublet and quartet pi states with even looser bonds are interpreted as the transfer of a strongly bonding electron from the wm orbital to the vm\* strongly antibonding orbital. The  $B'^2\pi_i$ ,  $D'^2\pi_r$ , and  $^4\pi_i$  states would fall into this category. Coquart et al. (60), and Roche and Lefebvre (101) have considered the possibility that the  $D'^2\pi_r$  state corresponds to high vibrational levels of the  $B'^2\pi_i$  state.

For the generation of the electron configuration of the Rydberg states an electron is added to the electron configuration of ground state  $P0^+$ :

...
$$(z\sigma)^2(y\sigma)^2(w\pi)^4(x\sigma)^2$$
  $(^1\Sigma^+)$ 

Verma et al. (67) suggest the following configurations for the Rydberg states, converging to the ground state of PO+:

$$A^2 \Sigma^+ - \sigma 4s$$
  $D^2 \pi_r - \pi 4p$   $G^2 \Sigma^+ - \sigma 4p$   $E^2 \Delta - \delta 3d$   $H^2 \Sigma^+ - \sigma 3d$   $I^2 \Sigma^+ - \sigma 5s$ 

Ackermann et al. (99) agree with this assignment except for H -  $\sigma$ 3d and I -  $\sigma$ 5s, which they think should be H -  $\sigma$ 5s and I -  $\sigma$ 3d.

The valence and Rydberg states have both been considered theoretically. Calculations on ground state PO have been performed by Boyd and Lipscomb (90) with a minimal basis set of Slater-type orbitals and by Mulliken and Liu (91) who performed an accurate SCF calculation to determine the role of d and f orbitals in the bond. Both groups found the d orbitals to be important.

The first calculation of excited states of PO was that of Ackermann et al. (99) on some of the Rydberg states of PO, the states  $A^2\Sigma^+$ ,  $D^2\pi_r$ , and  $E^2\Delta$ . The  $B^2\Sigma^+$  state was also considered but was withdrawn from the list of Rydberg states because it demonstrated  $\sim 50\%$  non-Rydberg character. By using the LCAO-MO SCF orbitals of the molecular ion core they obtained good agreement between calculated and experimental values for the other Rydberg states.

The excited valence state energies of PO have been calculated by Roche and Lefebvre by using SCF LCAO-MO wavefunctions with CI (101). Fair agreement with experimental term values was obtained except for the  $^2\pi$  states. An <u>ab initio</u> calculation for the spin-orbit coupling constants of the lowest  $^2\pi$  states shows large internuclear distance dependence. Tseng and Grein performed <u>ab initio</u> CI calculations upon some low lying valence states, using a minimal basis set of Slater-type orbitals (100). The agreement with experimental molecular parameters is not impressive.

### F. PO<sub>2</sub>

The next molecule is to be considered is the higher oxide,  $PO_2$ . It is to this molecule that Cordes and Witschel (50), and Davies and Thrush (53) attribute the emission continuum of phosphorus chemiluminescence. But this work does not support their analysis.  $PO_2$  is well established mass spectrally, at least in the hot hydrogen-phosphorus-compound flame (102), but its presence has never been definitely established in the cold phosphorus flame. For a hot, hydrogen rich flame the main species are  $P_2$ , PO, and  $PO_2$  with smaller amounts of P, HPO, and PN. In another related experiment, the flash photolysis of cold phosphine and molecular oxygen,  $PH_2$ , PH, PO, and OH were seen by electronic

absorption (103). In this case there was no suggestion of the presence of  $PO_2$  or HPO. Norrish and Oldershaw in these experiments observed PO in both oxygen sufficient and oxygen deficient systems, concluding that PO does not readily react with either  $PH_3$  or  $O_2$ . This suggests that  $PO_2$  is not readily formed from PO and  $O_2$  at room temperature under near atmospheric pressure.

The radical  $PO_2$  is a transient, odd electron species, making it a radical in both the physical and organic chemist's definition of the word.  $PO_2$  has seventeen valence electrons, is isoelectronic valencewise with  $NO_2$ , and is expected to be bent (104). This radical was detected by EPR in a calcite matrix (105). A similar type of instrumentation was used to detect OH radicals in the gas phase reaction of atomic oxygen and phosphine by Davies and Thrush but in spite of their suggestion that  $PO_2$  is present in these systems, apparently they did not detect it in their experiment (53).

Thus it appears certain that the species  $PO_2$  exists but its presence in cold phosphorus chemiluminescence has yet to be established and its mere presence does not necessarily mean that it is an emitter giving rise to a continuum of emission. For  $PO_2$  to exhibit continuum emission, by analogy to  $NO_2$ , it must show predissociative behavior at an appropriate energy region.  $PO_2$  has been produced directly in the  $1000\,^{\circ}\text{C}$  reaction of phosphorus and tin oxide (106).

$$PO_{2(g)} + 2Sn_{(g)} + 2Sn_{(g)} + 1/2 P_{2(g)}$$

By a mass spectrographic Knudsen cell method Drowart, et al., have thermodynamically determined the complete dissociation energy,  $PO_2 \rightarrow P + 20$ , for  $PO_2$ . The value obtained, 260 kcal/mole, is higher

than that of NO<sub>2</sub>, 224 kcal/mole. The PO bond energies in PO<sub>2</sub> were determined to be 118 kcal/mole and that in PO by similar experimental techniques was determined to be 142 kcal/mole (107). This implies that the high energy cut-off for the inverse predissociative recombination emission PO + O  $\rightarrow$  PO<sub>2</sub> + hv should be at 242 nm. The fact that a very sharp cut-off of the high energy end of the continuum of the phosphorus chemiluminescence is seen at 335 nm does not rule out PO<sub>2</sub> as the emitter responsible for the continuum but it is not entirely consistent.

Moreover, in later sections, experiments will be described that clearly rule out PO<sub>2</sub> as the emitter responsible for the green emission continuum.

The first well-defined spectrum of HPO was obtained by Ludlam by burning phosphorus in a hot hydrogen flame (51). He wrongly attributed the green bands to the species PH, as did initially Lam Thanh and Peyron, who studied the emission under somewhat different conditions and much higher resolution (52,108-110). The emission spectrum was obtained by allowing atomic hydrogen and molecular oxygen to react with molecular phosphorus at pressures lower than atmospheric. Only one electronic transition was observed and the transition was assigned as a  $^1A'' + ^1A'$ , by analogy to HNO, which has been studied by both absorption and emission (111-113). The analysis of the emission spectrum of HPO, extending from 450 to 700 nm, was aided by deuterium substitution for hydrogen. A similar isotope effect was observed in the chemiluminescence in this work (114). From a detailed rotational analysis they determined that  $r_{\rm PH} = 1.433 \ {\rm \AA}$ ,  $r_{\rm PO} = 1.512 \ {\rm \AA}$ , and  $\theta_{\rm HPO} = 104^{\rm O}$  44' for the ground state,  $^1A'$ . The fundamental frequencies of vibration were found to be

2308, 1179, and 983 cm<sup>-1</sup> for HPO and 1624, 1177, and 745 cm<sup>-1</sup> for DPO (52). Although Clement and Ramsay observed a sharp breakoff in the K-rotational structure due to predissociation in the excited state of HNO, Lam Thanh and Peyron did not observe direct evidence of predissociation in the excited state of HPO (109).

Because the luminescence of HPO extended far down their low pressure reaction chamber, Lam Thanh and Peyron attributed the probable formation of electronically excited HPO to a triple collision, analogous to that proposed for the formation of excited HNO by Clyne and Thrush (115). However, Ibaraki et al. (116) have proposed a different mechanism for the generation of electronically excited HNO, a hydrogen atom collision with NO dimer. It is quite possible that HPO is formed via a similar mechanism. This would explain the observations of Lam Thanh and Peyron and also some observations in this work much better than the mechanism of Clyne and Thrush.

Lam Thanh and Peyron do not specify in detail their experimental procedures, such as the length of time their photographic plates were exposed in obtaining the emission spectra of HPO and DPO (52), but they do indicate that there were intensity problems associated with obtaining the DPO spectrum (110). This experimental difficulty could explain the large differences in intensity between their DPO and HPO emission spectra. Their HPO spectrum is much more intense than their DPO spectrum whereas under the experimental conditions of this work all the DPO emission bands are at least five times more intense than the corresponding HPO emission bands and in addition there are many more of them (114). This very dramatic change in intensity resulting from

an isotopic substitution is indicative of a predissociative process (117). It occurs because the vibrational wave functions belonging to the two electronic states overlap substantially just below the point of intersection of the two potential surfaces and predissociation due to tunnelling occurs. Tunnelling is a very isotopic dependent phonomenon. Part of this intensity change is due to the fact that deuterium atoms tunnel less readily than hydrogen atoms. Part is due to the fact that for deuterium the vibrational levels of the upper state lie lower than the corresponding levels for hydrogen because of a lower zero-point energy; thus the width of the barrier through which the deuterium atom has to tunnel is greater (81). Striking examples of isotopic effects upon predissociation can also be seen in absorption and emission processes in radicals such as CH<sub>2</sub>, CD<sub>2</sub> and CH<sub>3</sub>, CD<sub>3</sub> (117).

The selection rules for predissociation are  $\Delta J = 0$ ,  $+ \leftrightarrow +$ ,  $- \leftrightarrow -$ ,  $A_1 \leftrightarrow A_1$ ,  $E \leftrightarrow E$ , etc., and  $\Delta S = 0$ , if spin-orbit interaction is weak (117). Because phosphorus is a rather heavy atom, it is expected that the last rule does not hold rigorously for HPO. Theoretically HPO and HNO should have a triplet state lower in energy than the  $^1A''$  excited state and if it lies close enough and is dissociative, then predissociation could be induced by spin-orbit interaction. Emission from the  $^3A''$  electronic state has never been reported for either HNO or HPO, but indirect evidence places the  $^3A''$  electronic state of HNO at about 1 ev (118). For HNO Bancroft et al. (112) favor a predissociation caused by a repulsive  $^1A''$  state or by a low-lying triplet state. A recent calculation on the potential energy curves for the HNO molecule using the UHF (unrestricted Hartree-Fock) method indicates that the predissociation is due to the small

magnitude of interaction between two closely approaching perturbed  $^1A''$  electronic states (119). These two states are the result of an application of the non-crossing rule. Each results from the interaction of two states, a repulsive state dissociating to ground state NO and a bound state dissociating to excited state NO. This occurs, they claim, because all the HNO states formed from ground state H and NO are repulsive and those formed from ground state H but excited state NO,  $^2\Sigma^-$  or  $^2\Delta$ , should be attractive. However, the  $^2\Sigma^-$  and  $^2\Delta$  states are far from being the lowest excited electronic states of NO.

## $H. OH, HO_2, H_2O^+$

In addition to HPO, it is reasonable to expect that there exists in the phosphorus chemiluminescent flame other hydrogen containing radicals such as OH,  $\mathrm{HO}_2$ , or  $\mathrm{H_2O}^+$ . No emission has been found in the chemiluminescent emission directly attributable to any of these species in the ultraviolet or visible, but there is emission at  $\sim 1.0~\mu$  possibly due to OH. The process by which protons and deuterons from water and heavy water, respectively, end up on the emitting species HPO and DPO could generate an OH radical. Davies and Thrush observed the OH radical by the use of ESR in the gas phase reaction of phosphine and atomic oxygen (53). There have been some preliminary results in this work by the use of ESR suggestive of an OH radical but the identification has not been positive. The OH radical is well known for its emission; in the ultraviolet at 306.4 nm and higher in energy, in the visible, and in the red and near-infrared where the rotational vibrational bands of the ground state of the ground state are known as the Meinel bands

(120). The ultraviolet transition is an  $A^2 \Sigma^+ \to X^2 \pi$  and the visible a  $B^2 \Sigma^+ \to A^2 \Sigma^+$  electronic transition (121).

The  $\mathrm{HO}_2$  radical has been observed directly by optical spectroscopic means in a number of systems (122-125), and mass spectrally in some hot hydrocarbon flames (126-127). The ground state of  $\mathrm{HO}_2$  is  $^2\mathrm{A''}$  and the first excited state is  $^2\mathrm{A'}$ . According to a recent calculation the energy separation is only 0.74 ev (128). The experimental value determined by Becker et al. (123) is very close to this.

In addition to OH and  $\mathrm{HO}_2$  one could expect also the species  $\mathrm{H_2O}^+$  to be present in this system.  $\mathrm{H_2O}^+$  has a  $^2\mathrm{B}_1$  ground state and transitions from an upper  $^2\mathrm{A}_1$  to the ground state have been observed in the visible region in absorption and in emission (129). However, emission that could be attributed to this species has not been seen in this work in spite of a careful analysis of the spectra. There are many other species likely to be involved in this chemiluminescence but they will not be discussed further. When the flame is subjected to mass spectral analysis as Hastie has done to a hot, atmospheric pressure hydrocarbon flame (127), these weakly and non-emitting species can be positively identified and their role in the mechanism of phosphorus chemiluminescence deduced. Attention will finally focus on the work about which this thesis is centered.

#### CHAPTER IV

# IDENTIFICATION OF THE EMITTING SPECIES IN PHOSPHORUS CHEMILUMINESCENCE

### A. Experimental Descriptions

#### 1. Chemicals

The white phosphorus used in these experiments was obtained from Baker Chemical Co., and was of  $\sim$  99% purity. The nitrogen, oxygen, and air were from Airco and were of sufficient purity that they were used directly. The water was distilled once and the deuterium oxide was from Columbia Organics Co. and was of 99.5% purity.

### 2. Equipment

Four different monochromators and six different photomultipliers were used to obtain the emission spectra. Some low-resolution emission spectra were recorded with a 0.3 meter McPherson Model 218 Monochromator. It is capable of 0.6 Å resolution. The grating has 1200 lines per mm and was blazed at 200 nm. Typical slit widths used on this monochromator were 250  $\mu$  to 300  $\mu$ . The detector was an EMI 9558 QB or a RCA 1P28 photomultiplier. The EMI has a S-20 response and is sensitive from 200 to 700 nm. The 1P28 has a S-5 response and is sensitive from 200 to 600 nm. The EMI was operated at 1.4 to 1.8 kv (kilovolts) and the RCA 1P28 at 1.0 to 1.1 kv. Current from each was fed into an Eldorado Model 201 Universal Photometer and from this to a Sargent Model TR

recorder. The major part of the emission studies of the  $\gamma$  system of PO and HPO and DPO was performed by using the above mentioned experimental apparatus.

Most of the latter work was done with a Heath Model EU-700, 0.5 meter monochromator with a grating of 1200 lines per mm and blazed at 250 nm. Typical slitwidths were 300 to 500  $\mu$ . This was used with a Heath Model EU-701-30 Photomultiplier Module which contained a RCA 1P28 photomultiplier different from the one used previously. The output of the photomultiplier tube was fed into a Heath Model EU-703-31 Photometric Readout unit, which was used with a typical sensitivity of  $10^{-8}$  amperes.

Another monochromator used was a Bausch and Lomb 0.25 meter instrument with an IR grating. The grating had 675 lines per mm and was used from 0.7 to 1.2 µ. Entrance and exit slit widths of 5 and 3 mm respectively and smaller were used. This monochromator was used with a RCA 7102 or RCA C31034 photomultiplier, both cooled with dry-ice. The RCA 7102 has a S-1 response and has a useful sensitivity from 0.5 to almost 1.2  $\mu$ . The RCA C31034 is a developmental type photomultiplier and has a gallium-arsenide photocathode. It can be used from 200 to 930 nm, has a very high sensitivity throughout the entire spectral range, and has an extremely low dark current. The housing for this photomultiplier was designed here. The machine and glassblowing shops produced some of the components, but it was assembled in this laboratory. The photomultiplier-cooler assembly performed up to specifications. The voltage used on the RCA 7102 was at most 1.17 kv and that on the RCA C31034, 1.90 kv. The Heath or Eldorado photometers were used with this set-up.

Highly resolved spectra of HPO and DPO emission were taken with a Spex 1401 Double Spectrometer. Typical slit-widths of 100-200-100  $\mu$  were used, there being three slits on the two monochromators. The photomultiplier used was another RCA C31034, which was cooled thermoelectrically to -20°C. This photomultiplier was used in a photon-counting mode and was operated always at 1.94 kv.

Medium and low resolution spectra were taken with the McPherson and Heath monochromators. High resolution spectra were taken with the Spex 1401 Double Spectrometer and very low resolution spectra were taken with the Bausch and Lomb monochromator. The overall spectral characteristics are discussed with reference to low resolution spectra, but spectral assignments and activation studies were made with reference to medium resolution spectra. (An exception to this statement are the near-infrared spectra, which were assigned with reference to low resolution spectra.) An attempt at rotational analysis of the DPO and HPO emission was made with the high resolution spectra. Only very low resolution spectra were taken for the near-infrared region because of the low sensitivity of detectors in this region.

### a. Room Temperature Emission Spectra

The spectra were obtained from a cool green phosphorus flame. The flame was produced from the following experimental arrangements. The P<sub>4</sub> was placed in a 50 ml glass flask which was placed inside of a beaker which was sealed around the top with a large rubber stopper. The neck of the 50 ml flask stuck through the rubber stopper. Through the stopper were connections for pumping hot water from a constant temperature water bath. Into the inner flask, containing the phosphorus,

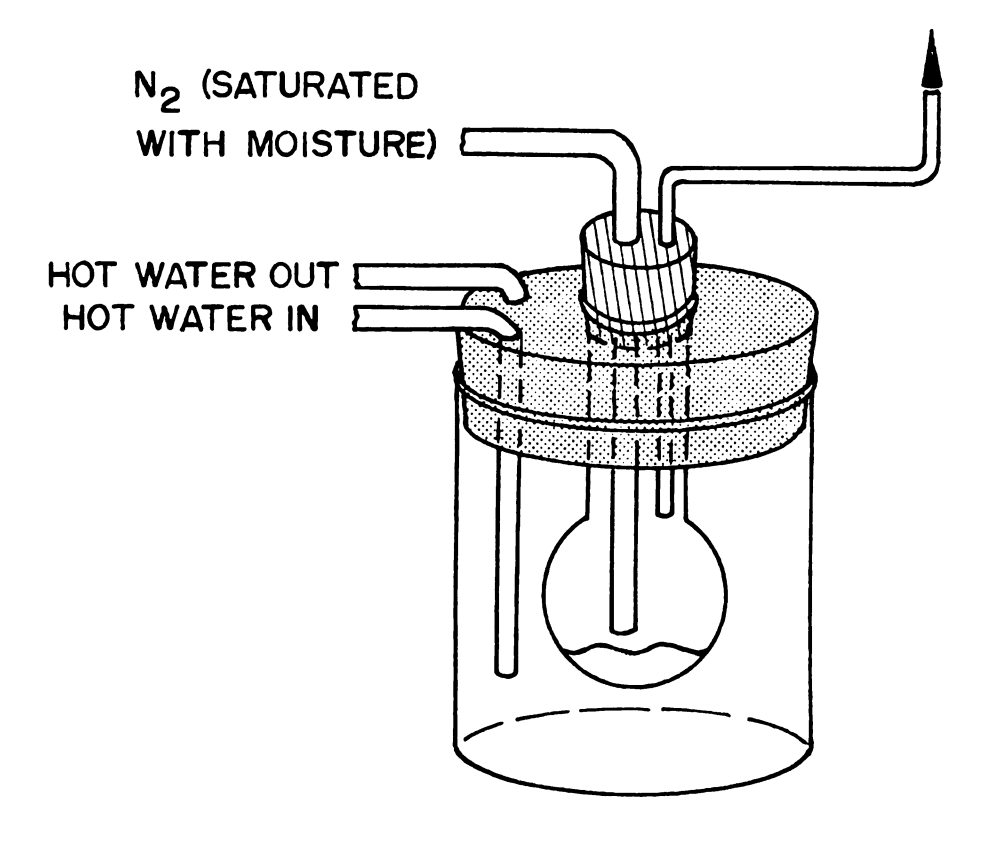


Figure 3. Diagram of the arrangement used for obtaining room temperature phosphorus chemiluminescence emission spectra

flowed nitrogen saturated with water or deuterium oxide. The nitrogen flowed into the container of water or deuterium oxide at room temperature where it was saturated and then the stream was led into the phosphorus container. A small 3 mm o.d. (outside dimension) heavy wall quartz tube led the mixture away, where the chemiluminescence occurred. A diagram of this is shown in Figure 3. Air was the source of molecular oxygen for the reaction.

The temperature of the water bath was maintained at  $57^{\circ}-60^{\circ}$ C. The temperature varied somewhat from experiment to experiment but was maintained constant to  $\pm$  0.5C° during each experiment. With spectra taken for comparison of intensity, the current to the electrical heater for the water bath was maintained at a constant value in order that there be no fluctuations in temperature and in voltage by the thermostat turning on and off.

### b. Temperature Dependent Emission Spectra

For the temperature dependent emission spectra the water bath around the phosphorus container was maintained at approximately the same temperature as described in the previous section but the tube carrying the phosphorus vapor, water or deuterium oxide vapor and nitrogen was heated electrically. Two different methods were employed for heating.

In the first method of heating the reactant vapors the quartz tube was wrapped with approximately three feet of #22 nichrome wire and covered with asbestos. The voltage across the two ends was regulated with a variable transformer to control the current through the heater and thus the temperature of the flowing reactants. The temperature was

measured with a fine #24 wire copper constantan thermocouple. The potentiometer used to measure the thermally induced EMF was a Model 8686 Leeds and Northrup millivolt potentiometer. The junction was held approximately 10 mm above the end of the tube. A diagram showing the setup is presented in Figure 4.

In the second method of heating the reactant vapors, the tube carrying the phosphorus vapor, water or deuterium oxide vapor, and nitrogen gas on the one hand and air in the other was heated before the two were allowed to mix and react. The air was commercially available cylinder air and was used directly from the tank. The thermocouple was held just to the side and top of the quartz tube carrying the unreacted vapors. The small tube was 3 mm o.d. as before, but it was inside of a 22 mm o.d. quartz tube. The heating wire was three feet of #14 nichrome wire. This wire was wrapped around the inside of the 22 mm o.d. quartz tube for 15 cm of the 30 cm total length. This tube was wrapped with aluminum foil followed by asbestos tape from one end to the other except for one small window, through which the monochromator observed the emission. The flow rate of air was about 2 to 3 liters per minute and it was found that the rate was not too critical. This apparatus is shown in Figure 5.

### c. Concentration Dependent Emission Spectra

For the concentration dependent emission spectra the phosphorus vapor, water or deuterium oxide vapor, and nitrogen gas were led into another 50 ml round bottom flask which was heated with an electric heating mantle to  $\sim 60^{\circ}$ C. On this flask was a connection for adding more nitrogen gas. Out of this flask flowed a constant amount of

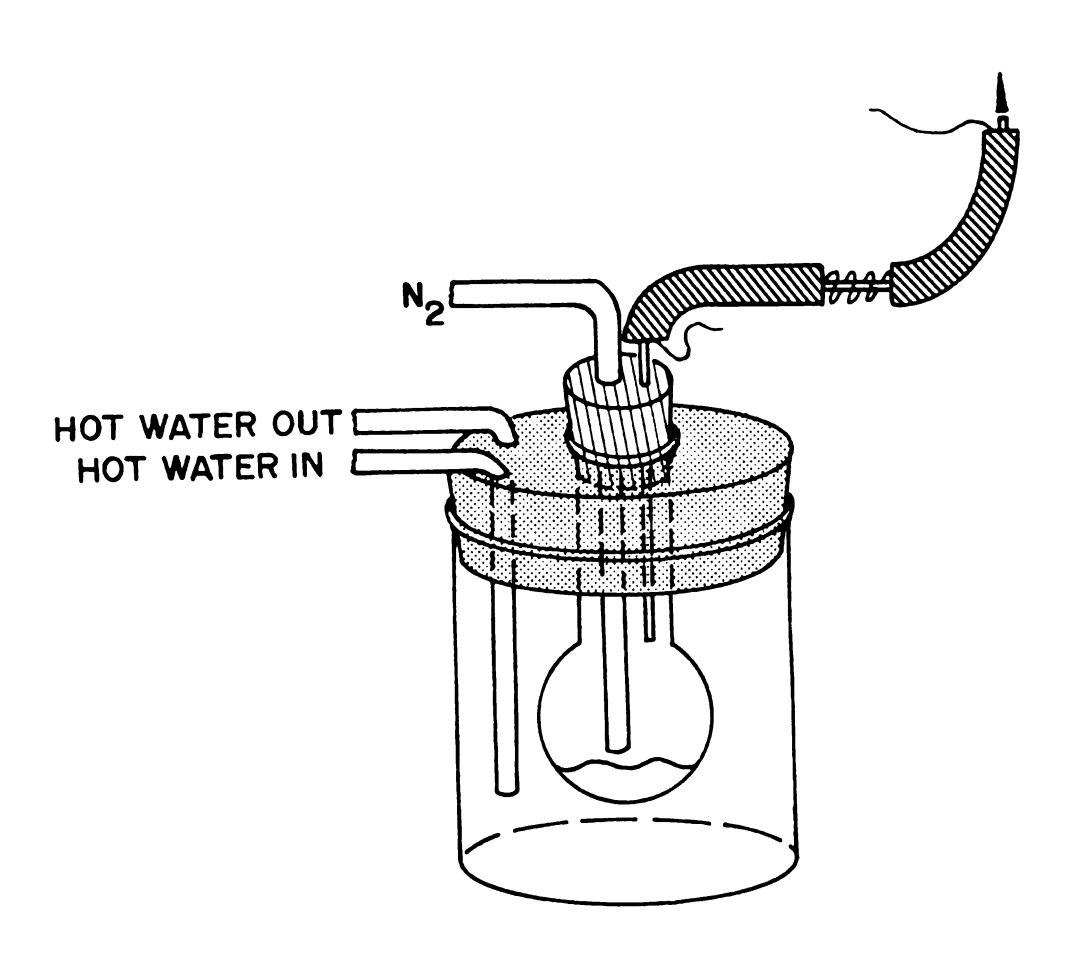
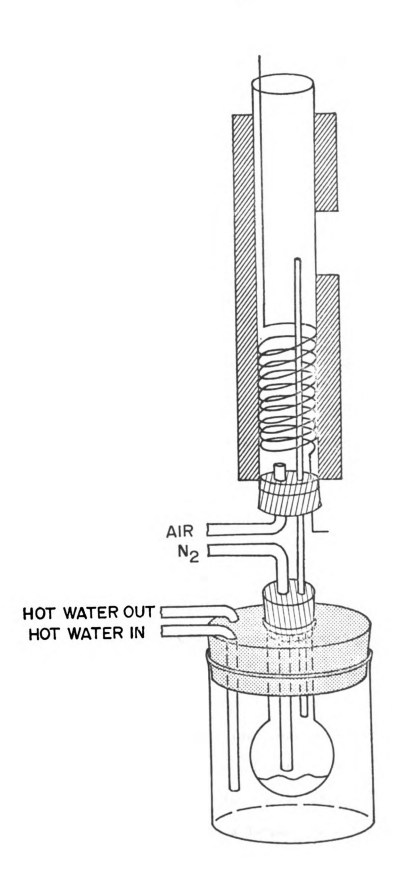


Figure 4. Diagram of the first arrangement used for obtaining temperature dependent phosphorus chemiluminescence emission spectra

Figure 5. Diagram of the second arrangement used for obtaining temperature dependent phosphorus chemiluminescence emission spectra



phosphorus and water vapor per unit time, but varying amounts of nitrogen. The 3 mm o.d. tube between the two flasks was heated slightly to prevent condensation and the 3 mm quartz tube leading to the site of the reaction was heated exactly as in the first method of obtaining temperature dependent emission spectra. The apparatus is shown in Figure 6.

d. Dehydrated Phosphorus Emission Spectra

To study the effect of drying the reactants in phosphorus chemiluminescence the phosphorus used was previously distilled over  $P_4O_{10}$  in a closed system in absence of air. The distilling apparatus is shown in Figure 7. Dried nitrogen was passed through the flask containing the phosphorus, which was heated to about  $60^{\circ}\text{C}$  with an electric heating mantle. The nitrogen stream carrying the phosphorus vapor was led into the reaction chamber where chemiluminescence occurred when dried oxygen was allowed to mix. The top of this chamber was open to the atmosphere but the flow rate of molecular oxygen was sufficiently fast to keep the inside of the reaction chamber free of outside oxygen and water vapor. The oxygen and nitrogen gases were both dried separately by bubbling through concentrated sulfuric acid followed by passing through a U-tube containing diphosphorus pentoxide.

e. Cross-Section of the Chemiluminescent Flame

To study the homogeneity of the chemiluminescent flame with respect to ratios of the emitting species, a system similar to that used in the experiment on Temperature Dependent Emission Spectra was used except that the heated tube was 7 mm in diameter instead of 3 mm (see Figure 4). This allowed a larger flame. A nitrogen flow rate of about 4 liters per minute was used. The resulting flame was a cone

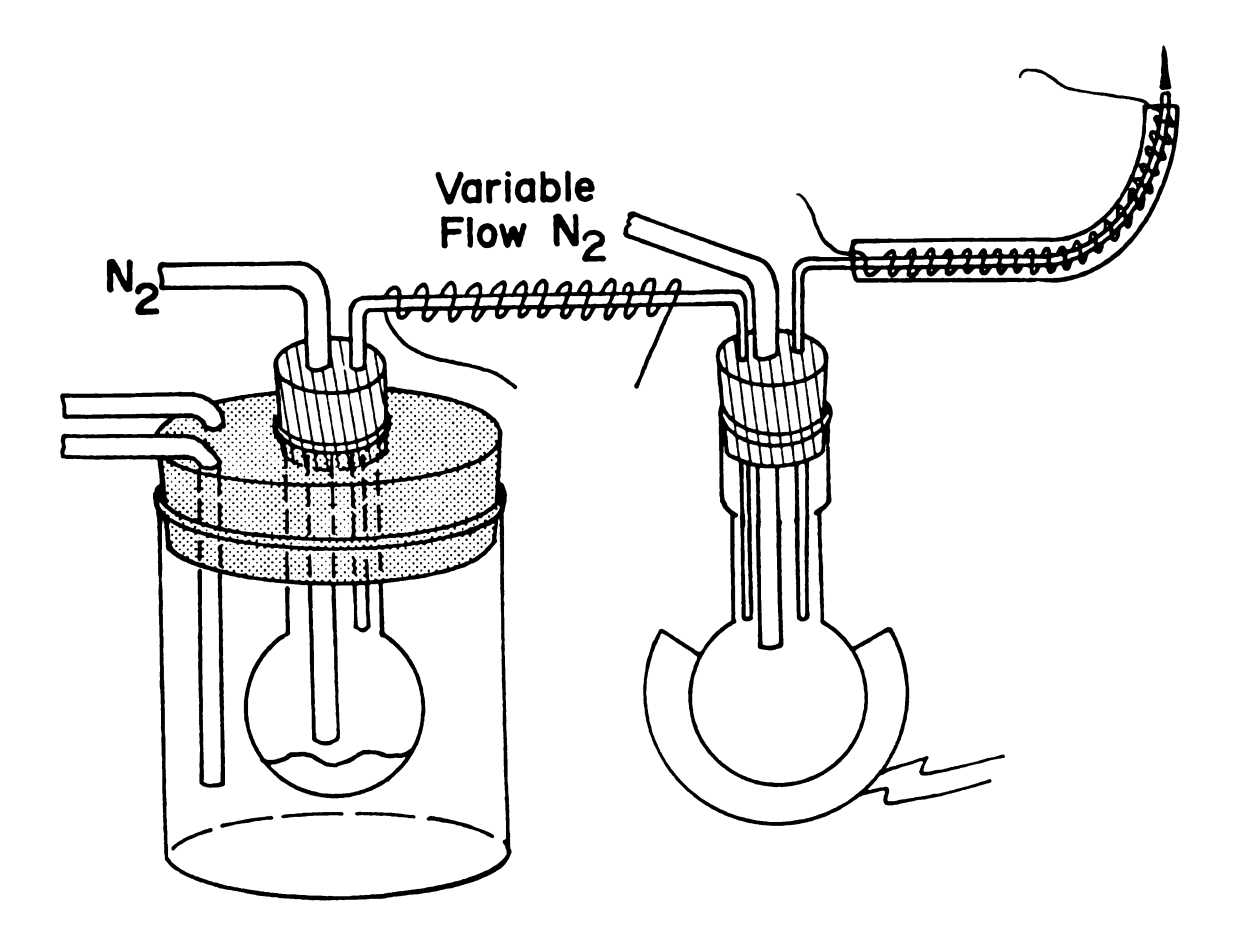


Figure 6. Diagram of the arrangement used for obtaining dilution

(concentration dependent) emission spectra from

phosphorus chemiluminescence

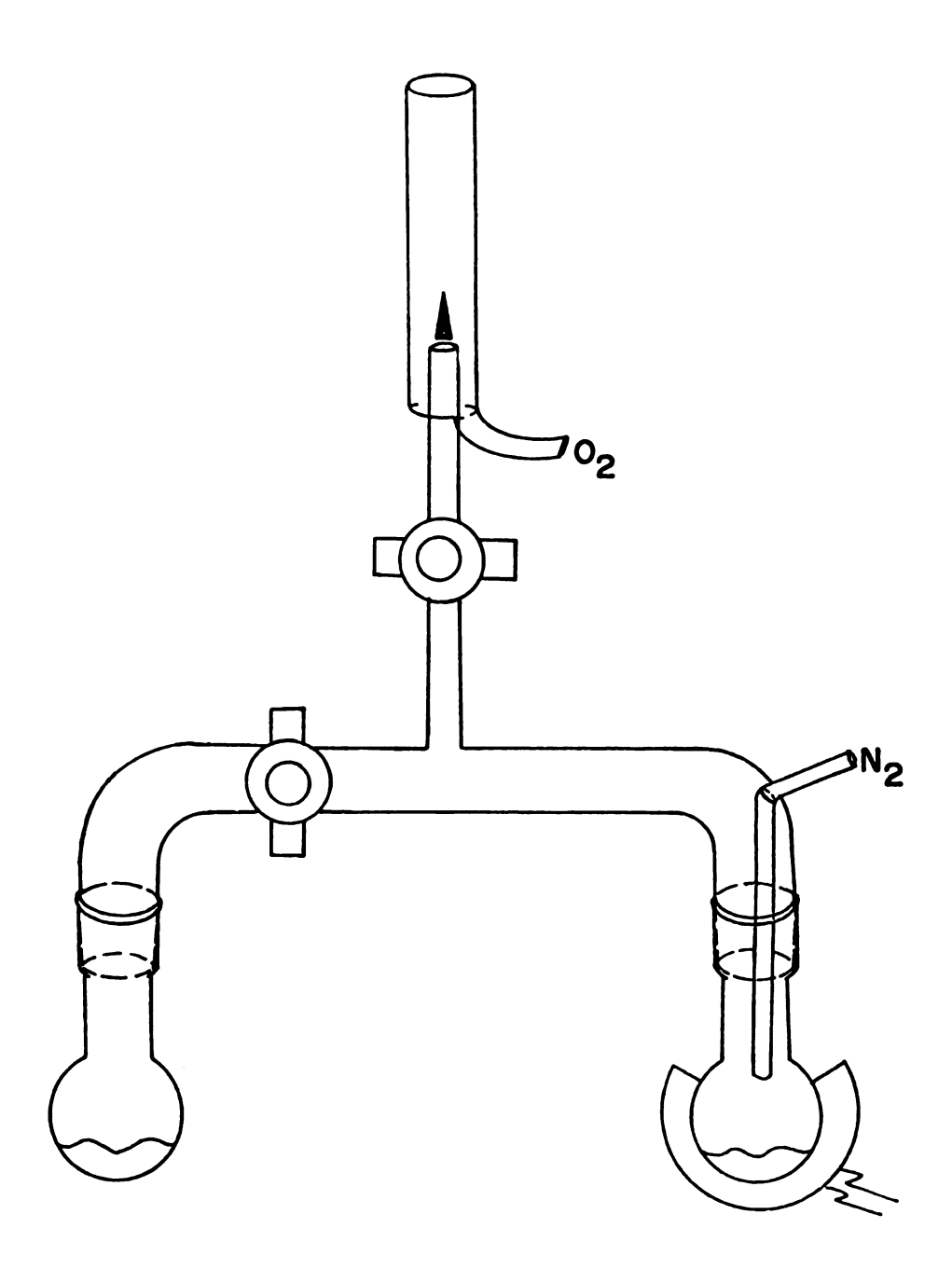


Figure 7. Diagram of the arrangement used for distilling dried phosphorus and obtaining dehydrated phosphorus chemiluminescence emission spectra

40 mm in height and 7 mm at the base. Cross-sections of the flame, which was 2 mm wide and 3 mm high, were spectrally analyzed at room temperature and at  $320^{\circ}$ C.

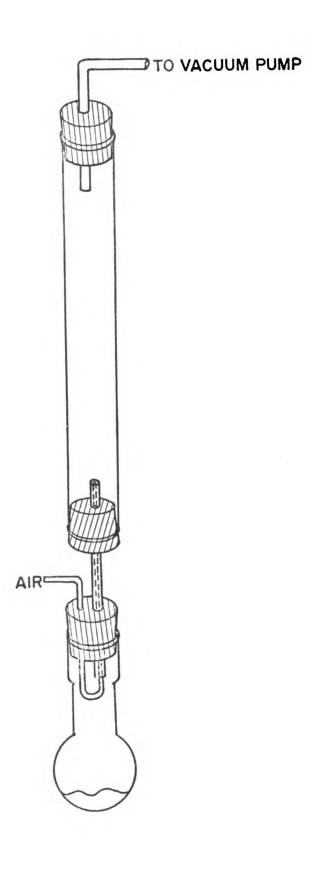
#### f. Low Pressure Studies

A vacuum pump was attached to a 22 mm o.d. and 20 cm long quartz tube with a liquid nitrogen trap between the pump and the tube. The pressure was approximately 0.1 torr in the tube during the reaction. Air was used as the source of molecular oxygen and was regulated into the system with a fine needle valve. The air entered the system in the middle of the concentric phosphorus inlet (Figure 8). A 50 ml round bottom flask containing phosphorus was connected directly to the quartz tube. At room temperature there was sufficient phosphorus vapor entering the quartz tube for visual observation of the chemiluminescence. A dim glow filled the entire length of the tube and hose to the trap, which also glowed.

#### B. The Cool Phosphorus Flame

The cool green phosphorus chemiluminescent flame is classified as a diffusion flame (130). In the flame, reactions take place at the interface of  $P_4$  vapor and atmospheric oxygen. In a premixed flame it is not necessary for oxygen to diffuse to react with the fuel, but the reactants are ignited by the high temperature of the flame as they move into the hot zone. In the cool phosphorus flame, on the other hand, the reactants are self-igniting upon contact with air without any perceptable temperature rise. Even though the phosphorus may be close to  $60^{\circ}$ C initially, at the point of contact with the atmosphere the flame feels cool to the touch. If enough phosphorus were pumped into the flame fast enough a hot flame would result.

Figure 8. Diagram of the arrangement used for obtaining low pressure, oxygen deficient chemiluminescent emission spectra



The phosphorus flame is slightly green in color and upon substituting  $D_2^0$  vapor for  $H_2^0$  vapor in the reaction a striking color change is noted, especially near the top of the flame. In going from water to deuterium oxide the flame turns a much darker green. In the experiment, Dehydrated Phosphorus Emission Spectra, however, the color is less green, almost yellow.

The shape of the flame for low flow rates is that of a perfect cone and is very still. There is no apparent movement of any part of the flame and it appears to be not a flame at all but a solid object, or if the room light is of sufficient intensity, a nearly transparent solid. At higher flow rates the shape mushrooms; the top part is of greater diameter than the bottom and the overall light intensity is increased.

Because the phosphorus oxide products of the flame are irritating and poisonous, the effluent gases must be pumped out of the environment of the experimentor. In almost all of these experiments a 4 inch flexible plastic hose was placed directly over the flame. This hose led to a hood where an electric motor and fan moved the phosphorus oxides into the hood. In performing a number of experiments, such as obtaining the highly resolved HPO and DPO emission spectra, where a hood was not available, a water aspirator was used with a 1 inch o.d. vacuum hose, and the hygroscopic oxides were hydrated and washed down the drain. This arrangement worked very well also but required the use of relatively large quantities of water.

Now that the physical properties of the flame have been described and the necessary precautions presented, the description and analysis of the emission spectra thus obtained constitute the subsequent discussion.

#### C. The Emission Spectra

#### 1. General Characteristics

Figure 9 shows a low resolution emission spectrum of the phosphorus flame at room temperature from 200 to 800 nm. The spectrum has discreet band emission in the ultraviolet from 228.0 to 274.6 nm, a continuum extending from 335.0 to 800.0 nm, and superimposed discrete bands in the region 450 to 650 nm. The emission in the region 228.0 to 274.6 nm was first assigned to PO by Ghosh and Ball (41). The continuum has been assigned by a number of investigators to various species (50,53) and one result of the present work is to prove that the species is a PO excimer, as we earlier proposed (114). The discrete bands superimposed upon the continuum have been assigned by others to PO also (16,44), but we have for the first time in this system assigned them to HPO (114). Details will be found in later sections. The band system to be discussed first is the system assigned to PO in the 228.0 to 274.6 nm region.

#### 2. PO y System

#### a. Assignment

The emission in the region 228.0 to 274.6 nm assigned to PO in the chemiluminescent reaction of phosphorus and oxygen is due to an  $A^2\Sigma^+ \to X^2\pi_\Gamma$  transition and is known as the  $\gamma$  system. A list of wavelengths along with the vibrational assignments and intensities is given in Table 1. Wavelengths obtained by Ghosh and Ball (41) from a discharge through phosphorus oxides are also given along with intensities for comparison. The spectrum from which the experimental wavelengths were taken is shown in Figure 10. The wavelength accuracy

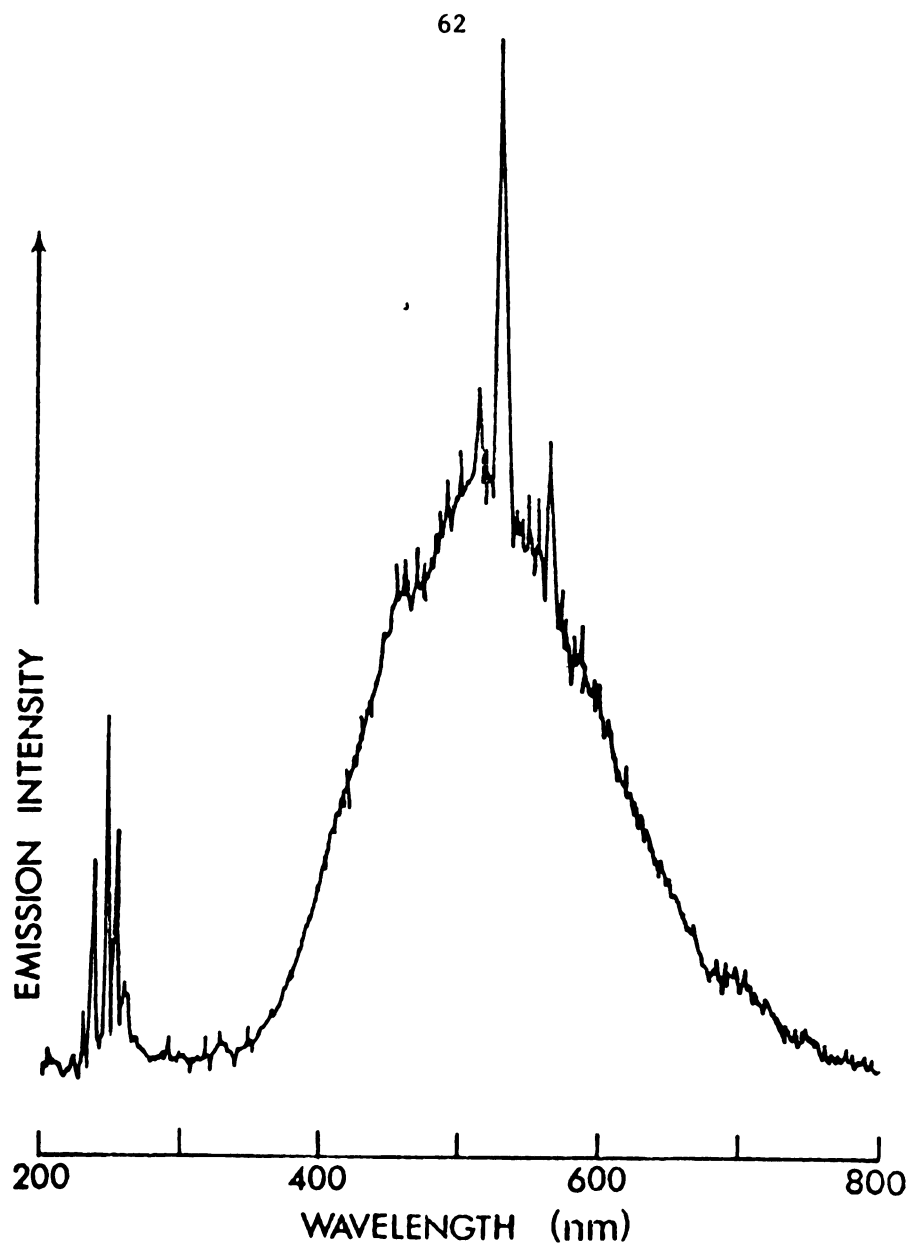


Figure 9. Ultraviolet and visible chemiluminescent emission spectrum of the gas phase reaction of  $\boldsymbol{P}_4^{},~\boldsymbol{O}_2^{},$  and a trace of  $H_2^0$ 

Table 1. Wavelengths of Band Heads of PO  $\gamma$  Emission System

	Ghosh and B	<u>all</u>	Present Work		
intensity	(v',v")	λ <sub>air</sub> (nm)	$\lambda_{air}^{(nm)}$	Intensity	
· • • • • • • • • • • • • • • • • • • •	6,4	228.070	228.1	1	
	6,4	8.173	8.3	1	
2	5,3	8,700	8.8	1	
2	5,3	8,819	8.9	1	
	6,4	9.230	9.2	1	
3	4,2	9.360	9.4	1	
3	4,2	9.487	9.5	1	
3	5,3	9.870	9.7	2	
3	5,3	230.036	9.8	2	
	3,1	0.166	230.2	ī	
4	4,2	0.534	0.4	1	
4	4,2	0.692	0.5	ī	
	• -		0.6	ī	
			0.8	1	
4	3,1	1.206	1.1	1	
4	3,1	1.370	1.2	1	
3	2,0	1.882		_	
3	2,0	2.060			
	•		2.2	1	
			2.3	1	
			5.0	1	
			5.5	1	
	4,3	5.800	5.9	2	
	4,3	5.945	6.0	2	
	5,4	6.270	6.2	2	
	5,4	6.405	6.4	2	
2	3,2	6.595			
2 2	3,2	6.729	6.7	2	
	4,3	7.054	6.9	2	
	4,3	7.194	7.1	2	
7	2,1	7.399	7.3	3	
7	2,1	7.523	7.4	3	
	3,2	7.847	7.8	4	
2 2	3,2	7.987	8.0	4	
8	1,0	8.223	8 1		
8	1,0	8,350	8,2	5 5	
	-		8.5	5	
			8.6	5	
7	2,1	8.647	8.7	5 5	
7	2,1	8.794	8.8	5	
	<del>-</del>		9.0	4	
8	1,0	9.465	9.5	3 2	
8	1,0	239.630	239.6		
	-		244.8	1	

Table 1 Continued

6	1,1	245.330	245.3	3
6	1,1	5.460		
2	2,2	5.740	5.7	4
2	2,2	5.896	5.9	5
10	0,0	6.291	6.4	10
10	0,0	6.423	6.5	10
6	1,1	6.675		
6	1,1	6.830	6.8	9
10	0,0	7.639	7,7	8
10	0,0	7.790	7.8	8
	3,4	250.700		
	3,4	0.807	0.8	1
	4,5	0.993	0,0	_
	4,5	1.142	1.1	1
	4,5	1,146	1.4	2
5	2,3	1.755	4.4	2
5	2,3	1.870	1.9	2
,	3,4	2.050	2.1	2
		2.220	2.2	2
	3,4	2.220	2.7	4
7	1 2	2 022		
7 7	1,2	2.823	2.8	4
,	1,2	2.942	2.9	4
	2,3	3.140	3.1	1
	2,3	3,300	3.4	1
			3.6	2
10	0.1	2 200	3.7	2
10	0,1	3.906	3.9	6
10	0,1	4.039	4.0	6
7	1 2	4.240	4.2	6
7	1,2	4.394	4.4	5
			4.7	1
			4.8	1
10	0,1	5.360	5.4	3
10	0,1	5.505	5.5	3
	5,7	5.910	5.9	1
	5,7	6.036	6.0	1
	4,6	7.070	7.1	1
	4,6	7.197	7.2	1
	3,5	8.247	8.2	1
	3,5	8.363	8.4	1
2	2,4	9.453	9.5	1
2	2,4	9.570		
	3,5	259.660	259.6	1
	3,5	259.810	259.8	1
7	1,3	260.676	260.7	2
7	1,3	0.799	0.8	2
2	2,4	0.913	0.9	2
2	2,4	1.070	1.1	2

Table 1 Continued

0	0.0	0(1 010	061 0	
8	0,2	261.918	261.9	2
8	0,2	2.054	2.0	2
7 7	1,3	2.190	2.3	2
7	1,3	2,342	2.4	2
			2.5	1
			2.8	1
7	0,2	3.484	3.4	1
7	0,2	3.630		
			3.7	1
			3.8	1
			4.3	1
	4,7	4.820	4.9	1
	4,7	4,980	5.1	1
3	3,6	6.155	6.2	1
3 3	3,6	6.290	6.3	1
	ŕ		6.6	1
			6.7	1
			7.2	1
4	2,5	7.545	. • =	_
4	2,5	7.672		
•	-,-		8.0	1
			8.1	ī
4	1,4	8.950	8.8	ī
4	1,4	9.080	9.0	1
4	2,5	269,240	269.3	1
•	2,3	207,240	270.1	1
			0.2	1
1	0,3	270.378	0.3	1
1	0,3	0.512	0.5	1
3	1,4	0.681	0.7	1
1	0,3	2.020	2.0	1
1				
1	0,3	2.020	2.2	1
			3.0	1
	2.7	/ (20	3.3	1
	3,7	4.630	4.5	1

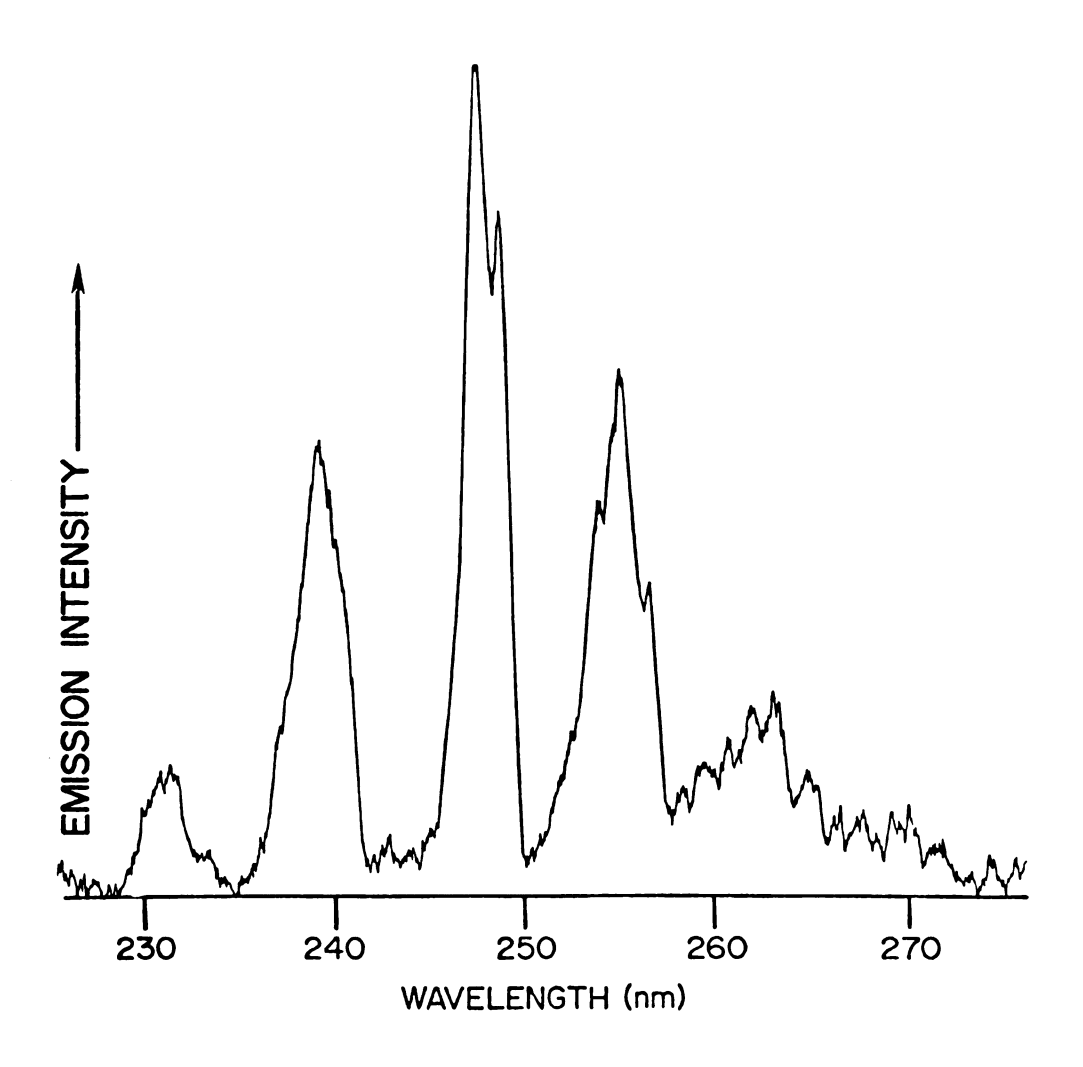


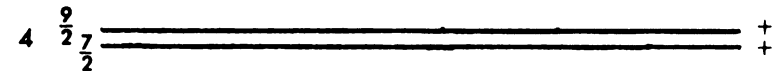
Figure 10. Medium resolution phosphorus chemiluminescent emission spectrum of the PO  $\gamma$  system in the region 228.8-272.1 nm

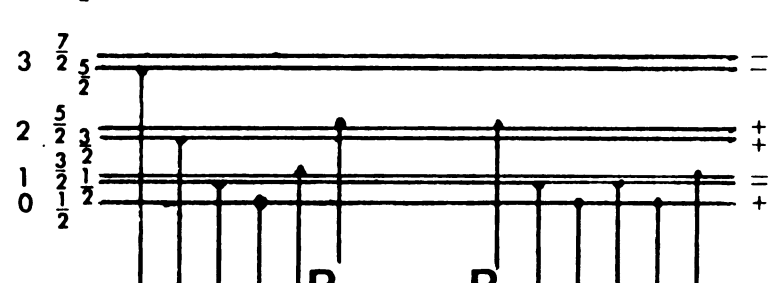
and resolution in this work are not as good as that of Ghosh and Ball but the wavelengths and intensities agree fairly well. At this resolution each band consists of two spin sub-bands, due to  $A^2\Sigma^+ \rightarrow X^2\pi_{3/2}$  and  $A^2\Sigma^+ \rightarrow X^2\pi_{1/2}$ , and each sub-band consists of two heads, which result from the combined effect of overlap and superposition of twelve different branch intensities. These consist of the main branches;  $P_1$ ,  $P_2$ ,  $Q_1$ ,  $Q_2$ ,  $R_1$ ,  $R_2$ , and the satellite branches, where  $\Delta N \neq \Delta J$ ;  $P_{12}$ ,  $P_{21}$ ,  $Q_{12}$ ,  $Q_{21}$ ,  $R_{12}$ , and  $R_{21}$ . Of these  $P_{21}$ ,  $\mathbf{Q}_{12}$ ,  $\mathbf{Q}_{21}$ , and  $\mathbf{R}_{12}$  are superimposed on the main branches for this transition even for resolution given by a third order spectrum on a 10 meter spectrograph (96). The origin of these twelve branches is shown on Figure 11 for the general case of a  $^2\Sigma^+$   $\rightarrow$   $^2\pi$  electronic transition in which the  $^2\pi$  state conforms closely to Hund's case (a). In Hund's case (a) the interaction of the nuclear rotation with the electronic spin and orbital motion is very weak but the electron spin and electronic orbital angular momentum couple very strongly. This means there is a large separation between the  $^2\pi_{3/2}$  and  $^2\pi_{1/2}$  electronic states (13). For the case of the  $\chi^2_{\pi_r}$  state of PO this separation is 224 cm<sup>-1</sup>. On the other hand, a  $^2$  electronic state always belongs to Hund's case (b), in which the electron spin is coupled to the axis of rotation of the molecule. In addition there is a spin splitting of the rotational levels of the  $^2\Sigma$  state which is dependent on N, the quantum number for the total angular momentum apart from spin (117). States which conform to Hund's case (a) for small rotation often undergo a transition to case (b) for large rotation. This is the reason for numbering by N in Figure 11, applicable for high J but formally extended to small J. The large number of branches result from the

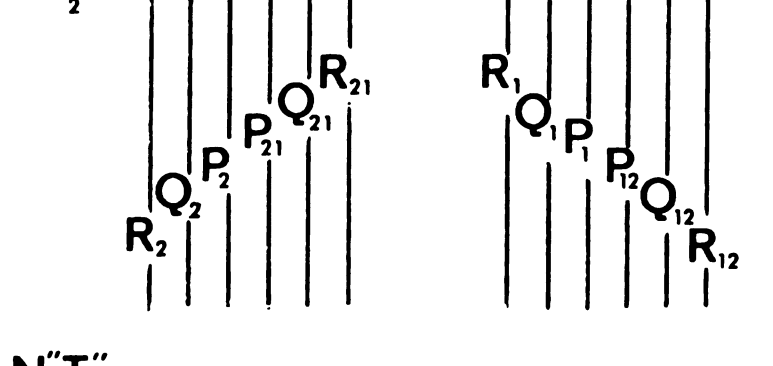
Figure 11. Energy level diagram for lines of a  $^2\Sigma^+ \rightarrow ^2\pi$ (a) band showing spin-doublet splitting and  $\Lambda$  doublet splitting in the lower state and spin-doublet splitting in the upper state

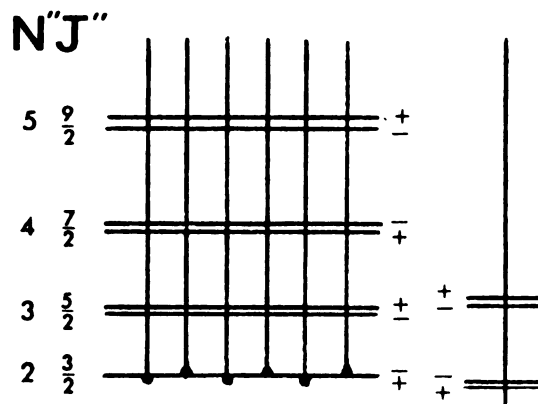
$$2\Sigma^+$$

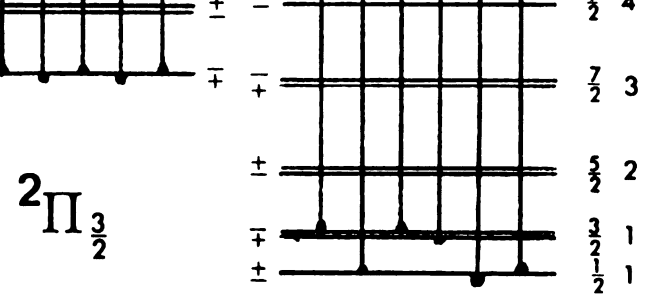
# N'J'











J″N″

fact that the selection rules for transitions between states conforming to different Hund's cases are rules that are common to both cases.

Although expressions have been worked out for the intensities of the branches of  $^2\Sigma$  -  $^2\pi$  transitions as a function of J for intermediate and limiting cases between Hund's cases (a) and (b) (131), our resolution is only sufficient to admit good correlation between intensities and wavelengths obtained by Ghosh and Ball (41). From a comparison of Ghosh and Ball's assignment of branches to Rao's assignment (96) it can be seen that Ghosh and Ball's assignment is inaccurate in so far as detailed branch assignments are concerned because of the huge increase in resolution in Rao's case. It is difficult to assign the correct branches to form the observed heads because of this. However, it appears that the branch head Ghosh and Ball assigned as  $\mathbf{P}_1$  is really  $P_{12}$ ,  $Q_1$  is  $P_2$ ,  $P_2$  is  $P_1$ , and  $Q_2$  is  $Q_1$ . This is because the  $P_{12}$ ,  $P_{2}$ ,  $P_{1}$ , and  $Q_{1}$  branches appear to form fairly strong heads and the other branches do not. The vibrational assignments of Ghosh and Ball and Rao's, however, agree. The (0,0), (0,1), (1,0), (0,2), (1,2), (2,4), and (5,3) transitions are the most intense under our experimental conditions. This means that emission is occurring under a population distribution far from vibrational equilibrium. With a vibrational spacing of 1391  $\,\mathrm{cm}^{-1}$  the Boltzmann ratio of populations in v' = 1 to v' = 2 is  $\sim 10^{-4}$  at  $100^{\circ}$ C. However, this is to be expected if PO is initially formed in very high electronic and vibrational states and high vibrational energy is lost in increments of a quantum at a time. Electronic transitions are seen in this work from up to and including v' = 5 of the  $A^2 \Sigma^+$  state. Vibrational and rotational

constants are given by Rao (96). Ghosh and Ball found  $\omega' = 1391.0$  and Rao found  $\omega' = 1391.16$  cm<sup>-1</sup>. It is easy to obtain a number close to this from our table of experimental wavelengths.

b. Interpretation of Temperature, Pressure, and Isotopic Substitution on the PO  $\gamma$  Emission Intensity

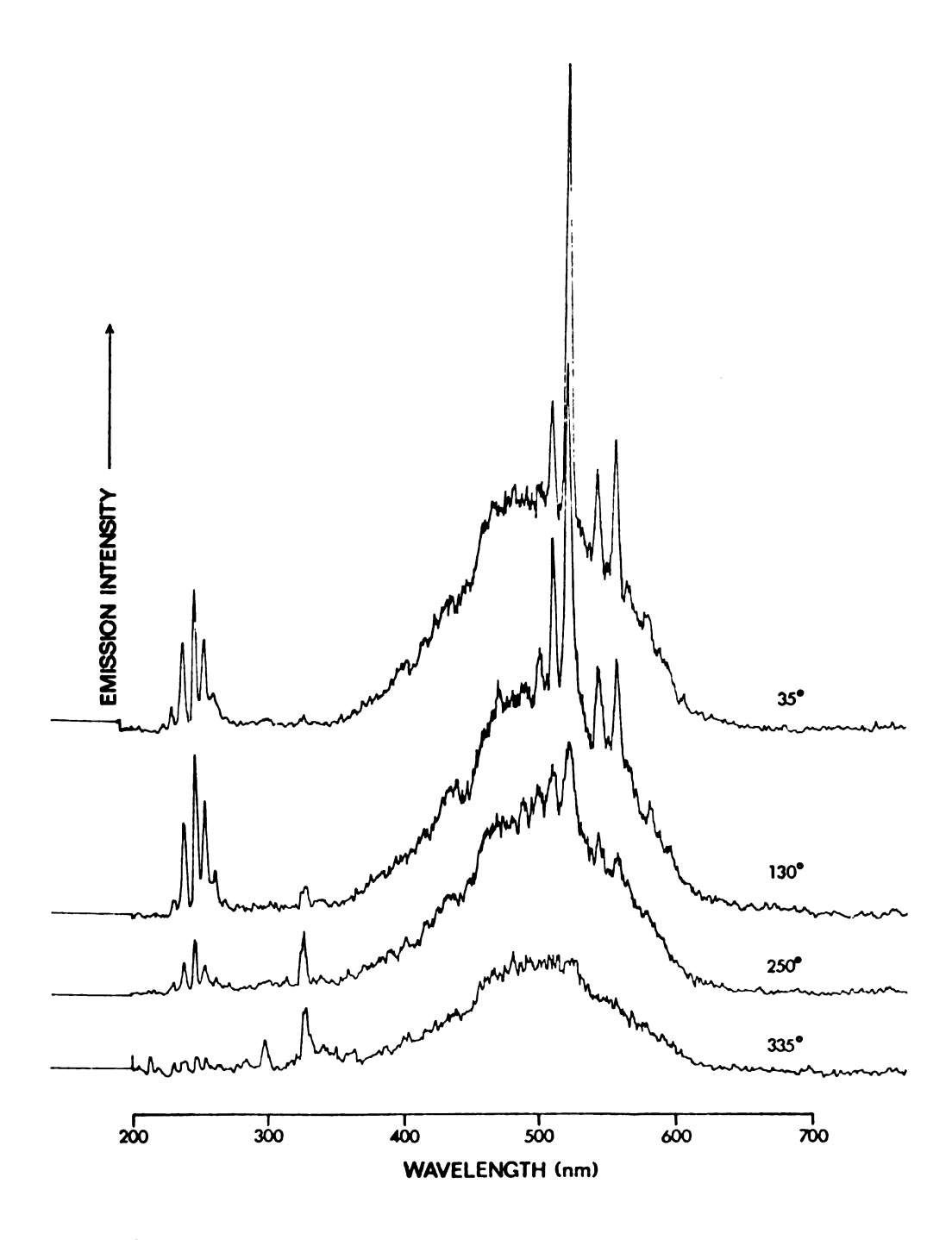
It is known from the work of others that the intensity of the PO  $\gamma$  system emission is pressure dependent. At low pressure PO  $\gamma$  emission is very weak (53). On the other hand as shown from the present work, at room temperature and under atmospheric pressure PO  $\gamma$  emission is relatively strong. This can be explained by the opposing effects of collisionally induced and collisionally compensated or suppressed depopulations. The two opposing effects upon depopulation of vibronic levels are discussed as follows:

- (i) The selection rules for predissociation:  $\Delta J=0$ ,  $+\leftrightarrow+$ ,  $-\leftrightarrow-$ ,  $A_1\leftrightarrow A_1$ , ...  $\Delta S=0$ ; have been derived for the free, unperturbed molecule. During collisions these rules are less valid. For example, during a collision of an excited state PO molecule with a ground state molecule the heavy atom effect of the ground state molecule will negate the  $\Delta S=0$  rule for the excited molecule. The higher the pressure, the more collisions there are per unit time and in some instances this leads to more depopulation of excited states via this depopulation mechanism.
- (ii) At higher pressures thermal equilibrium is attained more quickly and if depopulation is occurring from levels only significantly populated under non-equilibrium conditions, then

less depopulation will occur at higher pressure. Also at higher pressure depopulation can be compensated by an equal number of new molecules formed by inverse predissociation. According to Verma et al. (67), the depopulation in the  $A^2 \Sigma^+$ ,  $G^2 \Sigma^+$ ,  $H^2 \Sigma^+$ , and  $I^2 \Sigma^+$  states of PO, which are known to be accidentally pre

According to verma et al. (67), the depopulation in the A  $\Sigma$ , G  $\Sigma$ ,  $H^2\Sigma^+$ , and  $I^2\Sigma^+$  states of PO, which are known to be accidentally predissociated by the diffuse levels of the  $D^2\pi_r$  or  $D^{*2}\pi_r$  states, are collisionally compensated by inverse predissociation at higher pressures. (The D and D' states are diffuse because of predissociation interaction with a repulsive  $A^{*2}\Sigma^+$  state.) Thus it is possible that intensity alteration with temperature and pressure could be explained by these two opposing effects on depopulation. Except for a few spectra taken at low pressures, which will be presented later, and which do not show the PO  $\gamma$  system at all, no spectra were taken at intermediate pressures to show the buildup.

Many spectra were taken at a number of temperatures which show the decrease in PO  $\gamma$  system emission with increasing temperature. See Figure 12, which shows a series of temperature dependent chemiluminescence spectra for the reaction of  $P_4$  and  $D_2$ 0 vapors on contact with air in a heated chamber (the second arrangement for obtaining temperature dependent spectra). The vapors were carried by a nitrogen stream. They were taken with a Heath monochromator and RCA 1P28 photomultiplier. Emission from the (0,0) transition of the PO  $\beta$  system at 320-337 nm increases dramatically with increasing temperature, which is listed in  $C^0$ . Comparing the spectra taken at 35° and 130°C, the PO  $\gamma$  system emission is seen to be more intense at 130° than at 35°, but decreases rapidly at still higher temperatures, until at 335° the  $\gamma$  system is barely discernable. All these spectra were taken



a

at

In ap

st

op pa

a

s

g

fr

be le v'

ar

1

J

at atmospheric pressure. The  $\gamma$  system emission intensity goes through a maximum between 100° and 130° and decreases steadily thereafter. Increasing the temperature increases the collision frequency. Thus, apart from a change in the efficiency in the formation of excited state PO, this intensity alteration could be explained by the two opposing effects of pressure on depopulation presented in the preceding paragraph. The  $A^2\Sigma^+$  state potential curve of PO is perturbed by the  $^4\pi$ , state potential at v' = 0, by  $b^4\Sigma^-$  at v' = 1, by  $C^{*2}\Delta$  at v' = 2, and by  $C^{2}\Sigma^{-}$  at v' = 5. The v' = 0, 1, 2, 5 vibrational levels yield the most intense emission seen from the  $A^2\Sigma^+$  state. Thus the  $A^2\Sigma^+$ state is likely depopulated under low pressure conditions by the  $C^2\Sigma^-$  and lower states. The depopulation likely occurs in certain rotational levels that are not densely populated except for temperatures greater than 130°C. At higher temperatures the effect of depopulation from the  $A^2\Sigma^+$  state predominates and little emission intensity is seen from the state.

For the v' = 0 level of the  $A^2\Sigma^+$  state of PO perturbations have been seen by Verma and Jois (69) at the N = 10, 17, and 55 rotational levels; for v' = 1 at N = 30, 36; for v' = 2 at N = 19, 39, 45; for v' = 3 at N = 13, 14, 17, 44, 45; for v' = 4 at N = 31, 32, 38, 41, 42 and for v' = 5 at N = 33. N is the total angular momentum apart from spin. Now to show that there is significant population in rotational levels of these vibrational levels, in order to indicate the possibility of depopulation occurring from the rotational levels indicated, where J = N + 1/2, use of the Boltzmann distribution formula is warranted.

Boltzmann ratios at two temperatures for two rotational levels of some of the vibrational levels of the  $A^2\Sigma^+$  state of PO have been calculated and are reported here. The basic formula used is

$$N_J^{\alpha}$$
 (2J+1)e<sup>-BJ(J+1)hc/kT</sup>

where N here represents numbers of molecules and J is the rotational quantum number of the molecule. This states that the number of molecules in the J rotational level is proportional to the degeneracy (2J+1) times the exponential Boltzmann factor. For the ratio  $N_{33} \frac{1}{2}/N_{1/2}$ , using a value of  $B = 0.74 \text{ cm}^{-1}$ , this ratio is equal to 0.57 at  $300^{\circ}\text{K}$  ( $27^{\circ}\text{C}$ ) and 4.4 at  $600^{\circ}\text{K}$  ( $327^{\circ}\text{C}$ ), two typical temperatures at which PO  $\gamma$  system emission data were taken. The ratio in a particular rotational level to the total number in that vibrational level is

$$N_J/N_{total} = (hcB/kT)(2J+1)e^{-BJ(J+1)hc/kT}$$
.

The ratio  $N_{33\ 1/2}/N_{\rm total}=2.0\ {\rm X\ 10}^{-3}$  at  $300^{\rm O}{\rm K}$  and  $7.9\ {\rm X\ 10}^{-3}$  at  $600^{\rm O}{\rm K}$ . The rotational level of maximum population is  $J=11\ 1/2$  at  $300^{\rm O}{\rm K}$  and  $J=16\ 1/2$  at  $600^{\rm O}{\rm K}$ . The ratio  $N_{33\ 1/2}/N_{\rm J_{max}}$  is 0.078 at  $300^{\rm O}{\rm K}$  and 0.43 at  $600^{\rm O}{\rm K}$ . Thus it is seen that there is a very significant difference of population at the  $J=33\ 1/2$  rotational level of the ground or near ground vibrational level of the  $A^2\Sigma^+$  state of PO between  $27^{\rm O}$  and  $327^{\rm O}{\rm C}$ . Similar differences would be found for other values of N in each of the lower vibrational levels. These population differences could explain the large intensity change in emission with the change in temperature. In addition, each vibrational level is expected to be

affected differently with temperature. There are indications that this expectation holds. However, we are limited by our instrumental resolutions to make qualitative statements regarding this phenomenon. The  $\mathbf{v'}$  = 0 should show the largest dependence and it does. In addition this assumes that all the perturbations are of similar magnitude. The fact that we observe weak emission from the  $\mathbf{C'}^2\Delta$  state is consistent with an intermolecular energy migration concept. (A spectrum showing emission from the  $\mathbf{C'}^2\Delta$  state will be shown later.) This concept is central to the interpretation of temperature dependence obtained above. Another interpretation for the variation in the emission intensity of the PO  $\gamma$  system as a function of temperature has to do with the generation of PO in the oxidation of  $\mathbf{P_4}$  by  $\mathbf{O_2}$ . There could be different efficiencies of formation of excited state PO at different temperatures.

Deuterium oxide substitution for water also effects the PO  $\gamma$  system emission intensity. Under almost identical experimental conditions, the deuterium oxide substitution lowers the  $\gamma$  emission by  $\sim 15\%$ . (See Figure 13 which shows a chemiluminescence spectrum of the room temperature reaction, on contact with air, of  $P_4$  and  $D_2$ 0 vapors carried by a nitrogen stream. It was taken with a McPherson monochromator and an EMI 9558 QB photomultiplier. The discreet bands at 228.8-272.1 nm correspond to PO  $\gamma$  emission bands and those at 450-650 nm correspond to DPO emission.) The reason for the isotope effect is not clear. A number of possibilities exist. One of these could be an affect on the original formation of PO, since it is known that water is required for this chemiluminescence. In addition to the PO  $\gamma$  system, there is emission under certain conditions from the PO  $\beta$  system.

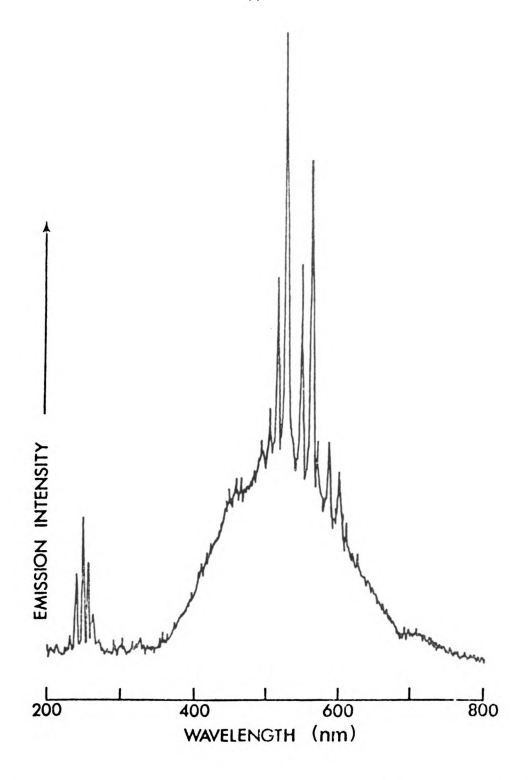


Figure 13. An ultraviolet and visible room temperature chemiluminescence emission spectrum for the gas phase reaction of  $P_4$ ,  $O_2$ , and  $D_2O$  vapors

#### 3. PO $\beta$ System

## a. Assignment

The PO  $\beta$  system consists of the transition  $B^2\Sigma^+ \to X^2\pi_r$ . The  $X^2\pi_r$  ground state, the same state to which the PO  $\gamma$  system radiates, belongs to Hund's case (a), as has been shown. The  $B^2\Sigma^+$  state of PO belongs to Hund's case (b), as does the  $A^2\Sigma^+$  state, and thus a similar branch designation is expected for both the emissions (see Figure 11). For some of the vibrational bands of the  $\beta$  system Singh has seen all twelve of the expected number of rotational branches (132).

An emission spectrum showing the PO  $\beta$  system is shown in Figure 14. (Figure 14 shows a medium resolution phosphorus chemiluminescence emission spectrum of PO  $\beta$  emission in the region 320-344 nm. It was taken at a temperature of  $\sim 300^{\circ}$ C with a Heath monochromator and RCA 1P28 photomultiplier and the first arrangement for obtaining temperature dependent emission spectra.) PO  $\beta$  emission is due to a  $B^2 \Sigma^+ \rightarrow X^2 \pi$ transition and extends from 323 to 340 nm. According to Dressler's discharge experiment there is significant emission intensity between 320 and 360 nm (48). In the present work most of the intensity for the PO  $\beta$  system is between 323 and 332 nm. The overall band system from Figure 14 appears to have a bimodal distribution, such as might occur for a (0,0) transition to the  $X^2\pi_{3/2}$  and  $X^2\pi_{1/2}$  sublevels of the ground state, and this does account for the majority of the emission. The intensity distribution is not very similar to that found by Dressler, as is seen in Table 2. This result is totally understandable in terms of the difference in the experimental conditions behind the two spectra. Even from the work of Singh (132) and Mohanty et al. (95),

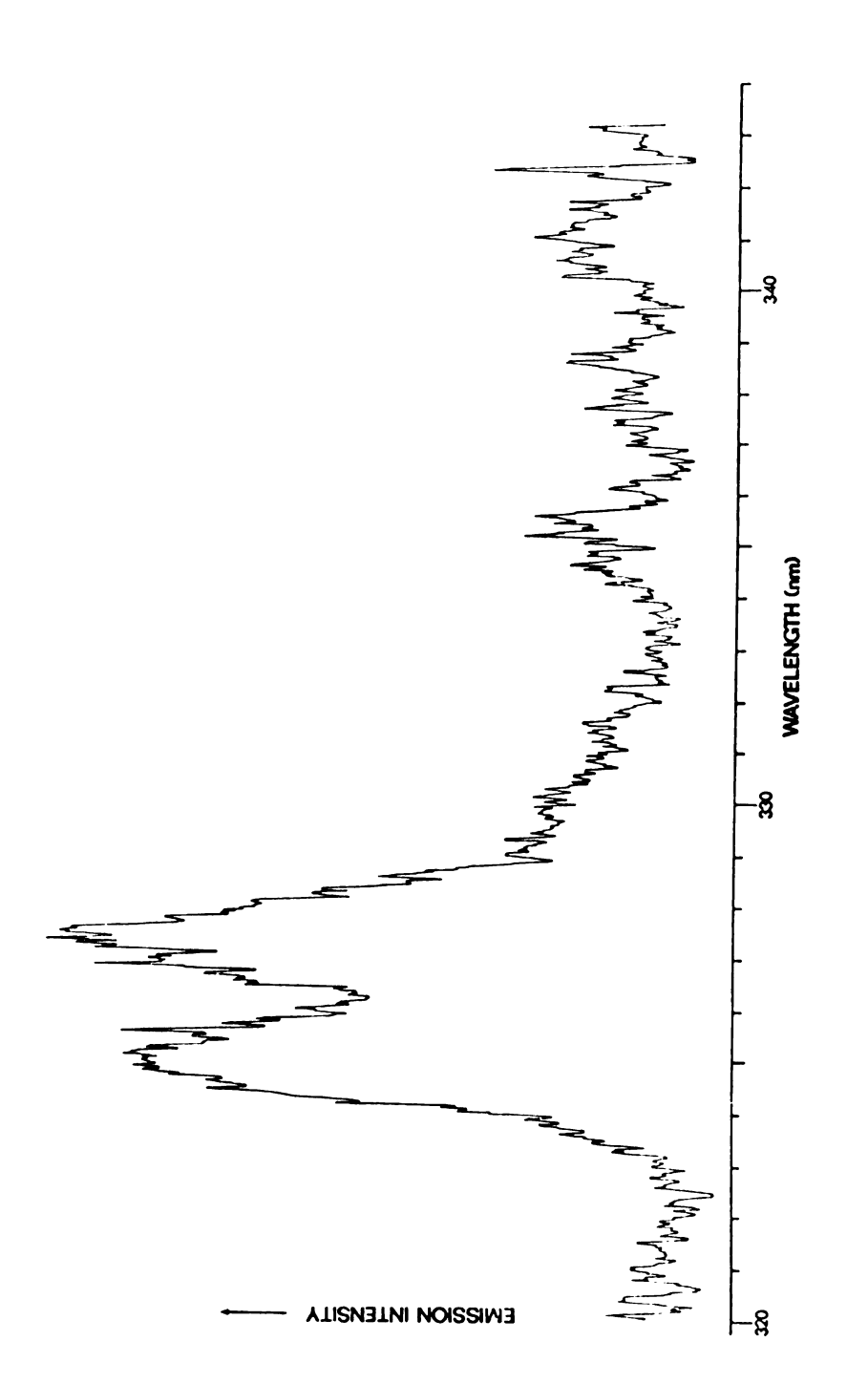


Figure 14. A medium resolution phosphorus chemiluminescence emission spectrum of the PO  $\boldsymbol{\beta}$ 

system in the region 320-344 nm

Table 2. Wavelengths of Band Heads of PO  $\beta$  Emission System

Dressler			Present Work	
Intensity	(v',v")	$\lambda_{air}^{(nm)}$	$\lambda_{air}^{(nm)}$	Intensity
2	6,5	319.873		
2	7,6	321.813	323.20	1
			3.35	1
			3.60	1
			3.75	
			3.90	3
			4.10	3
			4.15	4
			4.20	5
			4.30 (0,0)	6
10	0,0	324.621	4.65 $B^2 \Sigma - X$	$^{2}_{1/2}$ $^{7}_{9}$
			4.70	1 1/2 8
			4.80	8
			4.90	8
	1,1		5.00 (1,1)	8 8 8 8 8 8 7 7 8
			5.10	8
			5.26 $B^2 \Sigma - X^2$	π 1/2 8
8	1,1	325.529	5.50	1 4 2 7
			5.60	8
			5.70	7 6 6 5 5 5 5 5 10)2 5 13/2 6
			5.80	6
			6.05	6
			6.10	5
			6.20	5
			6.40 (9,0	), 5
			6.45 B <sup>2</sup> Σ-	$\frac{1}{1}^{2}\pi_{3/2}$
			0.30	1 3/2 6
	0,0		6.70	7
	2,2	326.856		
	0,0		6.90	9
	0,0		7.00	8
9	0,0	327.047	7.05	8
			7.20	9
			7.30	9
			7.40 (1,1)	10
			7.50 2 2	, 10
			7.55 $B^2 \Sigma - X^2$	π <sub>3/2</sub> 10
			7.60 1	10

Table 2 Continued

Intensity	(v',v")	λ <sub>air</sub> (nm)	λ <sub>air</sub> (nm)	Intensity
	1,1		327.80	8
	1,1		7.90	6
	0,1		7.95	6
			8.10	6
			8.25 8.35	5 5 3
			8.50	3
			8.60	4
			8.65	3
			8.70	2
			8.80	1
			9.05	1
			9.30	1
1	3,3	329.627	9.45	1
1	٥,٥	329.027	330.00	1
			0.10	1
			0.20	1
			0.30	1
5	5,5	330.284		
5 7	4,4	1.180		
	6,6	2.96		
7 7	5,5 7,7	2.824 4.058		
,	6,6	4.050	4.65	1
	.,.		5.30	1
			5.50	1
			5.65	1
3	8,8	6.205		
7	7,7	6.492		
6 3	0,1 8,8	7.978 8.759	8.70	1
6	1,2	8.792	8.85	1
4	2,3	9.781	- · - <del>-</del>	_
6	0,1	340.572		
2	3,4	0.98		
5 1	1,2	1.414		
	2,3	2.462		
1 1 2	5,6 7,8	6.009 7.089		
2	6,7	7.853		
2	7,8	7.089		
1	0,2	352.33		
1	1,3	3.04		
1	2,4	3.94		

who carried out rotational analyses on many of the vibrational bands, it is not possible to assign all the observed heads.

The  $\mathbf{v'}$  = 6 and 7 levels of the  $\mathbf{B}^2\Sigma^+$  states of PO are strongly perturbed by the  $\mathbf{B'}^2\pi_1$  and  $\mathbf{b}^4\Sigma^-$  states. Verma and Broida have noticed an abnormal population in these two levels (65). The two levels also have an abnormal intensity distribution in emission according to Dressler (48). In both cases the source was a relatively low pressure discharge. In Figure 15 is displayed an emission spectrum taken at room temperature and pressure that shows the (7,7)  $R_{12}$  transition of the PO  $\beta$  system at 336.5 nm to be more intense than any other of the system. (This spectrum was taken with a McPherson monochromator and RCA 1P28 photomultiplier.) It is likely that this unusually high emission intensity is due to an increased preferential population of the  $\mathbf{v'}$  = 7 level by an intersystem crossing from the  $\mathbf{b}^4\Sigma^-$  state (133). The  $\mathbf{b}^4\Sigma^- \to \mathbf{X}^2\pi_\Gamma$  transition is spin forbidden, rendering the  $\mathbf{b}^4\Sigma^-$  state a long lifetime, which in turn increases the probability of an inverse intersystem crossing.

## b. Effect of Temperature on PO $\beta$ Emission

The emission spectrum of the PO  $\beta$  system shown in Figure 14 was taken under higher than room temperature conditions. As Figures 13 and 15 show, the PO  $\beta$  system is very weak at room temperature under atmospheric pressure. The PO  $\gamma$  system appears to reach its maximum intensity under conditions such that the PO  $\beta$  system is a minimum. It is known that at low pressure the PO  $\gamma$  system is much stronger than the  $\gamma$  system (53). Moreover, it will be shown later in the excimer discussion and in the dilution experiment that our observation implying

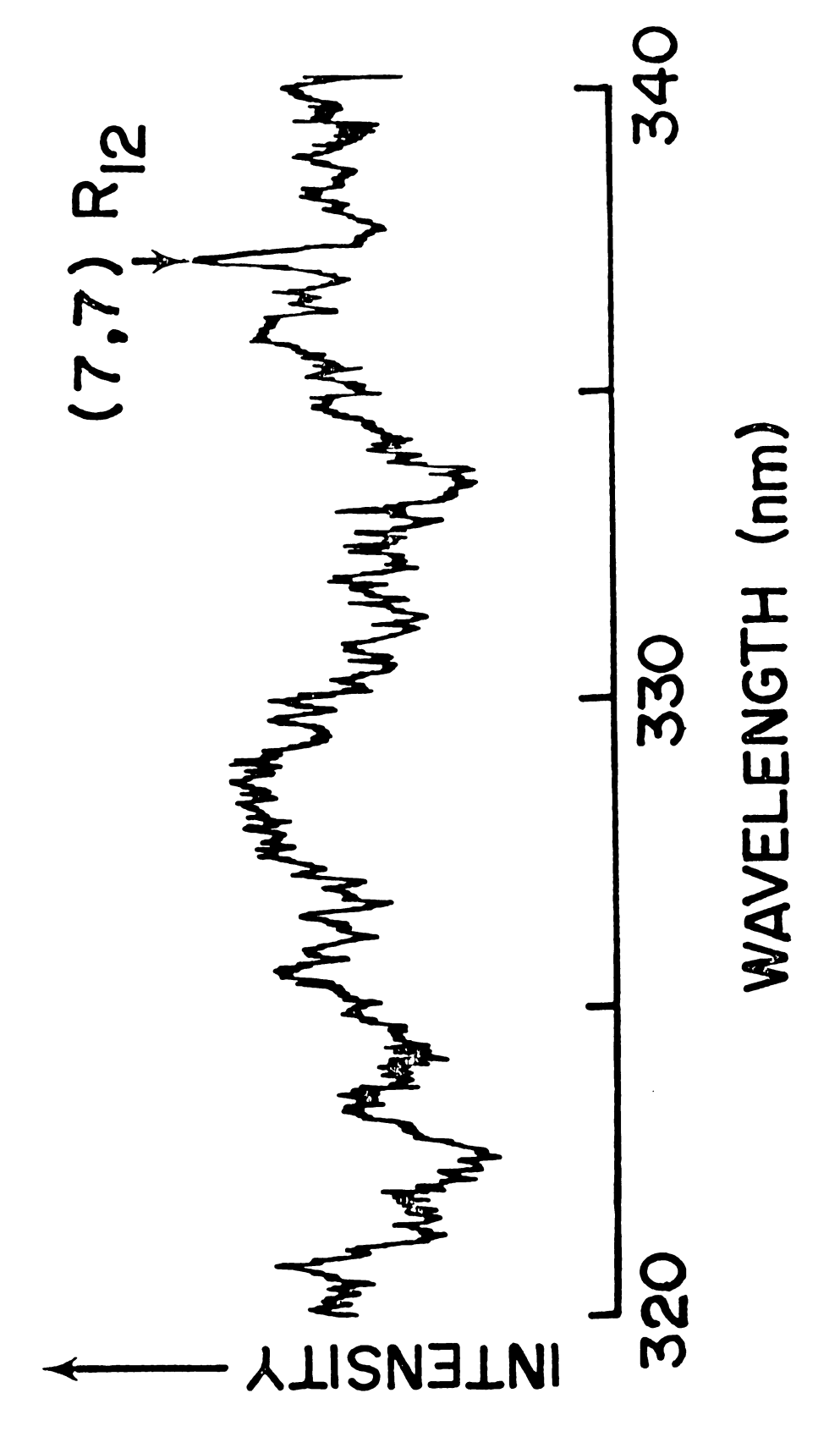


Figure 15. A room temperature phosphorus chemiluminescence emission spectrum of the PO  $\beta$ system showing an anomolously intense  $(7,7)\mathrm{R}_{12}$  transition at 336.5 nm

that the  $B^2\Sigma^+$  state is totally populated from the  $A^2\Sigma^+$  state is fortuitous. It will be shown that a plot of log (intensity) versus 1/T gives a different slope for the PO  $\gamma$  and  $\beta$  emission systems. For a series of emission spectra showing the effect of temperature on the system, where  $D_20$ and  ${\rm H_20}$  vapors were used in the  ${\rm P_L}$  oxidation, see Figures 12 and 16 respectively. Figure 16 shows temperature dependent chemiluminescence spectra for the reaction of  $P_4$  and  $H_2 O$  vapors on contact with air in a heated chamber (the second arrangement for obtaining temperature dependent spectra). The vapors were carried by a nitrogen stream. These were taken with a Heath monochromator and RCA 1P28 photomultiplier. Emission from the (0,0) transition of the PO  $\beta$  system at 320-337 nm increases dramatically with increasing temperature, which is in C<sup>O</sup>. There does not appear to be any deuterium isotope effect upon the temperature effect. A possible explanation for the temperature dependent intensity is that raising the temperature above room temperature supplies enough activation energy for intersystem crossing from the  $^4\pi_{_{\mbox{\scriptsize f}}}$  state to the  $B^2\Sigma^+$  state. Another way of stating this explanation is that a more favorable Boltzmann distribution is set up at higher temperatures between closely lying rotational and vibrational levels of the  $B^2\Sigma^+$  and  $4\pi_1$  electronic states of PO and because of the metastability of the  $4\pi_{i}$  state, higher probability of inverse intersystem crossing exists, similar to the discussion of the  $b^4\Sigma^-$  state. The weak under our experimental conditions of atmospheric pressure and this weakness is thought to be due to intermolecular coupling to populate the  ${}^4\pi_i$  state. At low pressure because of the absence of the intermolecular effects the  $B^2\Sigma^+$  state is not quenched and emits strongly.

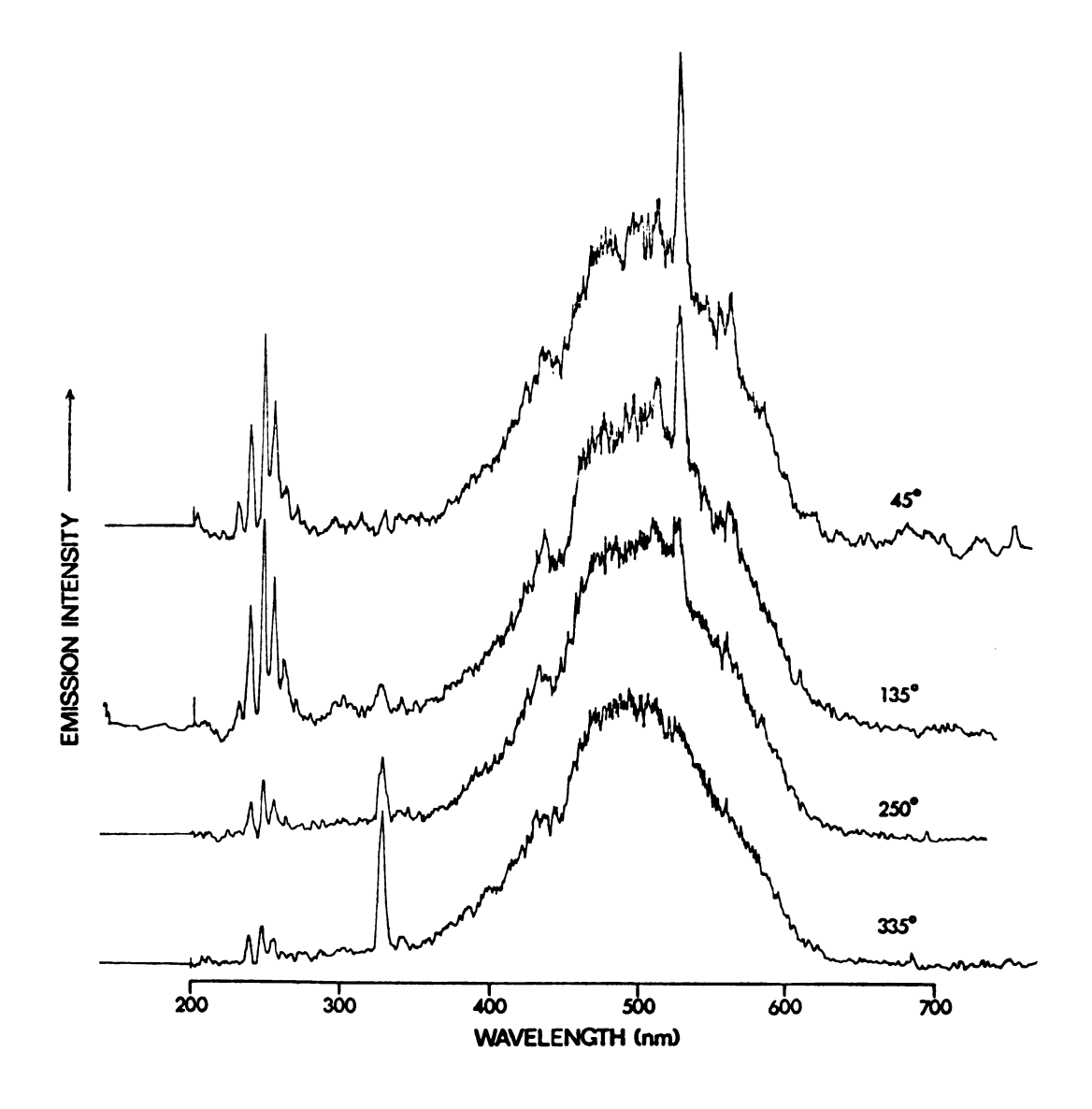


Figure 16. A series of temperature dependent chemiluminescence emission spectra for the ultraviolet and visible regions from the gas phase reaction of  $P_4$ ,  $O_2$ , and  $H_2O$  vapors

It is the  $^4\pi_1$  state that we propose is involved in the PO excimer formation, the species responsible for the visible emission continuum. Further discussion is deferred until the excimer section. Now the Dilution Experiment will be presented, showing that the  $B^2\Sigma^+$  and  $A^2\Sigma^+$  states are not directly coupled in their emissivity to the ground state.

#### c. Dilution Experiment

The emission spectra for the dilution experiment are shown in Figure 17. Both spectra were taken with a Heath monochromator and RCA 1P28 photomultiplier. Of the two spectra shown, the spectrum labeled (b) was obtained with a fixed nitrogen flow rate with the preheated  $P_4$ ,  $H_2O$ , and  $N_2$  stream and with the temperature recorded at  $\sim 300^{\circ}\text{C}$  in the middle of the flame. (See Figure 6 in the experimental section.) Spectrum (a) was taken under nearly identical conditions except that more nitrogen was added to the system. The dramatic increase in PO  $\beta$  emission with the PO  $\gamma$  emission and the continuum emission intensity remaining relatively constant confirms that the PO  $\beta$  system is not emitting at the expense of PO  $\gamma$  emission. The relationship of this spectacular increase in the PO β system emission intensity to the continuum emission intensity will be discussed later in the section dealing with the excimer formation. The next molecule to be discussed is HPO (DPO), which is possibly formed directly or indirectly from PO, (PO)2, or even (PO)\*2.

## 4. HPO (DPO)

# a. Assignment

The discrete HPO and DPO emissions have already been presented in Figures 9, 12, 13, 15, and 16 in the spectral region 450 to 700 nm.

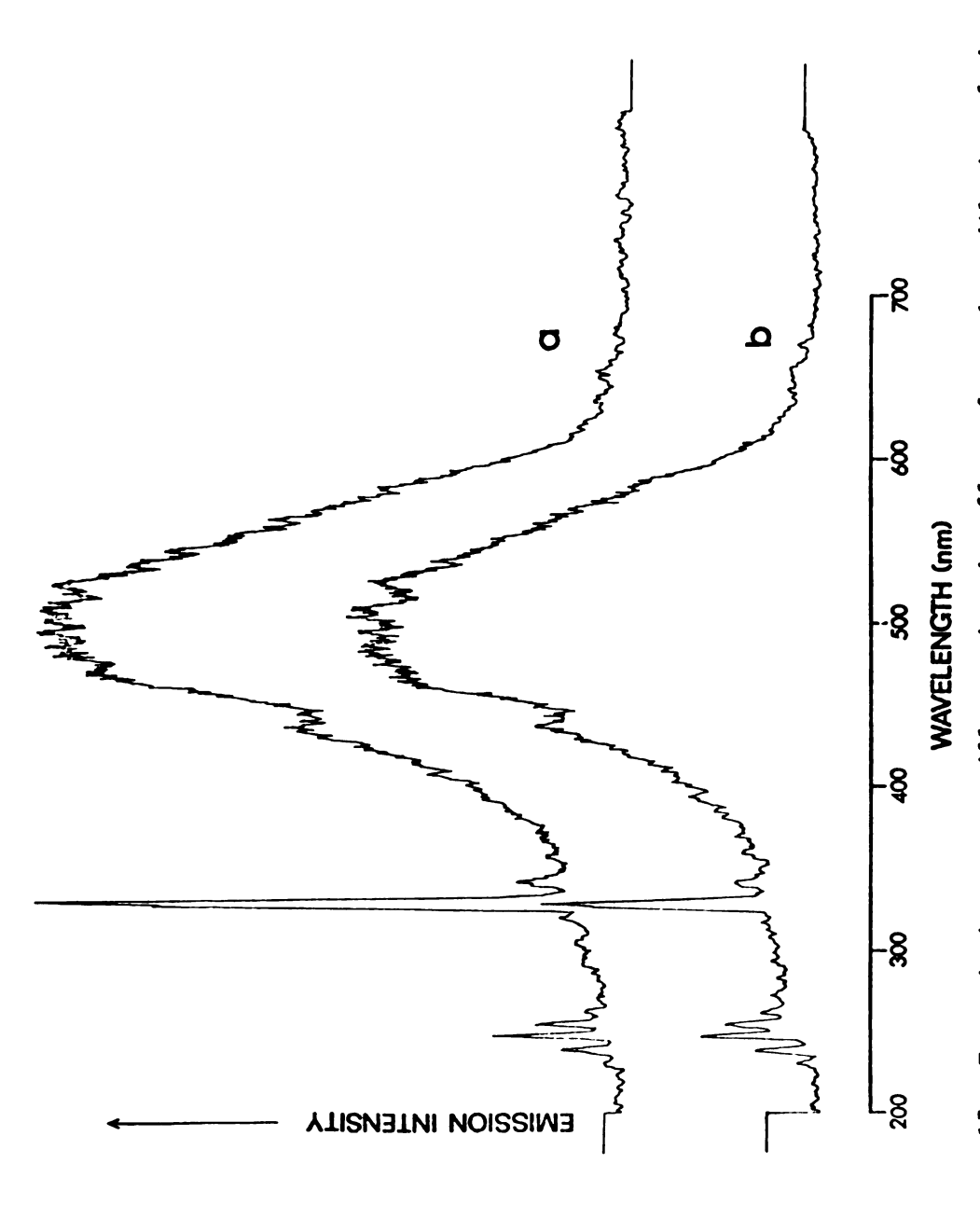
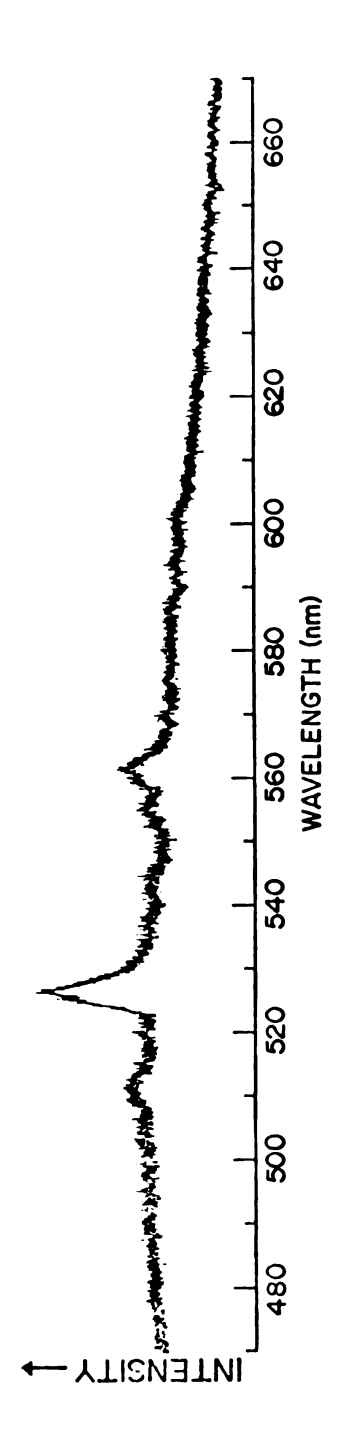
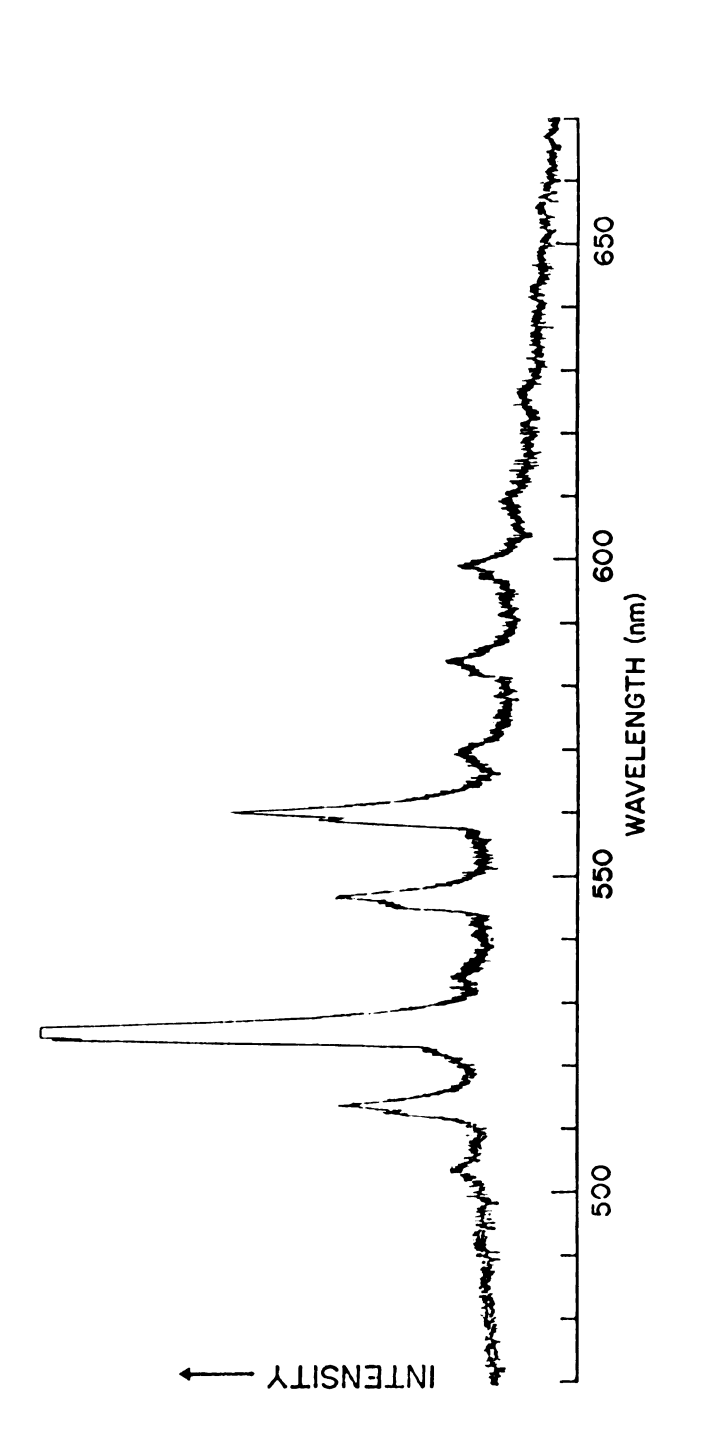


Figure 17. Two emission spectra illustrating the effect of gas phase dilution of the reaction of  ${\rm P_4},~{\rm O_2},~{\rm and}~{\rm H_2O}$  with additional  ${\rm N_2}$  buffer gas

More intense and better resolved spectra are shown in Figures 18 and 19. A McPherson monochromator and EMI 9558 QB photomultiplier were used to obtain these spectra. These two spectra were obtained under nearly identical conditions except that Figure 18 was taken with  $\mathrm{H}_2\mathrm{O}$ saturated nitrogen as the phosphorus carrier gas and Figure 19 was taken with  $\mathbf{D}_2\mathbf{0}$  saturated nitrogen. The temperature was very nearly room-temperature,  $\sim 30^{\circ}$ C, and the pressure was atmospheric. In Tables 3 and 4 are presented the observed emission wavelengths and intensities. Also included for comparison in these tables are emission wavelengths obtained by Lam Thanh and Peyron for these species in their discharge experiments under 20 mm of mercury (110). The wavelength correlation is excellent; however the intensity correlation shows a marked deviation. The difference in intensity distribution can be understood in terms of susceptibility to experimental differences. Lam Thanh and Peyron found many more bands toward the red for HPO. For DPO the difference is smaller. It is evident from Table 4 that there is more emission to the blue for DPO under ambient conditions than that obtained by Lam Thanh and Peyron in their discharge experiments. The substitution of deuterium in HPO has two effects on the emission from this species. First as expected, a frequency shift indicative of the change in mass occurs. Next, a striking effect on the intensity of the emission is seen; DPO emission is at least five times more intense than that from HPO. In addition, there is also an increase in the number of emission bands that can be counted. Aside from a difference in efficiency of generation of HPO upon isotopic substitution, the result can be explained as a decreased predissociation for DPO compared to HPO.



chemiluminescent gas phase reaction of  $\mathbf{P}_4$ ,  $\mathbf{0}_2$ , and  $\mathbf{H}_2\mathbf{0}$  vapors at room temperature A spectrum of medium resolution showing visible HPO emission produced by the Figure 18.



chemiluminescent gas phase reaction of  $P_4,\ 0_2,\ and\ D_20$  vapors at room temperature A spectrum of medium resolution showing visible DPO emission produced by the Figure 19.

Table 3. Medium Resolution HPO Emission Bands and Assignments

	T M1 . 1	1.0	110)		
	Lam Thanh and Peyron (110)			Present Work	
Intensity		$\frac{1}{v}(cm^{-1})$ -original	gin λ <sub>air</sub> (nm)		Relative
	$(v_1'', v_2'', v_3'')$			heads	Intensity
			<del> </del>		
	(001)-(000)			497.8	vw
4	(001)-(000)	19915	502.13	501.9	vw
	(002)-(010)			510.3	vw
	(002)-(010)			512.0	vw
10	(000)-(000)	19047	525.02	524.8	3
	(000)-(000)			526.3	4
6	(000)-(001)	18062	553.65	554.4	vw
	(000)-(001)			555.1	2
8	(000)-(010)	17860	559.91	559.7	2
	(000)-(010)			561.0	2 2
4	(001)-(020)	17544	570.00	567.9	2
	(001)-(020)			569.3	2
4	(000)-(002)	17091	585.10	583.9	vw
	(000)-(002)			585.9	vw
5	(000)-(011)	16879	592.45		
6	(000)-(020)	16687	599.27		
4	(001)-(030)	16386	610.28		
0	(000)-(003)	16136	619.73		
3	(000)-(012)	15912	628.46		
3 3	(000)-(021)	15 <b>713</b>	636.42		
3	(000)-(030)	15532	643.83		
1	(000)-(004)	15200	657.90		
1	(000)-(013)	14961	668.40		
1	(000)-(022)	14757	677.64		

vw = very weak

Table 4. Medium Resolution DPO Emission Bands and Assignments

	Lam Thanh and Peyron (110)			Present Work	
Intensity	$(v_1', v_2', v_3') - \overline{v}$	(cm <sup>-1</sup> )-ori; air	gin λ air (nm	) <sup>λ</sup> air(nm)-	Relative
	$(v_1'', v_2'', v_3'')$			heads	Intensity
	(001)-(000)			501.0	2
	(001)-(000)			502.5	2
	(002) - (010)			511.5	3
	(002)-(010)			512.5	4
10	(000) - (000)	19117	523.10	522.9	9
	(000)-(000)			523 <b>.9</b>	10
	(001)-(010)			531.5	2
	(001)-(010)			533.0	2
4	(000)-(001)	18367	544.46	543.9	3
	(000)-(001)			545.2	4
	(001)-(011)			555.2	2
6	(000)-(010)	17931	557.69	557.3	4
	(000)-(010)			558.5	6
1	(000)-(002)	17646	566.70	566.2	2
	(000)-(002)			568.5	
2	(000) - (011)	17191	581.70	581.0	2 2
	(000)-(011)			582.5	2
2	(000) - (020)	16759	596.69	596.5	2
	(000) - (020)			597.9	2
1	(000)-(012)	16472	607.09	607.0	1
	(000)-(012)			608.3	1
0	(000)-(021)	16028	623.91	623.3	1
	(000)-(021)			625.2	1
0	(000) - (030)	15610	640.62	640.3	vw
	(000) - (030)		- · · · · · · ·	641.5	vw
0	(000) - (022)	15305	653.38		

vw = very weak

Although predissociation will occur at nearly the same energy above the minimum of the potential curve or surface, because dissociation limits for isotopic molecules are the same, the predissociation occurs at different J or v' values (13). Also because of the greater mass of the deuterium atom, less tunneling below the intersection of the two crossing potential curves or surfaces will occur. This results in fewer radiationless transitions via predissociation and thus more emission. In addition to the isotopic effect, there is also an apparent temperature effect.

#### b. Temperature Effect on HPO(DPO) Emission

In Figures 12 and 16 are displayed the dependence of chemiluminescent emission intensities upon temperature. There appears to be a reduction in HPO and DPO emission intensity with increasing temperature over 130°C. We assumed that radiationless processes in the different species are similarly effected by temperature, and normalized the HPO and DPO emission intensities to 130°C for both lower and higher temperatures. 130°C was chosen because at this temperature there is a maximum in emission intensities. Normalization was done in luminous flux. After normalization the apparent decrease in HPO and DPO emission intensity as a function of temperature is not significant, the emission becoming more widely distributed over more roto-vibrational levels of the excited state. An activation energy plot of HPO and DPO normalized emission is shown in Figure 20. (Figure 20 shows plots of log(intensity) versus 1/T for (a) PO  $\beta$  system (0,0) emission; (b) PO  $\gamma$  system emission; and (c) HPO(DPO)  $^{1}A'' \rightarrow ^{1}A'$  emission. Intensity values were derived from temperature dependent chemiluminescence spectra for the reaction on

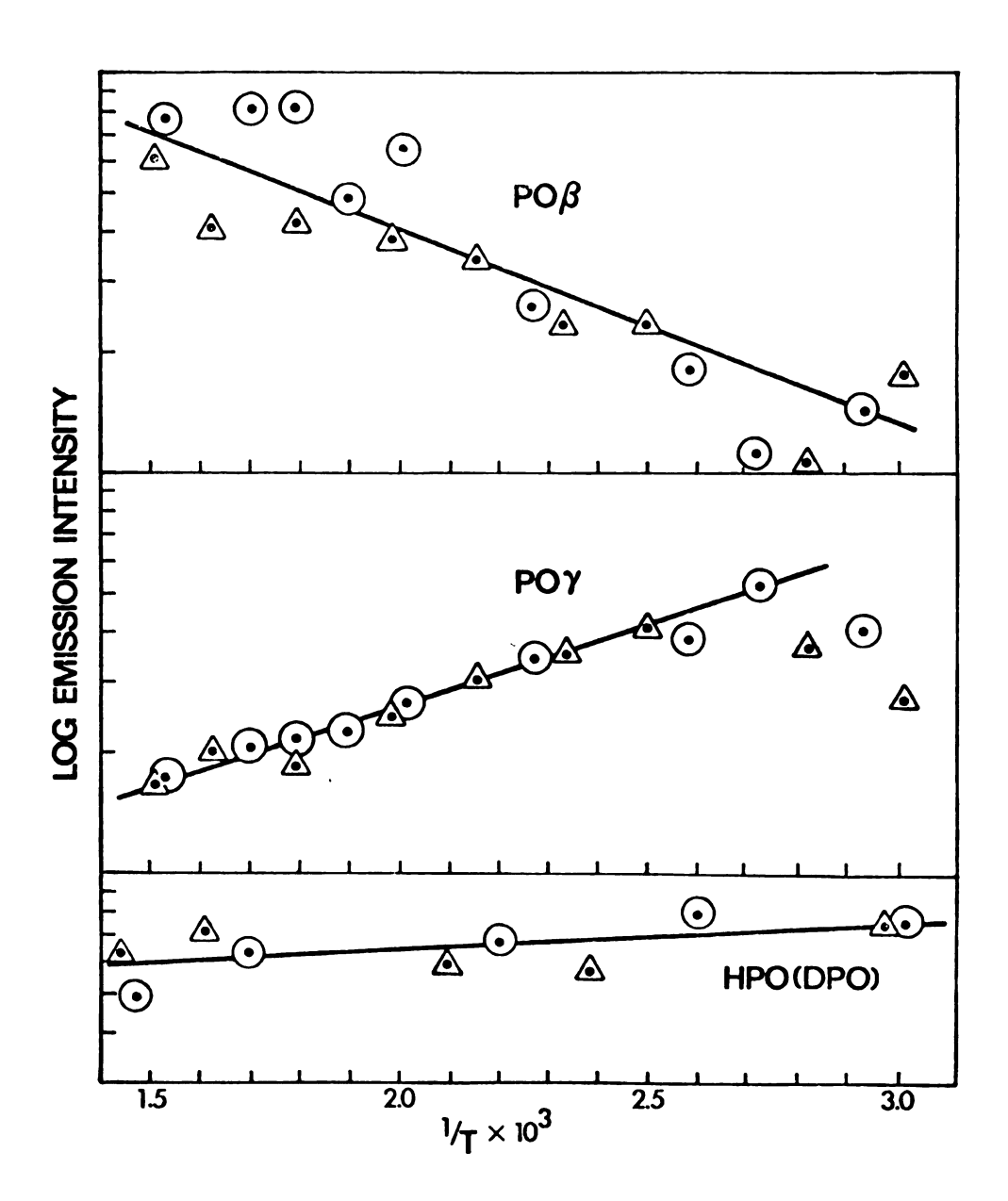


Figure 20. Plots of log(intensity) versus 1/T for a) PO  $\beta$  system (0,0) emission; b) PO  $\gamma$  system emission; and c) HPO(DPO)  ${}^1\!A'' \to {}^1\!A' \text{ emission}$ 

contact with air of  $P_4$  vapor and  $H_2^0$  vapor (triangular points) or  $D_2^0$  vapor (circled points) carried in a heated nitrogen stream (the first method of obtaining temperature dependent emission spectra). They were taken with a Heath monochromator and RCA 1P28 photomultiplier. The data were normalized with respect to total luminosity.) It is seen that HPO and DPO behave very similarly over the temperature range  $30\text{--}400^{\circ}\text{C}$ . The value of the slope is  $107 + 47 \text{ cm}^{-1}$ .

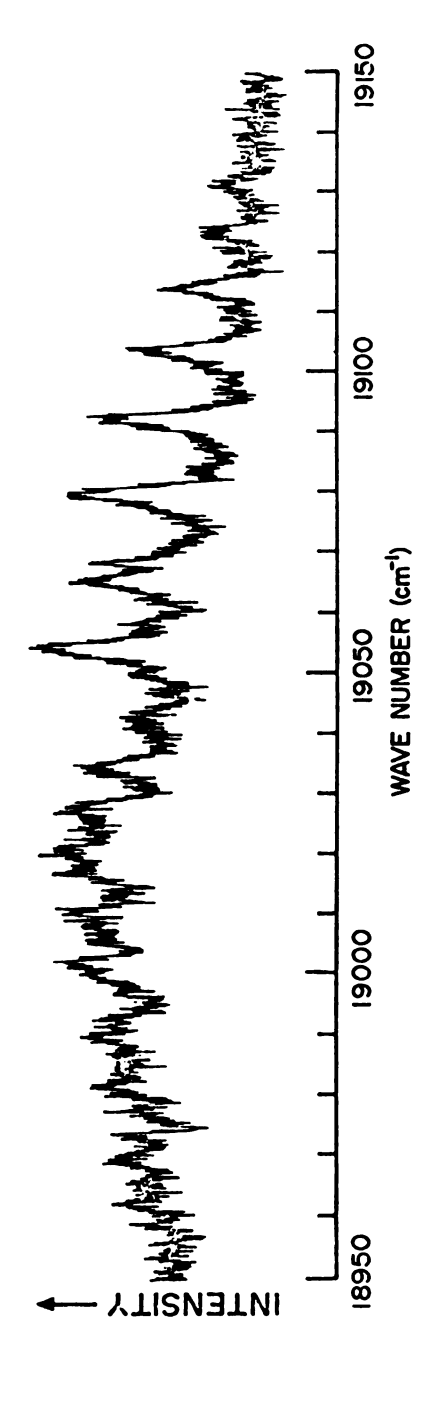
# c. Attempt at Rotational Analysis

An attempt was made to rotationally resolve the <sup>1</sup>A"(0,0,0) → <sup>1</sup>A'(0,0,0) transition of HPO and DPO emission by recording the spectrum on a 3/4 meter Spex 1401 Spectrometer and RCA C31034 photomultiplier with single photon counting ability. At medium resolution each emission band was double headed. At higher resolution each of these bands could be further resolved into smaller heads, but the resolution was not sufficient to individually resolve the rotational lines. The further resolved spectra are shown in Figures 21 and 22 and the wavenumbers and intensities of the heads are shown in Tables 5 and 6 for HPO and DPO respectively. A number of times we have alluded to the continuum underlying the HPO and DPO emission. Although this continuum can be seen in Figures 21 and 22, it is best seen in Figures 9, 12, 13, 16, and 17.

#### 5. The Continuum

#### a. General Characteristics

In general a continuum emission, which starts at about 335 nm, extends into the near-infrared and peaks at about 520 nm, dominates the visible portion of the emission spectrum of the phosphorus chemiluminescence



A spectrum of the partially resolved  $^1A''$  (0,0,0) +  $^1A'$  (0,0,0) transition of HPO Figure 21.

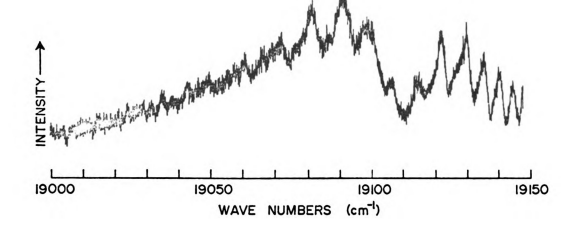


Figure 22. A spectrum of the partially resolved  $^1A''(0,0,0) \to ^1A'(0,0,0)$  transition of DPO

.

Table 5. Wavenumbers of Rotational Heads for the  ${}^{1}A''(000) \rightarrow {}^{1}A'(000)$  of HPO

Intensity	√(cm <sup>-1</sup> )	(Designation of Lam Thanh and Peyron)	Branch	K', K"
2	19130.5			
2	123.0			
3	113.7			
4	103.8		R	6,5
5	092.7		R Q	5,4 6,5
1	084.0		R	4,3
4	079.0		Q R	5,4 3,2
3	068.0		Q	4,3
4	065.0		R Q	2,1 3,2
5	054.0			
1	049.5		R	1,0
1	042.5			
2	034.6		Q	2,1
2	026.8		R Q	0,1 1,0
1	019.6		P	1,0
1	016.8		Q	0,1
2	19009.8			

Table 5 Continued

2	19002.0		
1	18989.6	Q	1,2
1	981.5	P	1 2
1	973.5	Q	1,2 2,3
1	969.0	P	2,3
1	965.4		
1	962.0	Q	3,4

Table 6. Wavenumbers of Rotational Heads for the  ${}^{1}A''(000) \rightarrow {}^{1}A'(000)$  of DPO

Intensity	$\overline{v}(cm^{-1})$	
2	19144.8	
3	140.5	
4	135.9	
5	130.2	
4	122.0	
1	114.1	
1	106.7	
2	098.5	
4	091.0	
3	081.0	
2	072.0	
1	065.7	
1	060.3	
1	049.0	
1	042.2	
1	19034.3	

under ambient conditions. Experimental results summarized in Figures 9, 12, 13, 16, and 17 were obtained with either a RCA 1P28 or an EMI 9558 QB photomultiplier. In Figure 23 is given the near-infrared emission spectrum. In Table 7 are shown wavelengths and intensities from band heads observed upon the continuum in the near-infrared. Wavelengths, intensities, and assignments from Verma et al. (69) are also given for comparison. The spectrum was taken with a cooled RCA 7102 photomultiplier and a Bausch and Lomb 0.25 meter (f = 3.5) monochromator with a grating of 675 lines per mm and blazed at 1.0  $\mu$ . With this fast optical detection system emission is seen to extend to 1.2  $\mu$ . An understanding of the origin of this visible and near-infrared continuum was slow and long in coming.

### b. Two Cases Resulting in Continuous Emission

Emission continua from molecules result from radiative transitions to or from a repulsive electronic state. Transitions from a repulsive state will be considered first. This case, the recombination of atoms, has already been discussed in the section on Examples of Chemiluminescent Reactions According to Complexity of Description. Because the kinetic energy of the colliding atoms may have a range of values, the emission which results from a transition to a lower bound electronic state is a continuum. It did not prove possible to resolve the apparent continuum in the spectrum of the phosphorus chemiluminescence. We are therefore interpreting it as true continuous emission.

Although important to astrophysical interpretations, the intensity of emission from two-body recombination at ordinary pressures is very weak for two reasons. First, this emission is weak because only one

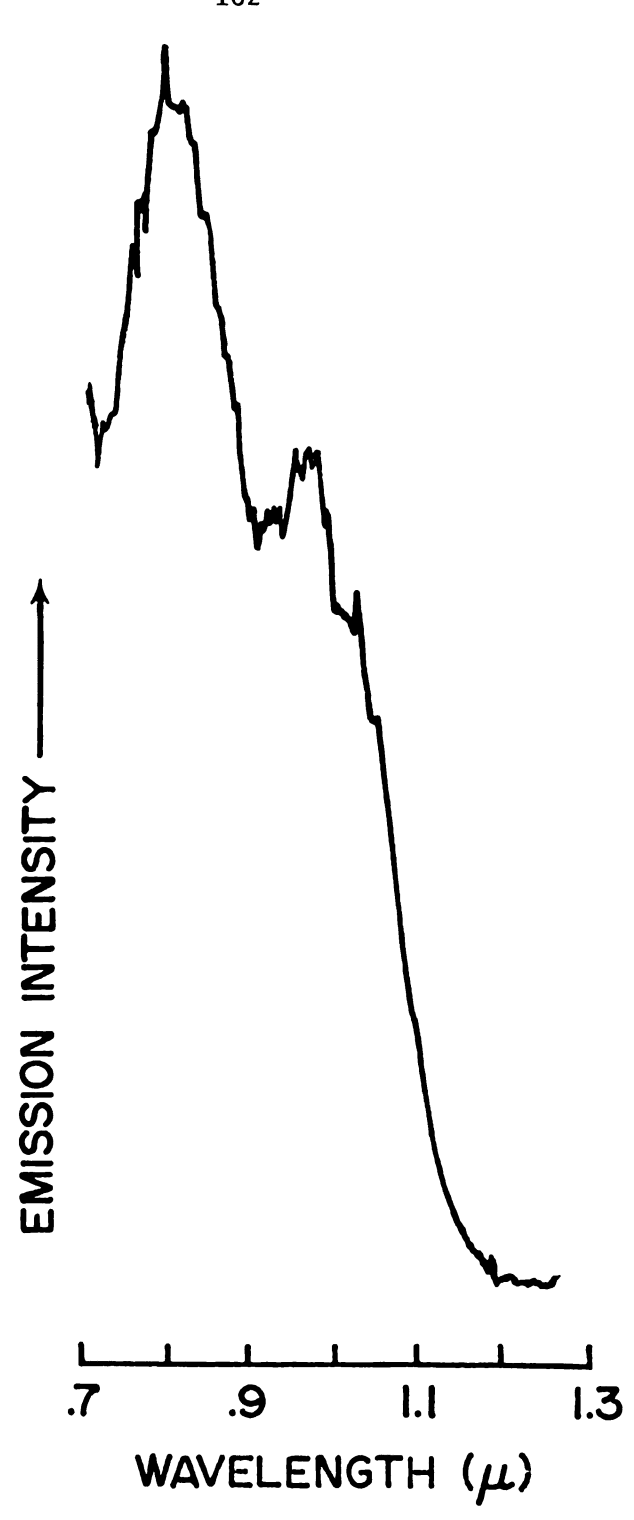


Figure 23. A low resolution chemiluminescence emission spectrum of the near-infrared 0.7 to 1.3  $\mu$  region

Table 7. Wavelengths of Band Heads of PO(A,F, $G^2\Sigma^+\to A,B^2\Sigma^+$ ) Emission in Near-Infrared

Verma and Jois (69)			Present Work	
(v',v")	Transition	λ <sub>air</sub> (μ)	λ <sub>air</sub> (μ)	Relative Intensity
7 <b>,</b> 5	A→B	0.72660	0.724	7
0,5	F→B	0.73238	0.734	7
6,4	A→B	0.74362	0.750	8
5,3	A→B	0.75794	0.756	8
4,2	A→B	0.77190	0.775	9
3,1	A→B	0.78554	0.783	9
2,0	A→B	0.79914	0.797	10
5,4	A→B	0.82390	0.810	10
2,2	G→A	0.82458	0.822	10
1,1	G→A	0.82607	0.830	9
0,0	G→A	0.84124	0.837	8
3,2	A→B	0.86062	0.860	7
3,0	F→A	0.86131	0.870	7
2,1	A→B	0.87868	0.875	7
1,0	A→B	0.89645	0.890	7
			0.900	6
			0.912	6
			0.918	6
			0.924	6
			0.930	6
			0.956	6
2,2	A→B	0.97369	0.968	6
1,1	<b>A</b> →B	0.99823	0.994	6
			0.998	5
			1.000	5
			1.008	5
			1.016	5
0,0	A→B	1.02274	1.024	5
			1.030	5
3,4	A→B	1.05484	1.045	4
2,3	A→B	1.08853	1.080	2
			1.100	1
1,2	A→B	1.12269	1.130	1

in  $10^4$  or  $10^5$  collisions can result in recombination. Secondly, it is usually a requirement that one of the two colliding atoms is excited. If the two atoms approach along the ground state potential curve the probability of radiation resulting in the visible or ultraviolet is negligible because the principal selection rule for vibrational transitions is  $\Delta v = \pm 1$ . The probability of  $\Delta v$  being large enough to bring the emission into the appropriate spectral region is vanishingly small. Also, in general an intraconfigurational transition has a very low oscillator strength. Thus, this type of reaction, which would lead to emission continua, is of very little interest in the present case.

In contrast to the case in which the upper state is unbound is the second case in which the lower electronic state is unbound. In general, the second case results in stronger continuum emission than the first case. We attribute the observed phosphorus chemiluminescent visible continuum to processes depicted by the latter situation.

Reasons for this interpretation will be discussed shortly, but first the process will be more fully described with additional examples.

A plot of the potential energy vs internuclear distance for a repulsive state is asymptotic to both the horizontal and vertical axes. Transitions take place from the bound upper state from various vibrational levels to points on the lower, asymptotic, dissociative potential curve. The products of the dissociation separate with kinetic energies that depend upon the height of the points above the zero of energy. If the part of the curve corresponding to the points at which the transitions end is steeply rising, then the spread of the continuum will be large. A good example of such a case is that of the lowest

excited triplet state of diatomic hydrogen (134). The transition from the bound  ${}^3\Sigma^+_{\phantom{1}}$  to the  ${}^3\Sigma^+_{\phantom{1}}$  state is dissociative because the  ${}^3\Sigma^+_{\phantom{1}}$  state is repulsive. This results in a continuum extending from 160 to 500 nm. Another example, and one which is probably an ideal case of an excimer emission, is that of the helium molecule (135). It is well known that two helium atoms in their ground states repel each other and do not form a diatomic molecule. On the other hand, an excited state helium atom and a ground state helium atom form a stable diatomic species that exists as long as the molecule resides in this state. Transitions between the bound excited state and the repulsive ground state of He $_2$  result in a continuous emission from 60 to 100 nm. A dissociative ground state entity with a bound excited state resulting in a strong continuous emission is the model which best fits the experimental evidence for the phosphorus visible chemiluminescent continuum. Reasons for this interpretation will now be discussed.

### c. The PO Excimer

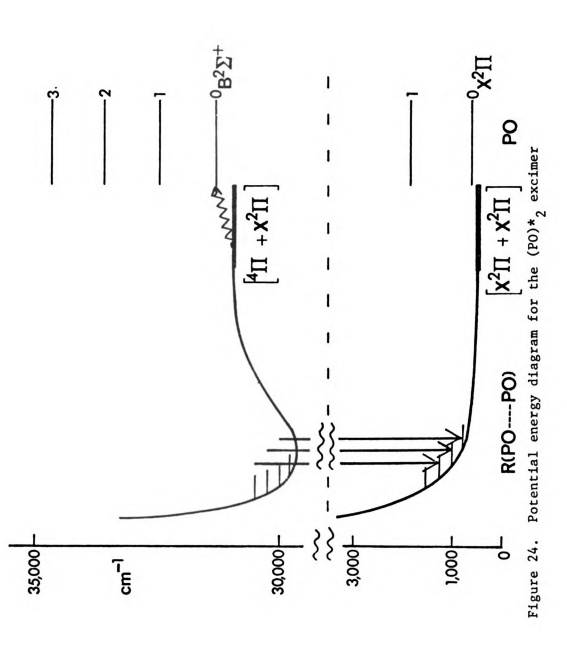
An excimer is an excited state dimer with a bound excited state and a dissociative ground state. We postulate that the visible continuum in phosphorus chemiluminescence is due to a PO excimer. A PO molecule in an excited state forms a metastable dimer,  $(PO)*_2$ , with a ground state PO. We propose that this species  $(PO)*_2$ , results from the collision of two PO molecules, one of which is ground state  $PO(X^2\pi_r)$  and the other  $PO(^4\pi_i)$ . The formation is reversible in that thermal dissociation of this excimer results in excited state PO emission. The  $^4\pi_i \to X^2\pi_r$  transition is forbidden and the only other nearby PO electronic state is  $B^2\Sigma^+$ . Figures 12 and 16 show the dramatic increase in

PO  $\beta$  emission with increasing temperature. Figure 24 shows the experimentally determined potential diagram for the excimer showing the dissociative ground state and the stabilized excited state of the excimer. The relative energies of the PO monomer states are shown on the right hand side. Energies for constructing this diagram were determined in this temperature study. It is seen that thermal dissociation of the excimer leads to one PO molecule being in the  $^4\pi_1$  state, from which a distribution can be set up into lower vibrational levels of the PO(B $^2\Sigma^+$ ) electronic state. This is shown in Figure 24 and by the equation

$$(PO---PO) \stackrel{?}{\leftarrow} PO(^{4}\pi_{i}) + PO(X^{2}\pi_{r}) \stackrel{?}{\leftarrow} PO(B^{2}\Sigma^{+}) + PO(X^{2}\pi_{r}) \rightarrow 2PO(X^{2}\pi_{r}) + h\nu.$$

(1) Determination of the PO Excimer Dissociation Energy The depth of this excimer well was obtained from the temperature study, emission spectra of which are shown in Figures 12 and 16. By plotting log (PO  $\beta$  photon flux) versus the inverse absolute temperature a value of the binding energy of the excimer could be obtained. The data are shown plotted in Figure 20. The binding energy is determined from the slope and is  $846 \pm 200 \text{ cm}^{-1}$ . (The fact that the slope for the PO  $\gamma$  system emission is  $650 \pm 26 \text{ cm}^{-1}$  further indicates that the two systems are not directly coupled.) The data were analyzed by using the least squares method of the KINET program (136).

The energy obtained in this manner is not exactly the dissociation energy because the internal energies of the species involved have not been taken into account (137). The complete, correct formulation for the system at equilibrium is as follows (138).



$$(PO) \star_2 \stackrel{\rightarrow}{\leftarrow} PO (B^2 \Sigma^+) + PO (X^2 \pi)$$

$$\frac{I_{PO \beta}}{I_{excimer}} = (constant) \frac{N_{PO (B^2 \Sigma^+)}}{N_{(PO) *_2}} = \frac{q_{PO (B^2 \Sigma^+)}}{q_{(PO) *_2}}$$

where I is the symbol for photon flux, N is the symbol for numbers of molecules and  $q = q_t q_r q_v q_e$ , where q is the overall partition function and is the product of the translational, rotational, and electronic partition functions.

$$q_{t} = \left[\frac{2\pi(\Sigma_{i}^{m_{i}})_{kT}}{h^{2}}\right]^{3/2} V$$

$$q_{r} = \frac{\pi^{1/2}}{\sigma} \left(\frac{T^{3}}{\Theta_{A}\Theta_{B}\Theta_{C}}\right)^{1/2} - \text{ for high temperature (classical)}$$

$$q_{v} = \frac{n'}{\pi} \left(\frac{e^{-\theta i/2T}}{1 - e^{-\theta i/T}}\right)$$

$$q_{e} = \sum_{i} \omega_{e^{-\epsilon e i/kT}} e^{-\epsilon e i/kT}$$

giving

$$\frac{I_{PO}}{I_{(PO)}}_{2} * = \left[\frac{\frac{\text{constants}}{\text{constants}}(T)^{3/2}(T)^{1/2} \left(\frac{e^{-\theta i/2T}}{1-e^{-\theta i}PO/T}\right) \left(\frac{e^{-\theta i/2T}(PO)}{e^{-\theta i/2T}(PO)}\right)^{-1} e^{\text{Do/kT}}\right] ^{1/2}$$

$$= (\text{constant}) (T) \left[\left(\frac{e^{-\theta i/2T}}{e^{-\theta i/2T}(PO)}\right) \left(\frac{e^{-\theta i/2T}(PO)}{e^{-\theta i/2T}(PO)}\right)^{1/2}\right] ^{1/2} e^{\text{Do/kT}}$$

In these equations  $^{\rho}$  is the symbol for density, m is the mass, V is the volume, k is the Boltzmann constant, h is Planck's constant, T is the absolute temperature,  $\sigma$  is the symmetry number and is the number of indistinguishable configurations a molecule can assume in space,  $\Theta_{A} = (h^{2}/8\pi^{2}I_{A}k), \text{ etc., } I_{A}, I_{B}, I_{C} \text{ are the principal moments of inertia}$  of a molecule,  $\theta_{1} = h\nu_{1}/k$  where  $\nu_{1}$  are the vibrational frequencies of a molecule of which there are n' frequencies, and  $\omega_{1}$  is the electronic degeneracy for state i and  $D_{O}$  is the dissociation energy for a given electronic state where the zero of energy is the dissociated excimer, and the depth of the potential minimum is  $D_{e}$ . For  $q_{e}$  usually only the first term is important, if any at all are.

The use of this equation presumes a state of equilibrium in translation, vibration, and rotation. The fact that the system under study is not at equilibrium but is at steady state nullifies the use of this equation for an exact excimer dissociation energy. It appears that the best solution is to treat the population in the two electronic states, the  $B^2\Sigma^+$  for the monomer PO and an unknown state for the excimer, as two Boltzmann energy levels, and ignore the internal energies of the two species. As in all dissociations, entropy will favor the monomer side of the conversion and energy will favor the excimer. What is assumed is that vibrational relaxation is very rapid for the excimer in order that the energy difference being monitored by the temperature study is the difference between the zero point vibrations of the two electronic states involved and not something much less. It is quite likely that this assumption holds, as some of the

vibrational spacings are of the order of only 100 cm<sup>-1</sup> as for (NO)<sub>2</sub>. For (NO)<sub>2</sub> the fundamental harmonic frequencies are 167, 196, 262, 478, 1788, and 1860 cm<sup>-1</sup> (137). The first is a torsion, the last two N-O stretches, and those inbetween N-N and O-O stretch, wag, and rocking frequencies. It is because an exact or empirical expression is lacking which relates transition probability, internal conversion, and electronic, vibrational and rotational degeneracies to the excimer dissociation energy, Boltzmann factors, and the emission intensities from the two species involved that the following simple, inexact expression was used to obtain the excimer dissociation energy:

$$I_{PO \beta}/I_{excimer} = constant e^{-D_o/kT}$$
.

If the data are normalized to a constant total photon flux, which was done in this case and which in essence is making  $I_{excimer}$  a constant, then a plot of log  $(I_{PO-\beta})$  versus (1/T) will yield  $D_O$ .

#### (2) Necessary Properties of the PO Excimer

In addition to thermal effects, the gas phase excimer and monomer should exhibit pressure effects and concentration effects upon their emission intensities. There is a very significant effect on concentration or dilution, as it will be referred to here. As shown in Figure 16, previously described in the section on the  $\beta$  system of PO, dilution of the gas phase reaction sphere with more nitrogen while keeping the temperature constant has a very striking effect: the PO  $\beta$  system intensity is greatly increased while the intensities of the other systems remain relatively constant. Concerning the species responsible for the continuum emission, this dilution experiment eliminates one of them, as will now be shown.

Some investigators have assigned the continuum to  $P0*_2$  (50,53) by analogy to  $N0_2$  where one of the reactions  $N0 + 0 + M \rightarrow N0*_2 + M$  (139-141),  $N0 + 0 \rightarrow N0*_2$  (142), or  $0 + N_20_2 \rightarrow N0*_2 + N0$  (116) gives rise to a diffuse continuum. However, the analogy does not carry over; thermal dissociation of  $N0_2$  does not give excited state N0 emission. The fact that upon thermal dissociation of the PO excimer almost all the emission in the PO system is due to the (0,0) and (1,1) transitions indicates that the PO  $B^2\Sigma^+$  state is probably not being populated from a higher electronic state but from one which is slightly lower in energy. The thermal effect as well as the buffer effect clearly eliminate the possibility that the two body recombination reaction  $P0 + 0 \rightarrow P0*_2$  or the three body recombination  $P0 + 0 + M \rightarrow P0*_2 + M$  is responsible for the reaction continuum.

Another method of changing the effective concentration for a constant flow rate of reactants is by changing the pressure. At low pressures the collision frequency of PO molecules, excited and ground state, will be less than at higher pressures. Thus the probability of excimer formation should be less if this model is true. Although we have only one spectrum which was obtained at less than atmospheric pressure – at a pressure of 0.1 torr – it shows a reduced continuum intensity and quite intense  $P_2$  emission. This spectrum will be shown in the section on low pressure work. Others, working at pressures of a few torr, have observed a weakened continuum relative to atmospheric pressure, a strong PO  $\beta$  system intensity, and a weak PO  $\gamma$  system emission intensity (53,65). Thus the low pressure requirements of the excimer model are upheld.

Because the ground state of an excimer is dissociative, there should exist no ground state absorption of the species. Although the evidence against an obtainable excimer absorption spectrum is not conclusive, none has been obtained in the present work to this time despite many attempts. Some of these attempts were made with a long pathlength apparatus consisting of 73 chemiluminescent flames in a row, each proceeding out of a hole 1.0 mm in diameter. The holes were 6.3 mm center to center. The estimated pathlength through the chemiluminescent flames was approximately 40 cm. With light sources ranging from a 75 watt xenon lamp to a 1000 watt xenon lamp, with direct illumination or illumination through a 0.25 meter Bausch and Lomb or 0.5 meter Heath monochromator, with a wide range of slit widths in order to give a wide range of intensities, no absorption spectrum could be obtained.

In addition to the excimer, the species HPO and PO should exist in the flame and discrete absorption spectra should have been obtained for them. It has been reported that absorption spectra of the PO  $\gamma$  and PO  $\beta$  systems have been obtained in a flash photolysis of phosphine and oxygen (103), but to this time none have ever been obtained for HPO or DPO. Thus, the fact that an absorption spectrum of the excimer could not be obtained is not conclusive evidence that such a spectrum does not exist.

According to the excimer model, the energy difference between the monomer emission and the on-set of the continuum should correspond closely to the binding energy of the excimer in the excited state. We call  $\Delta \overline{\nu}_{g}$  the ground state stabilization energy of the PO dimer with

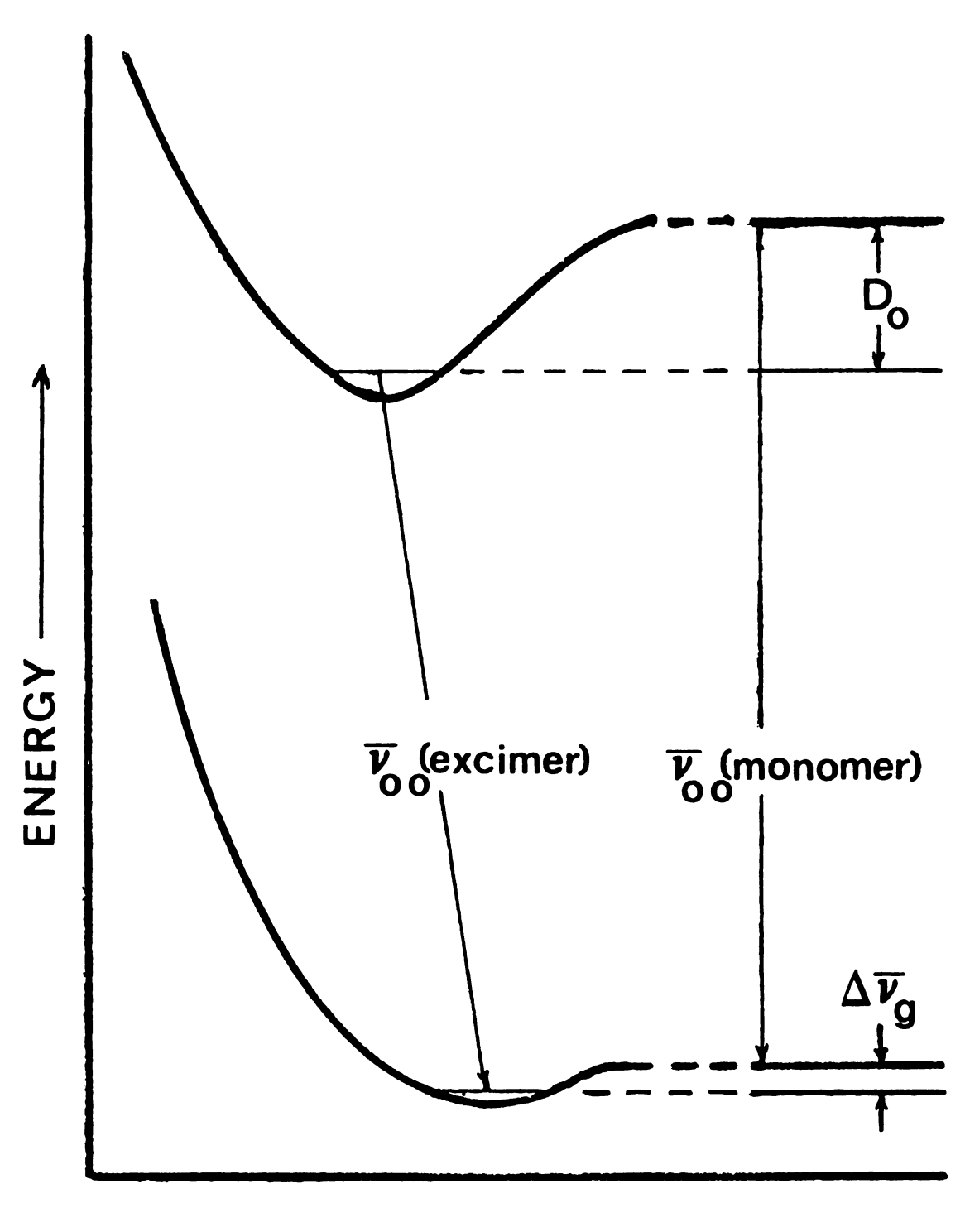
respect to monomer states. We designate  $\overline{\nu}_{00}$  (excimer) as the onset of the continuum excimer emission at the lowest temperature. From Figure 9  $\overline{\nu}_{00}$  (excimer) = 29850 cm<sup>-1</sup>. Temperatures lower than  $\sim 30^{\circ} \text{C}$  were not used, but the on-set of the continuum does not move to wavelengths lower than 335 nm until fairly high temperatures (200°C or higher); therefore, we can consider 335 nm to be the wavelength of the (0,0) emission. The value of  $\overline{\nu}_{00}$  (PO  $\beta$  system) is 30805 cm<sup>-1</sup> for the  $B^2\Sigma^+$  -  $X^2\pi_{1/2}$  sub-band. Because it is the higher energy sub-band it will be used as the limiting case for determining the maximum possible binding energy in the ground state of a PO dimer. It should be true that

$$\Delta \overline{\nu}_{g} = \overline{\nu}_{oo}(PO \beta) - \overline{\nu}_{oo}(excimer) - D_{oo}$$

where D<sub>o</sub> is the excimer dissociation energy of the stabilization of the excited state of the excimer with respect to the monomer states. See Figure 25 which shows a generalized potential energy diagram modified from Mataga et al. (143) for an excimer, illustrating the relations between various energies. As stated above, from temperature studies D<sub>o</sub> was found to be  $846 \pm 200 \text{ cm}^{-1}$ . With the above values  $\Delta v_g = 109 \pm 200 \text{ cm}^{-1}$ . Within the experimental limits it is seen that the ground state of the dimer is clearly dissociative. Only at temperatures much lower than room temperature could an associated ground state dimer of PO possibly be observed.

By analogy with  $NO_2$  and HONO the continuum in the near ultraviolet region in phosphorus chemiluminescence has been attributed to HOPO (53) in addition to  $PO_2$ . However, our experimental results do not

Figure 25. A generalized potential energy diagram for an excimer illustrating the origins of various energies



DISTANCE BETWEEN MONOMERS

support this attribution. Figure 26 shows a spectrum obtained by drying all the reactants fairly well, but not well enough to completely inhibit the reaction. (Taken with a McPherson Monochromator and EMI 9558 QB photomultiplier). It is seen that the spectrum shows a pronounced continuum relative to the PO  $\gamma$  emission. The HPO emission is practically non-existent and, because the spectrum was taken at room temperature, the PO  $\beta$  system emission is also essentially absent. The fact that the continuum is not shifted, changed in shape, or reduced in intensity indicates that the continuum is not due to the emission of any proton containing species. This rules against the involvement of HOPO and fits in with the excimer model very well.

Although the continuum of phosphorus chemiluminescence is not due to HOPO, and although there is not known to exist an (NO)\*2 excimer, there does exist an (NO)2 dimer. Gaseous (NO)2 has been characterized in the ultraviolet (137) and infrared (144). The association and dissociation of the NO dimer has been used by some to explain the rapid vibrational relaxation of NO (145), which is about 10<sup>4</sup> times more efficient than for similar molecules. Others (146-147) explain the rapid vibrational relaxation by a dipole-dipole interaction mechanism for energy transfer such as is used in excition theory (148) and in Forster theory (149). NO dimers have been detected in mass-spectrometric samplings of expanding NO jets (150,151). The structure is a near rectangular cis configuration (144). The weak bonding in NO dimer arises from electron pairing and involves overlap of p orbitals between both nitrogen and oxygen atoms (152,153). It is an oxygen bond that fixes the molecule into the rectangular shape. The binding energy of

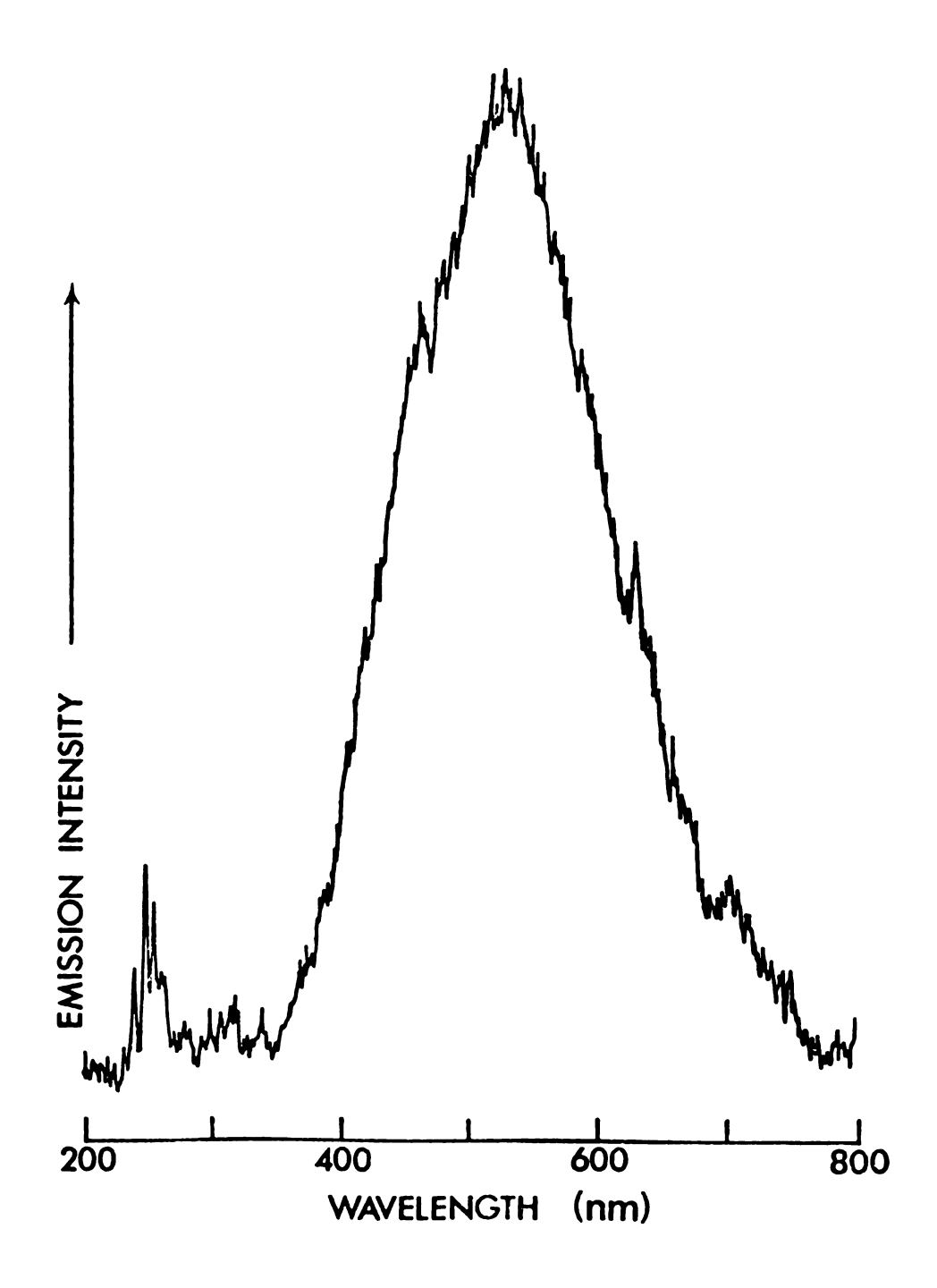


Figure 26. Dehydrated phosphorus chemiluminescence spectrum of the room temperature reaction of  $P_4$  and  $O_2$  vapor

NO dimer (137), 560 cm<sup>-1</sup>, is slightly less than that obtained for PO excimer. Although absolutely no structure determination has been made for the PO excimer, it is reasonable to assume that the conformation is similar. Some more detailed theory of excimers will now be dealt with in relation to PO.

## (3) Excimer Theory

Most of the work on excimers has been with large organic molecules and not small diatomics. Excimer formation is thought of as being another relaxation process, in addition to fluorescence, phosphoruescence, internal conversion, and intersystem crossing. Excimer formation is a bimolecular quenching process and as such is enhanced by increased collisional frequency, such as by an increase in monomer concentration. In this context the definition of excimer, due to Stevens, (154) is usually reserved for homomolecular excited double molecules formed by photoassociation after the absorption of light by one component without evidence for significant molecular association in the ground electronic state. For PO excimer the definition must be changed somewhat because the excited states are produced chemically rather than photochemically.

The electronic structure of the PO excimer can be expressed as a VB (valence-bond)  $\psi \stackrel{\sim}{\sim} \Sigma a_i \phi_i$  (PO\*-PO) +  $\Sigma b_i \phi_i$  (PO-PO\*) +  $\Sigma c_i \phi_i$  (PO<sup>+</sup>PO<sup>-</sup>) +  $\Sigma d_i \phi_i$  (PO<sup>-</sup>PO<sup>+</sup>) +  $\lambda \phi$  (PO-PO), a superposition of various configurations. The  $\phi_i$  wavefunctions are antisymmetric with respect to permutations of electrons within the monomer and the excimer and  $|a_i| = |b_i|$  and  $|c_i| = |d_i|$ , because all the monomers are identical. It was found for other systems that the first two terms of the expression are not

enough to explain completely the difference in energy between the monomer and excimer fluorescence (155). Some charge-transfer configurations were found to be necessary. The first two terms belong to what is known as the molecular exciton configuration (143). Because of the mixing of these configurations, the calculated value of the energy of the excimer emission will come much closer to the observed value than in the case of exciton type interaction only. The mixing of the electron transfer configurations is most likely stronger than their mixing with ground configurations. If the electronic delocalization over the monomers is fairly large, it is possible to describe the excimer state by the all-encompassing MO (molecular-orbital) method. MO's extending over the entire complex are constructed using the LCAO (linear combination of atomic orbitals) method. Although for large organic excimers such as pyrene such an ab initio approach is unrealistic because of the large number of integrals, such a calculation for the PO excimer is within reach of technology at this moment.

Although semi-empirical techniques do not give results of quantitative value, they do give useful qualitative concepts. A simple such method which could be applied to the PO excimer is a treatment given by Azumi, Andrews, and McGlynn (156) for polycyclic hydrocarbons. In this method which is here applied to PO the highest occupied molecular orbital and the lowest empty one of one PO molecule are designated  $\phi_1$  and  $\phi_2$ , respectively. The corresponding orbitals of the other PO are  $\theta_1$  and  $\theta_2$ , respectively. These are orthogonal. The overlap integrals are:

$$S_1 = \langle \phi_1 / \phi_1 \rangle$$
,

$$S_2 = \langle \phi_2 / \phi_2 \rangle$$
.

The simplicity of this method lies in the assumption that the excimer wavefunctions can be expressed only in terms of these four molecular orbitals. It is assumed that the more tightly bound molecular orbitals are not significantly involved in the formation of lower excimer states. This four-electron approximation means some exchange integrals over molecular orbitals are neglected, but these are assumed small. Molecular exciton states can be expressed by the following two wavefunctions:

$$\psi_{\mathbf{A}} = |\phi_{\mathbf{1}} \overline{\phi_{\mathbf{1}}} \theta_{\mathbf{1}} \overline{\theta_{\mathbf{2}}}| - |\phi_{\mathbf{1}} \overline{\phi_{\mathbf{1}}} \overline{\theta_{\mathbf{1}}} \theta_{\mathbf{2}}|$$

$$\psi_{\rm B} = |\phi_1 \overline{\phi}_2 \theta_1 \overline{\theta}_1| - |\overline{\phi}_1 \phi_2 \theta_1 \overline{\theta}_1|.$$

These Slater determinantal approximate wavefunctions are products of spatial functions and spin functions. Charge-transfer or charge-resonance states as they will be called here can be expressed by the following two wavefunctions:

$$\psi_{\text{C}} = |\phi_{1}\overline{\theta}_{2}\theta_{1}\overline{\theta}_{1}| - |\overline{\phi}_{1}\theta_{2}\theta_{1}\overline{\theta}_{1}|$$

$$\psi_{\rm D} = |\phi_1 \overline{\phi}_1 \phi_2 \overline{\theta}_1| - |\phi_1 \overline{\phi}_1 \overline{\phi}_2 \theta_1|$$

The bar denotes  $\beta$  spin. These wavefunctions do not constitute irreducible representations of the  $D_{\mbox{\sc 2h}}$  excimer point group but for the exciton states

$$\psi_{A} - \psi_{B}$$

and 
$$\psi_A + \psi_B$$
 do.

These transform as  $B_{3g}$  and  $B_{2u}$ . For the charge-resonance states

$$\Psi_{\mathbf{C}} - \Psi_{\mathbf{D}}$$

and 
$$\psi_C + \psi_\Gamma$$

are irreducible representations of the  $D_{2h}$  excimer point group and transform as  $B_{3g}$  and  $B_{2u}$  respectively. Organic excimer-forming molecules such as anthracene, pyrene, and perylene belong to the  $D_{2h}$  point group but it is expected that the PO excimer, if it is similar in conformation to the NO dimer, will belong to the  $C_{2v}$  point group. The species  $B_{3g}$  and  $B_{2u}$  both transform as  $B_2$  in the  $C_{2v}$  point group. They correspond to the triplet and quintet states of the PO excimer formed from  $PO(^4\pi)$  and  $PO(X^2\pi)$  and will be differentiated as  $a^3B_2$  and  $b^5B_2$  respectively.

Some normalized zeroth-order excimeric wavefunctions which are bases for irreducible representations of the PO excimer point group are as follows.

$$|\tilde{a}^{3}B_{2}(\text{exciton})\rangle = 1/2 \frac{\{|\phi_{1}\overline{\phi_{1}\theta_{1}}\overline{\theta_{2}}| - |\phi_{1}\overline{\phi_{1}\theta_{1}\theta_{2}}| - |\phi_{1}\overline{\phi_{2}\theta_{1}\theta_{1}}| + |\overline{\phi_{1}\phi_{2}\theta_{1}\theta_{1}}|\}}{\sqrt{(1 - S_{1}^{2})(1 + S_{1}S_{2})}}$$

$$|\tilde{b}^{5}B_{2}(\text{exciton})\rangle = 1/2 \frac{\{|\phi_{1}\overline{\phi_{1}\theta_{1}\theta_{2}}| - |\phi_{1}\overline{\phi_{1}\theta_{1}\theta_{2}}| + |\phi_{1}\overline{\phi_{2}\theta_{1}\theta_{1}}| - |\overline{\phi_{1}\phi_{2}\theta_{1}\theta_{1}}|\}}{\sqrt{(1 - S_{1}^{2})(1 - S_{1}S_{2})}}$$

$$|\tilde{a}^{3}B_{2}(\text{charge-resonance})\rangle = 1/2 \frac{\{|\phi_{1}\overline{\theta_{2}\theta_{1}\theta_{1}}| - |\overline{\phi_{1}\theta_{2}\theta_{1}\theta_{1}}| - |\phi_{1}\overline{\phi_{1}\phi_{2}\theta_{1}}| + |\phi_{1}\overline{\phi_{1}\phi_{2}\theta_{1}}|\}}{\sqrt{(1 - S_{1}^{2})(1 + S_{1}S_{2})}}$$

$$|\tilde{b}^{5}B_{2}(\text{charge-resonance})\rangle = 1/2 \frac{\{|\phi_{1}\overline{\theta_{2}\theta_{1}\theta_{1}}| - |\overline{\phi_{1}\theta_{2}\theta_{1}\theta_{1}}| - |\phi_{1}\overline{\phi_{2}\theta_{1}\theta_{1}}| + |\phi_{1}\overline{\phi_{1}\phi_{2}\theta_{1}}|\}}{\sqrt{(1 - S_{1}^{2})(1 - S_{1}S_{2})}}$$

Although the ground state of the excimer should not exist as a stable form, the wavefunction may be expressed as

$$|A_1\rangle = \sqrt{\frac{|\phi_1 \overline{\phi_1} \theta_1 \overline{\theta_1}|}{(1 - 2S_1^2 - S^4)}}$$

with energy  $E_0 = \langle A_1 | H | A_1 \rangle$  where

$$H = H_c + \sum_{v < u} (1/r_{v\mu})$$

and  $1/r_{\nu\mu}$  is the electrostatic repulsion between  $\pi$  electrons  $\nu$  and  $\mu$  and  $H_c = \sum_{\nu} H_c(\nu)$  where  $H_c(\nu)$  represents the effect of the core on electron  $\nu$ . The other matrix elements are:

To evaluate the integrals Slater type orbitals can be used as basis functions for atomic orbitals or extended Gaussian type functions can be used. The Slater type orbitals can be of the type used by Boyd and Lipscomb (90) or Mulliken and Liu (91). The Gaussian type

have been extended to include second row elements such as phosphorus by Hehre and Latham (157) and by Huzinaga and Arnau (158). Thus the problem reduces to the solution of a secular equation of the type

where

and

In addition to this model of the excimer as a mixed state produced by configuration interaction of charge-resonance and excitor-resonance states there are approaches where the whole excimer is treated as one entity by the <u>ab initio</u> method. No calculation was done on the PO excimer but some possible approaches have been outlined with the expectation that a calculation will be done.

#### 6. Cross-Section of the Flame

Because of possible variations in local concentrations of various emitting species in different parts of the flame of the reaction of phosphorus and oxygen which could change with temperature, a spectral study was made of several small cross-sections of a rather large flame at two different temperatures. The flame, under the described experimental conditions, is a diffusion limited flame with chemiluminescent reactions taking place at the interface of the  $P_{\Delta}$  vapor and atmospheric molecular

oxygen. With phosphorus vapor moving out in almost every direction, it will be true that all short-lived species will be present in every macroscopic cross-section. All the emitting species are expected to have very short lifetimes because they undergo allowed transitions,  ${}^2\Sigma^{+} \ + {}^2\pi \text{ or } {}^1A'' \ + \ ^1A'.$  In this study the relative ratios of emission of PO  $\gamma$ , PO  $\beta$ , HPO, and (PO)\* $_2$  remained almost the same in every small horizontal rectangular cross-section of the flame. The overall luminous flux varied somewhat from position to position with the maximum about two-thirds up from the bottom but the relative ratios remained constant.

# 7. Oxygen Deficient Phosphorus Chemiluminescent Systems

Under low pressure conditions of about 1 torr some authors have observed a strong PO  $\beta$  system, a weakened PO  $\gamma$  system, and a weakened (PO)\*, emission from phosphorus chemiluminescence, all at room temperature (53,65). An attempt to repeat these conditions was made except with molecular oxygen instead of atomic oxygen and at a pressure of 0.1 torr instead of 1 torr. The result is shown in Figure 27. The PO  $\gamma$  system is not seen at all, the visible continuum is greatly reduced in intensity, and there is fairly strong emission in the region 250 to 300 nm which is attributed to P<sub>2</sub>. Verma and Broida have seen P<sub>2</sub> emission in this region belonging to the  $A^{1}\pi_{g} - X^{1}\Sigma_{g}^{+}$ electronic transition in the reaction of atomic oxygen with molecular phosphorus at 0.4 to 1 torr pressure (65). But according to this work under these experimental conditions the emission appears to belong also to the  $C^1\Sigma^+_{ii}-X^1\Sigma^+_{g}$  electronic transition (see Table 8). The resolution is not sufficient to make an unambiguous assignment but a comparison to this system is shown in Table 8.

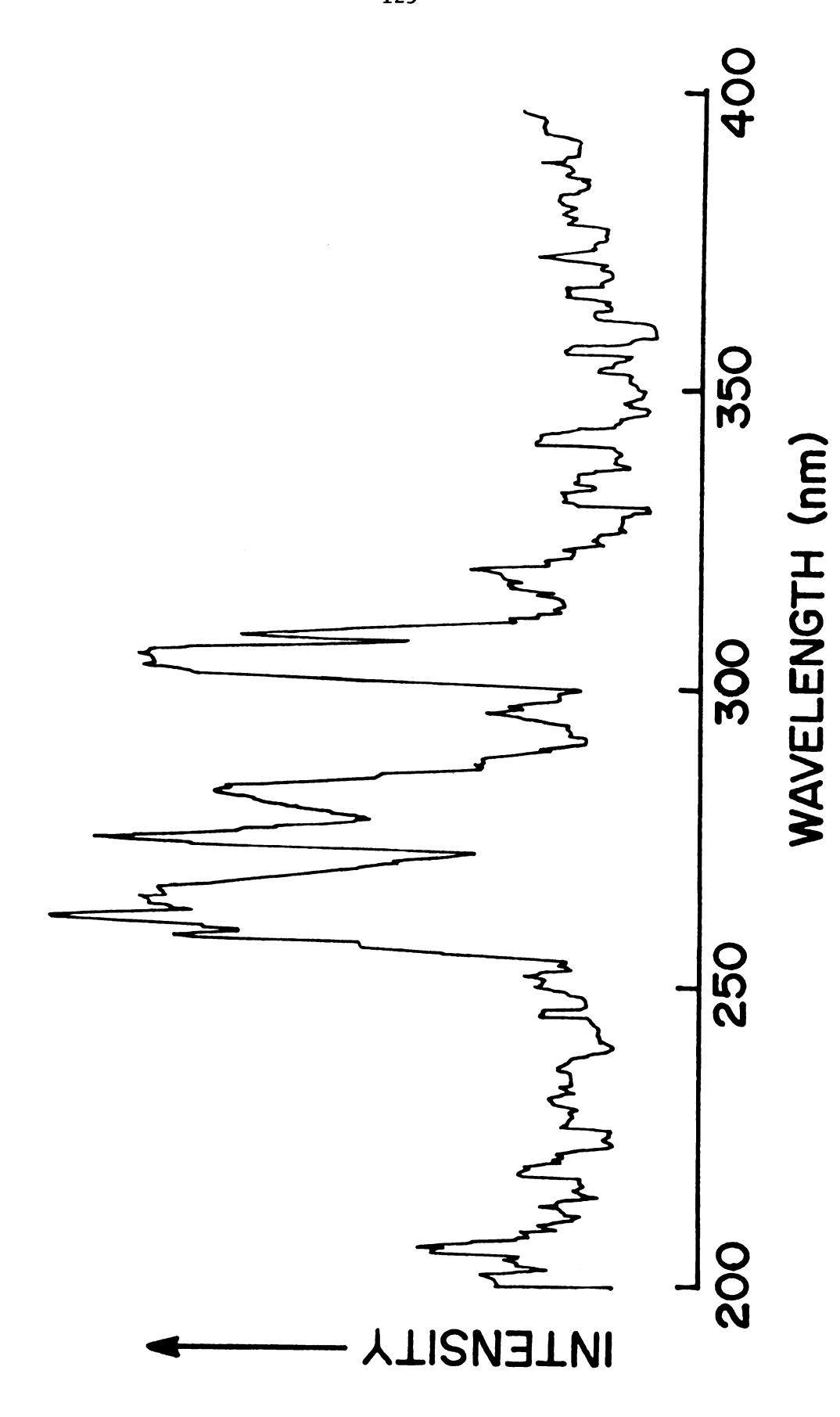


Figure 27. Spectrum showing ultraviolet  $P_2(A^1_{\pi} \to \chi^1_{\Sigma}^+)$  emission from an oxygen deficient,

low pressure system

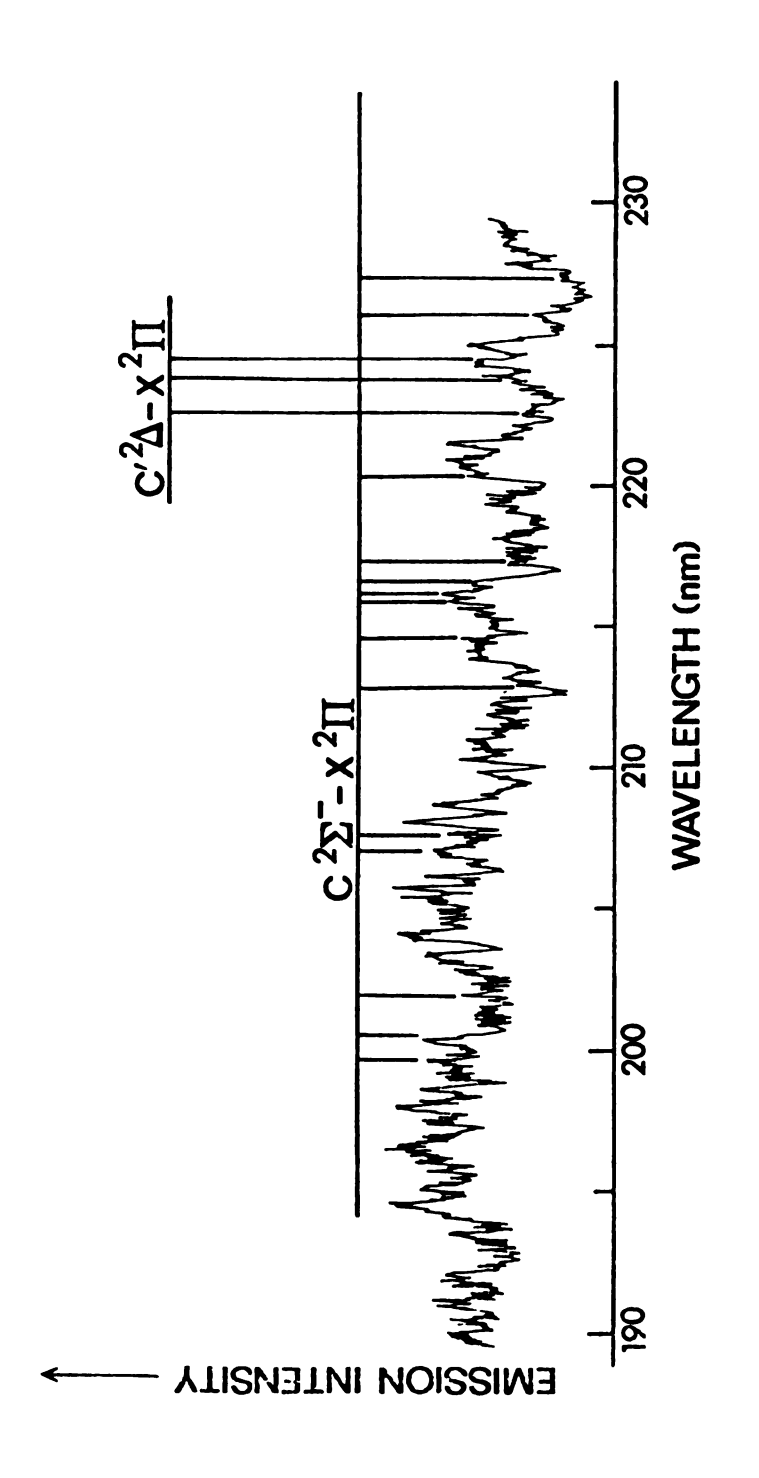
Table 8. Wavelengths of Band Heads of  $P_2$   $C^1\Sigma_u^+ - X^1\Sigma_g^+$  and  $A^1\pi_g - X^1\Sigma_g^+$  Emission

	Litera	Present Work				
Intensity		Transition	_	Reference		Intensity
4	7,15	C-X	256.56	153	257.0	5
5	11,18	C-X	258.66	153	259.5	8
5	5,15	C-X	262.55	153	262.5	10
5 4	9,18 6,16	C-X C-X	264.52 264.21	153 153	265.5	8
	,				266.5	8
6	3,0 4,17	A-X C-X	275.82 275.71	64 153	275.0	9
	5,19	C-X	283.0	153	283.5	7
	0,1	A-X	296.984	86	296.0	2
4	7,24	C-X	302.87	153	302.5	8
	0,2 8,25	A-X C-X	303.929 304.64	86 153	304.0	8
4	1,3 9,26	A-X C-X	305.37 306.42	64 153	305.5	8
5	10,27	C-X	308.20	153	308.5	7
	0,3 8,26	A-X C-X	311.243 310.54	86 153	310.5	6
4	10,29	C-X	320.19	153	320.0	2

Aside from spectral evidence of P, involvement in the lowpressure reaction between phosphorus and oxygen there is physical evidence. Physical evidence of the participation of  $P_2$  is the fact that the walls of the quartz tube containing the reaction quickly became covered with red phosphorus. The structure of red phosphorus is not definitely known but it is thought to be a polymer of  $P_{L}$  (159). Ordinarily, red phosphorus is formed from the white only by photochemical means, or by temperatures of 300 to  $400^{\circ}$ C (160). The fact that relatively massive amounts of red phosphorus are rapidly formed under low pressure conditions under neither intense photo-illumination nor high temperatures indicates that fairly high concentrations of P, are present, presumably from an oxygen induced dissociation of  $\mathbf{P}_4$ . Red phosphorus is not formed under any of the other experimental conditions performed in this work. Perhaps with a more abundant supply of oxygen the  $P_4$  entity is broken up into more PO instead of  $P_2$ . More of this will be discussed under the section on mechanism.

## 8. Weak Near-Vacuum Ultraviolet Emission

In addition to the major visible and ultraviolet emission from phosphorus oxidation under ambient conditions of temperature and pressure, there is weak emission in the near-vacuum ultraviolet region. This emission extends from at least 195 to 227 nm. It is very weak and the assignment is admittedly somewhat ambiguous, but the fact that there is emission is definite. A spectrum showing this emission is presented in Figure 28 and the assignments are shown in Table 9. It is thought to be due to  $C^2\Sigma^- - \chi^2\pi_r$  and  $C^{*2}\Delta - \chi^2\pi_r$  electronic transitions. Verma and Broida have seen emission from these states



Gas phase room temperature phosphorus chemiluminescence showing weak high energy emission from the  $C^2\Sigma^-$  and  $C'^2\Delta$  electronic states of PO Figure 28.

Table 9. Wavelengths of Band Heads of the  $PO(C^2\Sigma^- \to X^2\pi_r)$  and  $C'^2\Delta \to X^2\pi_r$ ) Weak High Energy Electronic Transitions

Assigned Transition (65)	$\lambda_{air}$ (Å) (65)	This Work
$C^2\Sigma \to X^2\pi$		
n+6)* - 1	1997.5	1996
(n+6) - 1	2006.2	2007
(n+9) - 3	2022.2	2021
(n+7) - 3	2072.6	2071
(n+7) - 3	2078.4	2077
(n+7) - 4	2130.9	2130
n+1) - 1	2148.4	2147
n+1) - 1, (n+4) - 3	2160.2	2160
n+9) - 6	2164.9	2164
n+4) - 3	2170.1	2168
n+9) - 6	2175.7	2174
n+3) - 3	2205.0	2205
n+1) - 3	2266.3	2263
n+1) - 3	2277.3	2275
$^{2}$ $^{2}$ $^{\Delta}$ $^{-}$ $^{2}$ $^{\pi}$		
- 1	2229.8	2227
- 3	2238.0	2238
- 0, 6 - 3	2247.3	2246

 $\underline{\textbf{n}}$  is an unknown number

also (65). Thus, it appears that PO is chemically generated in very high energy electronic states such as the  $C^2\Sigma^-$  and  $C^{*2}\Delta$  states. At atmospheric pressure inverse intersystem crossings are induced into the  $A^2\Sigma^+$  state, from which strong PO  $\gamma$  emission is seen. The Franck-Condon factors are not as high for the transitions  $C^2\Sigma^- - \chi^2\pi_{r}$  and  $C^{2}\Delta - X^{2}\pi_{r}$  as for the transition  $A^{2}\Sigma^{+} - X^{2}\pi_{r}$ , which explains the difference in emission intensity from the various PO electronic states. Under all conditions there would be transitions such as  $C^2\Sigma^- - B^{*2}\pi_{4}$ and  $C^{12}\Delta$  -  $B^{12}\pi_4$  occurring (see Figure 2). This emission would be in the near-infrared spectral region,  $\sim$  1.6  $\mu,$  outside the spectral sensitivity range of any photodetector which was used. These transitions have high Franck-Condon factors and are allowed. The  $B'^2\pi_1 - X^2\pi_1$ transition is allowed but was not definitely seen under these experimental conditions, possibly only because it was weak. However, Verma has seen and rotationally analyzed a number of bands belonging to the  $B^{2}\pi_{i} - X^{2}\pi_{r}$  transition (64). It occurs in the region 380 to 480 nm and involves only high vibrational levels of the  $PO(X^2\pi_r)$  ground state. The shoulder on the visible continuum at 470 nm in Figure 9 is possibly part of this system. It could not be resolved into heads corresponding to those seen by Verma and thus is only speculative. Transitions from the  $B''^2\pi_i$  to the  $4\pi_i$  state are spin forbidden, but are not impossible because phosphorus is a rather heavy atom.

#### 10. The Near-Infrared Emission

Shown in Figure 23 is a spectrum of near-infrared phosphorus chemiluminescence emission. Though of very low resolution, it shows hints of structure. Part of the spectrum is no doubt a continuation of the visible continuum, but the structure may be due to the  $A^2\Sigma^+ - B^2\Sigma^+$ 

transition as seen by Verma and Jois (69) in the region 700 to 1200 nm. Table 7 is a comparison of some of these band heads with the corresponding ones obtained by Verma and Jois. Other transitions from excited PO electronic states to other excited states such as the  $F^2\Sigma^+ - A^2\Sigma^+$ ,  $G^2\Sigma^+ - A^2\Sigma^+$ , etc., are also possible and highly probable. More work needs to be done in this area. Besides the PO and (PO)\*2 emission in this spectral region, there is a possibility that if a triplet state of HPO is populated, the triplet to singlet ground state transition would be in this region.

#### CHAPTER V

## THE MECHANISM OF PHOSPHORUS CHEMILUMINESCENCE

## A. General Considerations

The cool chemiluminescent reaction of molecular oxygen, molecular phosphorus, and water vapor under atmospheric conditions is a gasphase reaction which gives off light, phosphorus oxides, and very little thermal energy. The overall chemical reaction,

$$P_{4(g)} + 50_{2(g)} \rightarrow P_{4}0_{10(s)}$$

has  $\Delta H_{298}^{=}$  - 730 kcal/mole, an enormous quantity of energy. On a molecular basis, if this energy were concentrated into a single photon, it would have a wavelength of  $\sim$  40 nm, which is in the far vacuum ultraviolet region. Even if this energy is split four ways, for example into 4PO\* molecules, this means an energy of  $\sim$  160 nm, still well into the vacuum ultraviolet region. Bowen and Pells have established that at least one visible photon is produced per 2000  $P_4$  molecules undergoing oxidation (38). It is not clear whether all the  $P_4$  molecules give excited state PO upon oxidation or whether only a small fraction proceeds through the generation of excited state PO. The fact that the reaction is highly exothermic but does not produce local heating suggests that electronic excitation may be the major energy channel.

#### B. The Role of PO

By analogy to NO, Walsh has proposed the following mechanism for the generation of PO electronic excited states (16):

$$P(^{4}S) + O(^{3}P) + PO(X^{2}\pi_{r}) \rightarrow PO(X^{2}\pi_{r}) + PO(A^{2}\Sigma^{+} \text{ or } B^{2}\pi)$$

(The  $B^2\Sigma^+$  state was misassigned in Walsh's time. It is worthwhile to note that by an adiabatic state correlation the  $A^{2}$  and  $B^{2}$  states are not attainable by this reaction. However,  $P(^{2}D) + O(^{3}P)$  will give  $^{2}\Sigma^{+}$  states.) Walsh has seen emission from levels v' = 10 and below of the  $B^2\Sigma^+$  state of PO and v' = 2 of the  $A^2\Sigma^+$  state. From the fact that this cut-off in both excited states is the same energy above the ground state, he suggested that the single reaction listed was responsible for the production of three different electronic excited states and that transitions from these states were responsible for all the emission bands. However, in the present work emission has been seen from electronically excited states as high in energy as the  $G^{2}\Sigma^{+}$  state of PO. All the states involved in the transitions observed in the present work are shown in Figure 29. A direct transition from the  $G^2\Sigma^+$  state to the ground state would produce emission in the vacuum ultraviolet, a region that was not spectrally searched for emission in the present work. But from the work of Downey there is strong evidence that there is emission in the region 160 to 180 nm (31). The difference between the present work and that of Walsh stems from the fact that he probably used atomic species and we used molecular species as reactants. Now the question remains as to how electronically excited PO is obtained from P<sub>4</sub>.

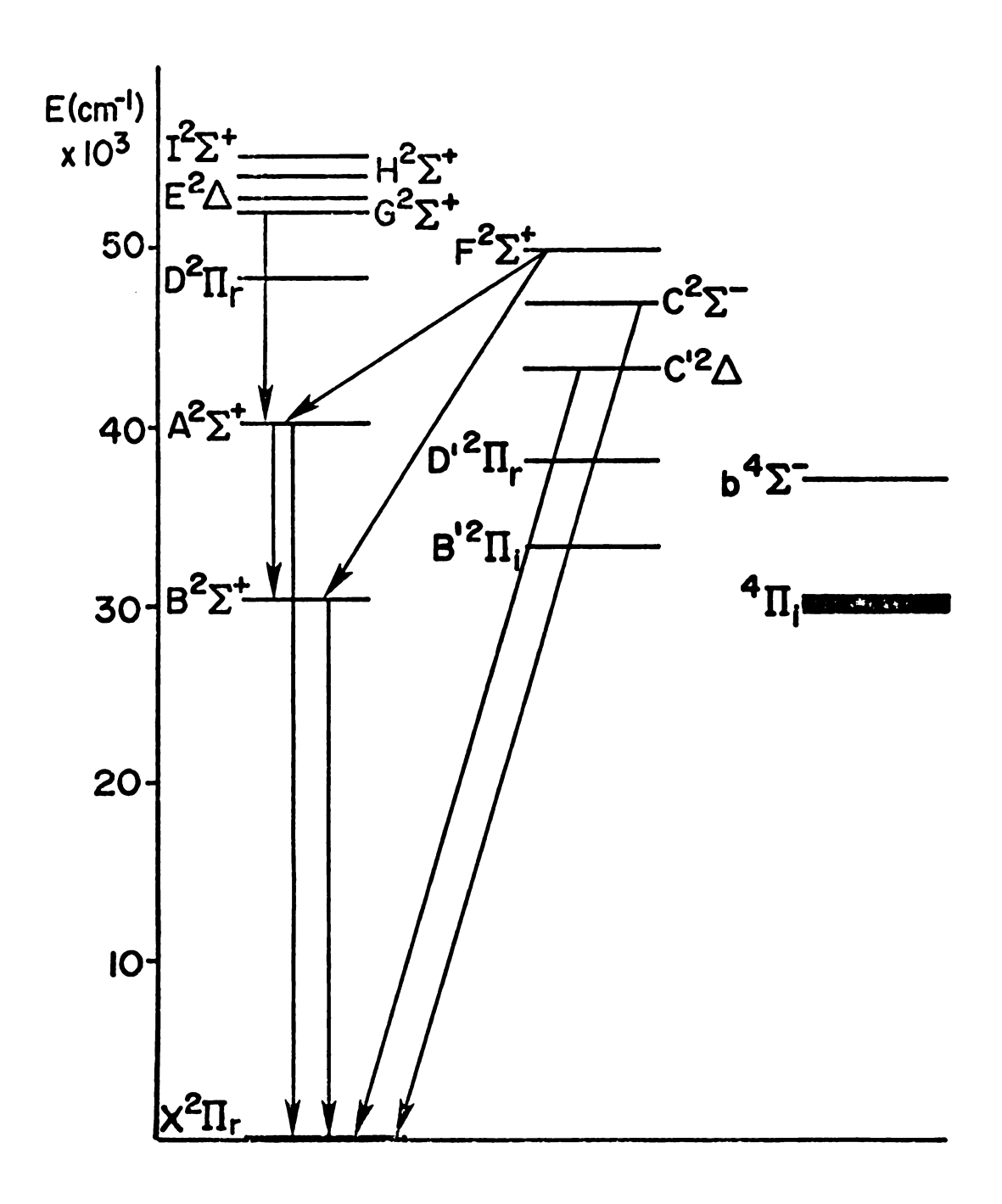


Figure 29. Potential energy diagram of PO showing all the electronic transitions which have been observed in this work

# C. Production of PO\* from $P_4$ , $O_2$ , and $H_2O$

In the mechanism for  $P_4$  oxidation proposed by Semenoff (40) and by Dainton et al. (46) there is no allowance for the production of PO. There is proposed instead a direct insertion of oxygen atoms into  $P_{L}$  to eventually produce  $P_{L}O_{10}$ . There is no allowance for the necessary role of a proton in the reaction. (The necessity of a proton source was shown by Baker (26).) Dainton, et al. (46), have suggested that the production of light is only a minor side product, an assertion supported by Bowen and Pells (38). However, the work of Baker also established that there is no oxidation reaction without a proton source such as water present (26). Thus it appears that the role of a proton should appear in the mechanism. We propose as a possible alternate mechanism that the oxygen molecule can form a stable, reversible, polar complex with the non-polar  $P_{\underline{\lambda}}$  entity. This complex can be ruptured, including the tetrahedral  $P_{\underline{\mathsf{d}}}$ , by attack with a proton. In oxygen-sufficient systems the rupture of the complex results in the production of excited state PO\* and perhaps HPO\*. In the present work it was shown that in oxygen deficient systems the rupture results in the production of significant amounts of excited state  $P_2$ \* in addition to excited state The fact that Davies and Thrush (53), under corresponding conditions, observed a ten-fold enhancement in the total glow emission upon going from  $0_2 + P_4$  to  $0 + P_4$  indicates that oxygen atoms could be the chain carriers in this branched chain reaction, or that the oxygen atom reaction with  $P_{\Lambda}$  molecules is merely one step ahead of the oxygen molecule reaction with  $P_{\underline{\lambda}}$  molecule. That is, oxygen molecules undergo a dissociation process while in the complexation step with  $P_4$ . The

fact that ozone is produced in the reaction is not positive evidence that oxygen atoms are the chain carriers in the reaction; the work of Downey showed that  $\mathbf{0}_3$  was produced by the vacuum ultraviolet radiation emitted by the reaction (31). The work of Backstrom showed that ultraviolet radiation was very effective in accelerating the solution phase oxidation of  $\mathbf{P}_4$  (36). It is therefore reasonable to assert that the reaction could be partially photochemical. Our proposed phosphorus-oxygen complex could also be induced to rupture upon absorption of an ultraviolet or vacuum ultraviolet photon. As long as more than one excited species is formed per  $\mathbf{P}_4$  entity ruptured, the reaction would have characteristics of a branched chain reaction. The idea that a  $\mathbf{P}_4$  molecule is susceptible to rupture by light absorption is supported by the experimental observation that ultraviolet light causes  $\mathbf{P}_4$  to polymerize. This polymerization involves bond transformations of some type.

## D. Proposed Reaction Scheme

The proposed scheme of phosphorus chemiluminescence is as follows:

$$P_4 + O_2 \rightarrow P_4 O_2$$
 $P_4 O_2 + H^+ \rightarrow P^*_2 + PO^+ + HPO^*$  oxygen deficient

 $P_4 O_2 + O_2 \rightarrow P_4 O_4$  oxygen sufficient

 $P_4 O_4 + H^+ \rightarrow PO^+ + HPO^* + 2PO^*$  initiation

 $PO^* \rightarrow PO + hv_{uv}$  and vac uv

$$P0^+ + e^- \rightarrow P0 + hv$$
 vac uv

initiation

$$^{\text{hv}}$$
uv or vac uv +  $^{\text{P}}_{4}^{\text{O}}_{2}$   $\rightarrow$   $^{\text{P*}}_{2}$  +  $^{\text{2PO*}}$ 

propagation

$$P0 + P0* + (P0)*_{2} + 2P0 + hv_{ex}$$

termination for oxygen sufficient and oxygen deficient systems

$$hv_{uv}$$
 or vac  $uv + P_4O_4 \rightarrow 4PO*$ 

propagation

$$P_{2}^{*} + P_{0} + (P_{0}^{---P_{2}})^{*} \rightarrow P_{2}^{+} + P_{0} + h_{ex}^{*}$$

termination for oxygen deficient systems

$$P_2 + P0* \rightarrow (P0--P_2)* \rightarrow P0 + P_2 + hv_{ex}$$

termination for oxygen deficient systems

$$P0* \rightarrow P0 + hv_{11}v$$

propagation

$$P*_2 \rightarrow P_2 + hv_{uv}$$

propagation

$$HPO* \rightarrow HPO + hv_{vis}$$

termination

PO + PO 
$$\rightarrow$$
 (PO)<sub>2</sub>

dimer formation

$$(PO)_2 + H_2O \rightarrow PO + HPO* + OH$$

side reaction

$$(PO)*_{2} + H_{2}O \rightarrow PO* + HPO* + OH$$

slight degradation

Verma and Broida have shown that even when using atomic oxygen in this chemiluminescent reaction, a trace of protons is necessary in order to observe discrete emission (65). In the present scheme this implies that a certain minimum number of proton sources must be present in order to have a certain minimum number of active centers present.

The oxygen upper and lower limits of pressure could be explained as

follows: at high pressures the  $P_4$ -oxygen complex would be surrounded by a maximum of  $O_2$  molecules and would retain the original  $P_4$  tetrahedral, nonpolar symmetry. Under these conditions it would be less susceptible to attack by a proton. At low pressures the important effect would be one of enough  $P_4$ -oxygen complexes to absorb chain carrying photons.

In this proposed mechanism we have included the possibility of exciplex formation between  $P_2$  and PO, with one of the two species being excited. This speculation is enforced by comparing the states of PO and the states of  $P_2$ , as is shown on Figure 30. There also exists the possibility that  $P*_2$  forms by energy transfer from PO\*.

E. Major Energy Decay Modes in Phosphorus Chemiluminescence

From this work it is seen that PO\* is the central species in phosphorus chemiluminescence. The major radiative modes of decay are as follows:

1. 
$$\gamma$$
-band  $PO(A^2 \Sigma^+) \rightarrow PO(X^2 \pi_r) + h\nu$ 

2. 
$$\beta$$
-band  $PO(B^2\Sigma^+) \rightarrow PO(X^2\pi_r) + h\nu$ 

3. 
$$PO(B^2\Sigma^+) + PO(X^2\pi_r) \rightarrow PO(^4\pi_i) + PO(X^2\pi_r) \stackrel{?}{\leftarrow} (PO) *_2 \rightarrow 2PO(X^2\pi_r) + hv$$

In addition to these modes of decay there is seen emission from the very high PO excited states,  $G^2\Sigma^+$ ,  $C^2\Sigma^-$ ,  $F^2\Sigma^+$ , and  $C^{\prime 2}\Delta$ . The G and F states are seen only by a near-infrared transition to other lower excited states. Thus it is seen that PO\* is probably initially generated in very high electronic states and the energy degrades into lower electronic states by various energy transfer methods, such as the

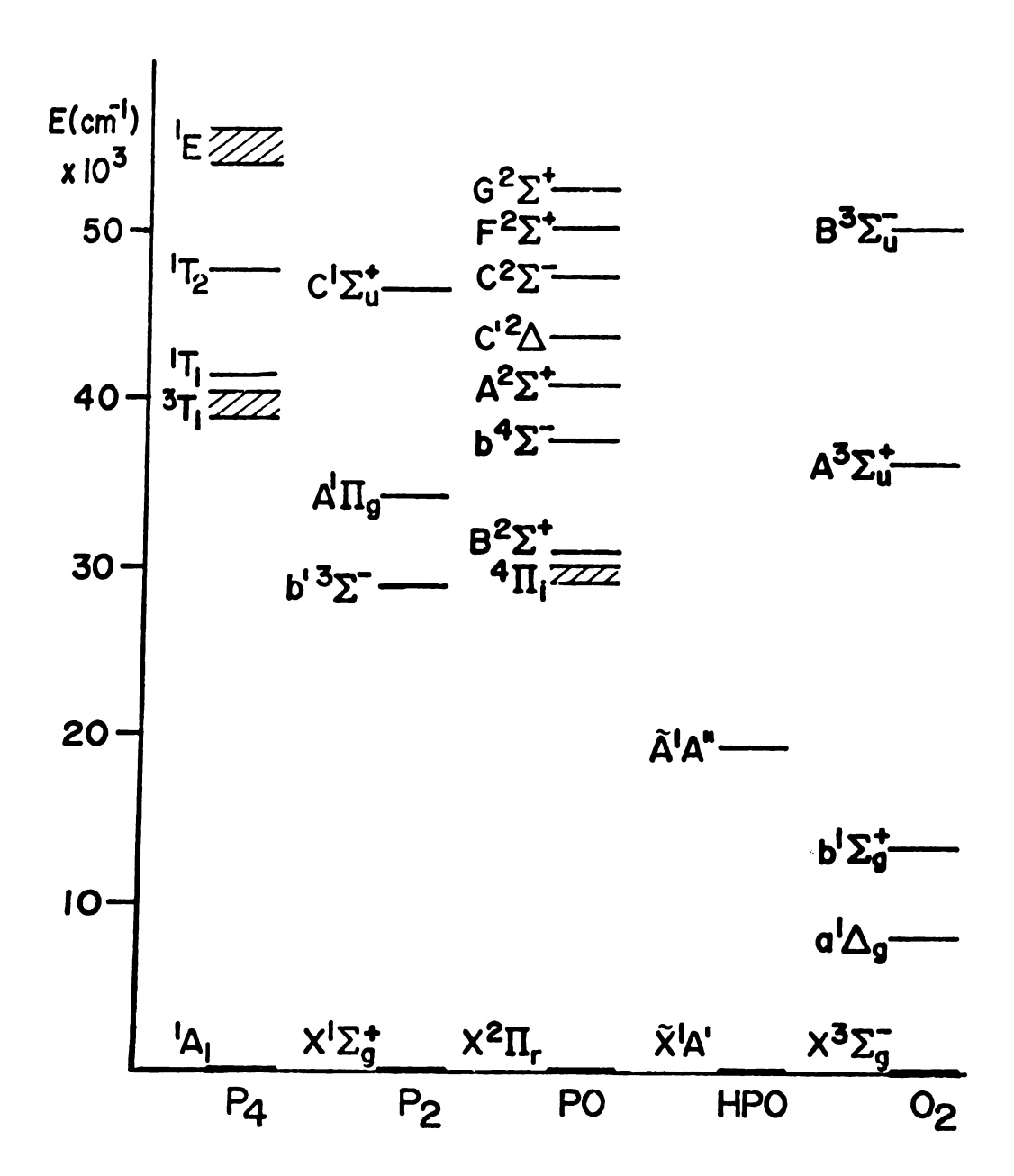


Figure 30. Potential energy diagram showing simultaneously a number of electronic states of the species  $P_4$ ,  $P_2$ ,  $P_3$ ,  $P_4$ ,  $P_5$ , and  $P_6$ 

dipole-dipole interaction proposed by Gorden and Chiu for NO (147). The net result is some emission from nearly all the upper electronic states, especially the  $A^2\Sigma^+$  and  $B^2\Sigma^+$  states for various conditions, and a net accumulation in the  $^4\pi_1$  state, from which excimer formation occurs upon collision with ground state PO. Under the conditions of this work significant HPO(DPO) emission is seen from the transition

4. 
$$\bigwedge^{\circ}(^{1}A'') \rightarrow X(^{1}A') + hv$$

## F. Correlation of States for the Formation of HPO

The species, HPO\*, is possibly formed by a mechanism similar to the sequence proposed by Ibaraki et al. for the generation of HNO\*,

$$H + (NO)_2 \rightarrow HNO* + NO$$
 $HNO* \rightarrow HNO + hv.$ 

A group theoretical adiabatic state correlation diagram for the formation of HPO\* by this mechanism is shown as follows:

$$H + (PO)_{2} \rightarrow H - P - O \rightarrow HPO* + PO$$

$$^{2}S_{g} \quad ^{1}A' \quad C_{s} \quad ^{1}A'' \quad ^{2}\pi \qquad \text{states and symmetries}$$

$$^{2}A' \quad ^{1}A' \quad ^{1}A'' \quad ^{2}A'' \qquad \text{transformation into } C_{s} \text{ symmetry}$$

$$^{2}A' \quad X \quad ^{1}A' \quad = \quad ^{1}A'' \quad X \quad ^{2}A'' \qquad \text{direct product}$$

$$^{2}A' \quad = \quad ^{2}A' \quad = \quad ^{2}A' \qquad \text{equality}$$

Also (P0)\*2 in an excited triplet or quintet state will correlate with an excited state PO as follows:

where the  $^3A'$  and  $^5A'$  states of (PO)\* $_2$  were chosen by assuming a  $^2C_2$  symmetry and the spin was chosen by the addition of  $PO(X^2\pi_r)$  and  $PO(^4\pi_f)$ .

An additional point to consider is whether predissociation of HPO\* will yield excited state PO(B $^2\Sigma^+$ ). An adiabatic state correlation shows that it will not.

HPO\* 
$$\rightarrow$$
 H + PO reaction

 $^{1}A''$ 
 $^{2}S_{g}$ 
 $^{2}\pi$ 
states

 $^{1}A''$ 
 $^{2}A'$ 
 $^{2}A''$ 
direct product

 $^{1}A'' = ^{1}A''$ 
equality

The species  ${}^2\Sigma^+$ , which transforms as  ${}^2A^{\prime}$ , does not correlate with the  ${}^1A^{\prime\prime}$  excited state of HPO.

G. Breakdown of the Analogy Between PO $_2$  and NO $_2$  in this System

Thus far in the mechanism we have made several assumptions by analogy to NO and the manner in which this molecule is known to behave. However, there is a point at which this analogy must cease. It has been suggested that the continuum in phosphorus and oxygen

chemiluminescence is due to  $PO_2$  emission in analogy to  $NO_2$  emission, which is continuous (53). However, thermal dissociation of  $NO_2$  does not yield emission from the lowest allowed electronic excited state of NO, the  $\gamma$  system.

## H. Suggested Further Experiments

The role of the proton has already been discussed at some length and the necessity suggests further experiments. If it is the positive charge of the proton which is necessary to cause attraction to a dipole induced by a non-symmetric  $P_4$ -oxygen complex, then a doubly charged species, such as an  $\alpha$  particle, should work even better. In a proposed experiment a very low energy source of  $\alpha$  particles is to be brought near a completely dried phosphorus-oxygen supply and the effect noted. If, as has been suggested in this mechanism the chain carriers are photons, then another experiment to try is to bring a very low intensity ultraviolet light source near a quartz container of a completely dried sample of phosphorus and oxygen to determine whether there is an induced effect.

#### CHAPTER VI

#### SUMMARY

In this work we have spectrally analyzed the ultraviolet, visible, and near-infrared emissions from the chemiluminescent oxidation reaction of phosphorus under various conditions, including ambient. The results of this work are given as follows:

- (1) The emitter HPO has been identified for the first time in naturally occurring phosphorus chemiluminescence. This was done by a deuterium isotopic substitution in the cool reaction of molecular phosphorus, molecular oxygen, and traces of water vapor under ambient conditions.
- (2) Our proposal that the chemiluminescent visible continuum emission is due to PO excimer has been confirmed by thermal and dilution studies. From thermal studies the binding energy of this excimer in its first excited electronic state has been determined to be 846 ± 200 cm<sup>-1</sup> and the binding energy in the ground state 109 ± 200 cm<sup>-1</sup>. From this information an approximate potential energy surface of the excimer has been constructed.
- (3) By confirming the identity of the continuum emitter as (PO)\*2, we have eliminated the possibilities of PO<sub>2</sub> and HOPO. Also the thermal studies and the dried sample studies have directly ruled out PO<sub>2</sub> and HOPO respectively as emitters.

- (4) We have determined the effects of temperature, diluent gas, pressure, and deuterium substitution upon the emissivities of the  $PO(A^2\Sigma^+)$  and  $PO(B^2\Sigma^+)$  excited electronic states.
- (5) The deuterium oxide vapor substitution for water vapor and the subsequent dramatic increase in DPO emission intensity over HPO emission intensity indicates a predissociation in the  $A(^1A'')$  electronic state of HPO(DPO).
- (6) From small rectangular cross-section spectral studies of the cool phosphorus-oxygen diffusion flame it has been determined that the relative ratios of emission from the transient species are the same regardless of the cross-section chosen.
- (7) Weak transitions from the very energetic  $G^2\Sigma^+$ ,  $F^2\Sigma^+$ ,  $C^2\Sigma^-$ , and  $C^{\prime 2}\Delta$  electronic excited states of PO have been observed under ambient conditions, indicating that the reaction mechanism differs from that in the reaction of atomic phosphorus and atomic oxygen in gas discharge experiments.
- (8) In a low pressure, oxygen deficient system significant  $P_2$  emission has been observed, indicating a possible different mechanism for oxygen deficient systems.
- (9) A possible alternate, photochemical mechanism for the phosphorus oxidation branched chain reaction has been proposed.
- (10) A probable mechanism for formation of HPO\* from both (PO)<sub>2</sub> and (PO)\*<sub>2</sub> is presented.
- (11) Suggestions for further experiments to confirm our mechanism are presented.

REFERENCES

#### REFERENCES

- F. McCapra in "Essays in Chemistry", vol. 3, J. N. Bradley,
   R. D. Gillard, and R. F. Hudson, Eds., Academic Press, N.Y., 1972,
   pp. 102-105.
- 2. F. McCapra, Quart. Rev. (London), 20, 485 (1966).
- 3. H. H. Seliger in "Chemiluminescence and Bioluminescence", M. J. Cormier, D. M. Hercules, and J. Lee, Eds., Plenum Press, N.Y., 1973, p. 461.
- 4. D. M. Hercules, Accts. Chem. Res., 2, 301 (1969).
- 5. A. U. Khan and M. Kasha, J. Amer. Chem. Soc., <u>92</u>, 3292 (1970).
- 6. R. D. Kenner and A. U. Khan, J. Chem. Phys., In press.
- 7. W. S. Struve, T. Kitatagawa, and D. R. Herschbach, J. Chem. Phys., 54, 2759 (1971).
- B. A. Thrush in "Annual Review of Physical Chemistry", vol. 19,
   H. Eyring, C. J. Christensen, and H. S. Johnston, Eds., Annual
   Reviews, Inc., Palo Alto, Ca., 1968, pp. 383-384.
- 9. E. A. Chandross and F. I. Sonntag, J. Amer. Chem. Soc., <u>88</u>, 1089 (1966).
- A. U. Khan and M. Kasha, J. Chem. Phys., <u>39</u>, 2105 (1963); Nature,
   204, 241 (1964); J. Amer. Chem. Soc., 88, 1574 (1966).
- T. Carrington in "Chemiluminescence and Bioluminescence",
   M. J. Cormier, D. M. Hercules, and J. Lee, Eds., Plenum Press,
   N.Y., 1973, p. 7-24.

- 12. H. B. Palmer, J. Chem. Phys., 47, 2116 (1967).
- 13. G. Herzberg, "Molecular Spectra and Molecular Structure, I. Spectra of Diatomic Molecules", D. Van Nostrand, New York, N.Y., 1950.
- 14. F. Ackerman and E. Miescher, J. Mol. Spec., 31, 400 (1969).
- 15. G. D. Gillispie, Ph.D. Thesis, Michigan State University, East Lansing, Michigan, 1975.
- 16. A. D. Walsh in "The Threshold of Space", M. Zelikoff, Ed., Pergamon Press, London, 1957, p. 165.
- 17. P. N. Clough and B. A. Thrush, Trans. Farad. Soc., 63, 915 (1967).
- R. F. Vassil'ev, Prog. Reaction Kinetics, 4, 305 (1967).
- 19. M. M. Rauhut, Accts. Chem. Res., 2, 80 (1969).
- 20. H. H. Seliger and W. D. McElroy, "Light: Physical and Biological Action", Academic Press, N.Y., 1965.
- 21. O. Shimomura, F. H. Johnson, and Y. Saiga, Science, 140, 1339 (1963).
- 22. W. A. Kummer, J. N. Pitts, Jr., and R. P. Steer, Environ. Sci. Tech., <u>5</u>, 1045 (1971).
- 23. A. Fontijn, A. J. Sabadell, and R. J. Ronco, Anal. Chem., <u>42</u>, 575 (1970).
- 24. W. R. Seitz and D. M. Hercules in "Chemiluminescence and Bioluminescence", M. J. Cormier, D. M. Hercules, and J. Lee, Eds., Plenum Press, N.Y., 1973, p. 427.
- 25. E. N. Harvey, "A History of Luminescence", The American Philosophical Society, Philadelphia, Pa., 1957.
- H. B. Baker, J. Chem. Soc., <u>47</u>, 349 (1885); Phil. Trans., <u>179A</u>,
   571 (1888).

- 27. T. E. Thorpe and A. E. Tutton, J. Chem. Soc. (Trans.), <u>57</u>, 545 (1890); 59, 1019 (1891).
- 28. E. J. Russell, J. Chem. Soc., 83, 1263 (1903).
- 29. P. Geuter, Z. Wiss. Phot., <u>5</u>, 1 (1907).
- 30. M. Centnerszwer and A. Petrikaln, Z. Phys. Chem., 80, 235 (1912).
- 31. W. E. Downey, J. Chem. Soc., 347 (1924).
- 32. H. J. Emeleus and W. E. Downey, J. Chem. Soc., 2491 (1924).
- 33. H. J. Emeleus and R. H. Purcell, J. Chem. Soc., 788 (1927).
- 34. H. J. Emeleus, J. Chem. Soc., 1362 (1925).
- 35. C. C. Miller, J. Chem. Soc., 1823 (1929).
- 36. H. L. J. Backstrom, Medd. Vestenskapsadad Nobel Inst., 6, 1 (1927).
- 37. E. Q. Adams, Phys. Rev., 23, 771 (1924).
- 38. E. J. Bowen and E. G. Pells, J. Chem. Soc., 1096 (1927).
- 39. E. J. Bowen and A. C. Cavell, J. Chem. Soc., 1920 (1929).
- 40. N. Semenoff, Z. Physik., 46, 109 (1927); Chem. Rev., 6, 347 (1929).
- 41. P. N. Ghosh and G. N. Ball, Z. Physik., 71, 362 (1931).
- 42. F. Hund, Z. Physik., 36, 657 (1926).
- 43. R. S. Mulliken, Phys. Rev., 30, 785 (1927).
- 44. K. Rumpf, Z. Phys. Chem., Abt. B., 38, 469 (1938).
- 45. F. S. Dainton, Trans. Farad. Soc., 42, 244 (1947).
- 46. F. S. Dainton and H. M. Kimberley, Trans. Farad. Soc., <u>46</u>, 629 (1950).
- 47. F. S. Dainton and J. C. Bevington, Trans. Farad. Soc., <u>42</u>, 377 (1946).
- 48. K. Dressler, Helv. Physica Acta, 28, 563 (1955).
- 49. N. L. Singh, Can. J. Phys., 37, 136 (1959).
- 50. H. Cordes and W. Witschel, Z. Phys. Chem., 46, 35 (1965).

- 51. E. B. Ludlam, J. Chem. Phys., 3, 617 (1935).
- 52. M. Lam Thanh and M. Peyron, J. Chim. Phys. Physicochim. Biol., 60, 1289 (1963).
- 53. P. B. Davies and B. A. Thrush, Proc. Roy. Soc. A., 302, 243 (1968).
- 54. H. Guenebaut, C. Couet, and B. Coquart, J. Chim. Phys. Physicochim. Biol., 63, 969 (1966).
- 55. B. Coquart, C. Couet, T. A. Ngo, and H. Guenebaut, J. Chim. Phys. Physicochim. Biol., 64, 1197 (1967).
- 56. C. Couet, T. A. Ngo, B. Coquart, and H. Guenebaut, <u>ibid.</u>, <u>65</u>, 217 (1968).
- 57. B. Coquart, C. Couet, H. Guenebaut, and T. A. Ngo, Can. J. Phys., 50, 1014 (1972).
- 58. J. C. Prudhomme, M. Larzilliere, and C. Couet, ibid., 51, 2464 (1973).
- 59. T. A. Ngo, M. DaPaz, B. Coquart, and C. Couet, ibid., 52, 154 (1974).
- 60. B. Coquart, M. DaPaz, and J. C. Prudhomme, <u>ibid.</u>, <u>52</u>, 177 (1974).
- 61. J. C. Prudhomme and B. Coquart, ibid., 52, 2150 (1974).
- 62. B. Coquart, M. DaPaz and J. C. Prudhomme, <u>ibid.</u>, <u>53</u>, 377 (1975).
- 63. R. D. Verma and M. N. Dixit, ibid., 46, 2079 (1968).
- 64. R. D. Verma, ibid., 48, 2391 (1970).
- 65. R. D. Verma and H. P. Broida, ibid., 48, 2991 (1970).
- 66. R. D. Verma, <u>ibid.</u>, <u>49</u>, 279 (1971).
- R. D. Verma, M. N. Dixit, S. S. Jois, S. Nagaraj, and
   R. Singhal, ibid., 49, 3180 (1971).
- 68. S. Guha, S. S. Jois, and R. D. Verma, ibid., 50, 1579 (1972).
- 69. R. D. Verma and S. S. Jois, ibid., 51, 322 (1973).
- 70. R. D. Verma and S. R. Singhal, <u>ibid.</u>, <u>53</u>, 411 (1975).

- 71. H. R. Zaidi and R. D. Verma, ibid., 53, 420 (1975).
- 72. L. R. Maxwell, S. B. Hendricks, and V. M. Mosely, J. Chem. Phys.,

  3, 699 (1935).
- 73. D. MacRae and C. C. Van Voorhis, J. Amer. Chem. Soc., <u>43</u>, 547 (1921).
- 74. J. R. Arnold, J. Chem. Phys., 14, 351 (1946).
- 75. M. Mashima, J. Chem. Phys., 20, 801 (1952).
- 76. L. Pauling and M. Simonetta, ibid., 20, 29 (1952).
- 77. W. Moffit, Trans. Farad. Soc., 44, 987 (1948).
- 78. R. R. Hart, M. B. Robin, and N. A. Kuebler, J. Chem. Phys., <u>42</u>, 3631 (1965).
- R. M. Archibald and P. G. Perkins, Chem. Commun., 569 (1970).
- 80. I. H. Hillier and V. R. Saunders, ibid., 1223 (1970).
- 81. G. Herzberg, "Molecular Spectra and Molecular Structure, III.

  Electronic Spectra and Electronic Structure of Polyatomic

  Molecules", D. Van Nostrand, New York, N.Y., 1966.
- 82. J. D. Carette and L. Kerwin, Can. J. Phys., 39, 1300 (1961).
- 83. P. K. Carroll and P. I. Mitchell, Proc. Roy. Soc. (London),
  A., 342, 93 (1975).
- 84. J. Brion, J. Malicet, and H. Guenebaut, Can. J. Phys., <u>52</u>, 2143 (1974).
- 85. G. Herzberg, Ann. Physik, 15, 677 (1932).
- 86. E. J. Marais, Phys. Rev., 70, 499 (1946).
- 87. A. E. Douglas and K. S. Rao, Can. J. Phys., 36, 565 (1958).
- 88. S. Mrozouski and C. Santaram, J. Opt. Soc. Amer., <u>57</u>, 522 (1967).
- 89. F. Creutzberg, Can. J. Phys., 44, 1583 (1966).

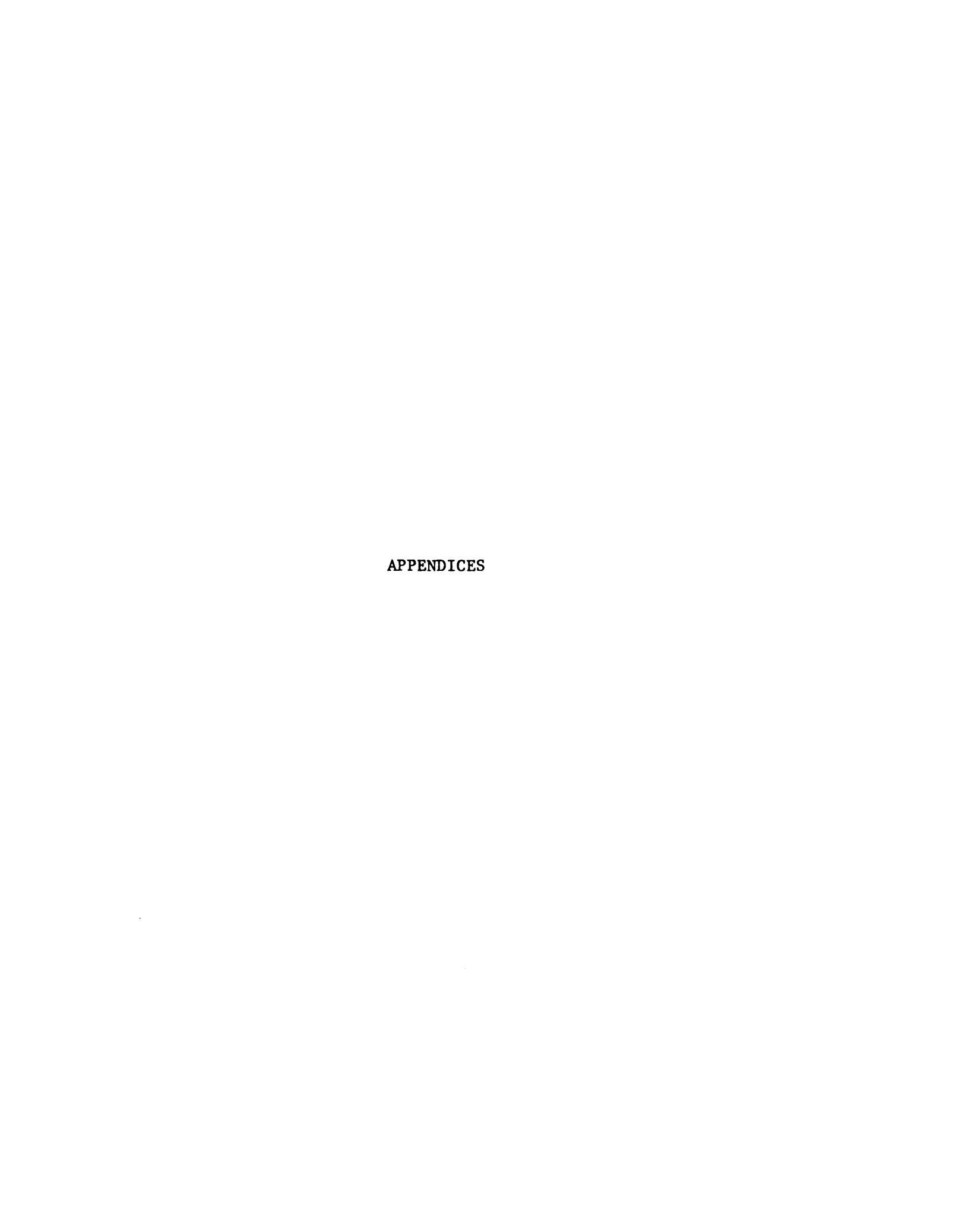
- 90. D. B. Boyd and W. N. Lipscomb, J. Phys. Chem., 46, 910 (1967).
- 91. R. S. Mulliken and B. Liu, J. Amer. Chem. Soc., <u>93</u>, 6738 (1971).
- 92. W. S. Martin, J. Opt. Soc. Amer., 49, 1071 (1959).
- 93. A. U. Acuna, D. Husain, and J. R. Wiesenfeld, J. Chem. Phys., 58, 494 (1973); 5272 (1973).
- 94. J. Curry, L. Herzberg, and G. Herzberg, Z. Physik., 86, 348 (1933).
- B. S. Mohanty, K. N. Upadhya, R. B. Singh, and N. L. Singh,
   J. Mol. Spectry., 24, 19 (1967).
- 96. K. S. Rao, Can. J. Phys., 36, 1526 (1958).
- 97. K. K. Durga and P. T. Rao, Indian J. Phys., 32, 223 (1958).
- 98. S. Mrozowski and C. Santaram, J. Opt. Soc. Amer., <u>56</u>, 1174 (1966).
- 99. F. Ackerman, H. Lefebvre, and A. L. Roche, Can. J. Phys., <u>50</u>, 692 (1972).
- 100. T. J. Tseng and F. Grein, J. Chem. Phys., 59, 6563 (1973).
- 101. A. L. Roche and H. Lefebvre-Brion, ibid., 1914 (1973).
- 102. J. W. Hastie, J. Res. Nat. Bur. Stand. (US), 77A, 733 (1973).
- 103. R. G. W. Norrish and G. A. Oldershaw, Proc. Roy. Soc., <u>A262</u>, 10 (1961).
- 104. A. D. Walsh, J. Chem. Soc., 2266 (1953).
- 105. L. V. Bershov, Teor. Eksp. Khim., 6, 397 (1970).
- J. Drowart, C. E. Myers, R. Szwarc, A. Vander Auwera-Mahieu, andO. M. Uy, Trans. Farad. Soc., 67, 1749 (1972).
- 107. L. Brewer and G. Rosenblatt, Chem. Rev., <u>61</u>, 257 (1961).
- M. Lam Thanh and M. Peyron, J. Chim. Phys. Physicochim. Biol.,
   59, 688 (1962).
- 109. <u>Ibid.</u>, <u>61</u>, 1531 (1964).
- 110. <u>Ibid.</u>, <u>63</u>, 266 (1966).

- 111. F. W. Dalby, Can. J. Phys., 36, 1336 (1958).
- 112. J. L. Bancroft, J. M. Hollas, and D. A. Ramsay, <u>ibid.,40</u>, 322 (1966).
- 113. M. J. Y. Clement and D. A. Ramsay, ibid., 39, 205 (1961).
- 114. R. J. Van Zee and A. U. Khan, J. Amer. Chem. Soc., 96, 6805 (1974).
- 115. M. A. A. Clyne and B. A. Thrush, Discuss. Farad. Soc., <u>33</u>, 139 (1962).
- 116. T. Ibaraki, K. Kodera, and I. Kusunoki, J. Phys. Chem., <u>79</u>, 95 (1975).
- 117. G. Herzberg, "The Spectra and Structures of Simple Free Radicals",
  Cornell Univ. Press, Ithaca, N.Y., 1971.
- 118. T. Ishiwata, H. Akimoto, and I. Tanaka, VIII Inter. Conference on Photochem., Edmonton, Canada, v11, Aug., 1975.
- 119. A. W. Salotto and L. Burnelle, Chem. Phys. Lett., 3, 80 (1969);
   J. Chem. Phys., 52, 2936 (1970).
- 120. A. B. Meinel, Astrophys. J., 111, 555 (1950).
- 121. C. E. Moore and H. P. Broida, J. Res. Nat. Bur. Stand. (US), 63A, 279 (1959).
- 122. H. E. Hunziker and H. R. Wendt, J. Chem. Phys., 60, 4622 (1974).
- 123. K. H. Becker, E. H. Fink, P. Langen, and U. Schurath, <u>ibid</u>., 4623 (1974).
- 124. T. T. Paukert and H. S. Johnson, ibid., 56, 2824 (1972).
- 125. C. J. Hochanadel and J. A. Ghormley, ibid., 56, 4426 (1972).
- 126. S. N. Foner and E. H. Fink, R. L. Hudson, ibid., 36, 2681 (1962).
- 127. J. W. Hastie, Combust. Flame, 21, 187 (1973).
- 128. J. C. Gole and E. F. Hayes, J. Chem. Phys., 57, 360 (1972).
- 129. H. Lew and I. Heiber, <u>ibid.</u>, <u>58</u>, 1246 (1973).

- 130. A. G. Gaydon and H. G. Wolfhard, "Flames", Chapman and Hall Ltd., London, 1970, p. 141.
- 131. L. T. Earls, Phys. Rev., 48, 423 (1935).
- 132. N. L. Singh, Can. J. Phys., 37, 136 (1959).
- 133. R. J. Van Zee and A. U. Khan, Chem. Phys. Lett., 36, 123 (1975).
- 134. J. G. Winans and E. G. G. Strueckelberg, Proc. Nat. Acad.

  Amer., 14, 867 (1928).
- 135. J. J. Hopfield, Astrophys. J., 72, 133 (1930).
- 136. J. L. Dye and V. A. Nicely, J. Chem. Ed., 48, 433 (1971).
- 137. J. Billingsley and A. B. Callear, Trans. Farad. Soc., <u>67</u>, 589 (1971).
- 138. T. L. Hill, "An Introduction to Statistical Thermodynamics",
  Addison-Wesley Publishing Co., Inc., Reading, Mass., 1960.
- 139. H. P. Broida, H. I. Schiff, and T. M. Sugden, Trans. Farad. Soc., 57, 259 (1961).
- 140. M. A. A. Clyne and B. A. Thrush, Proc. Roy. Soc., A269, 404 (1962).
- 141. A. McKenzie and B. A. Thrush, Chem. Phys. Lett., 1, 681 (1968).
- 142. A. G. Gaydon, Proc. Roy. Soc., A183, 111 (1944).
- 143. N. Mataga and T. Kubota, "Molecular Interactions and Electronic Spectra", Marcel Dekker, Inc. New York, 1970.
- 144. C. E. Dinerman and G. E. Ewing, J. Chem. Phys., 53, 626 (1970).
- 145. J. Billingsley and A. B. Callear, Nature, <u>221</u>, 1136 (1969); Trans. Farad. Soc., 67, 257 (1971).
- 146. L. A. Melton and W. Klemperer, J. Chem. Phys., <u>55</u>, 1468 (1971);59, 1099 (1973).
- 147. R. G. Gordon and Y. N. Chiu, ibid., 55, 1469 (1971).

- 148. D. P. Craig and S. H. Walmsly, "Excitons in Molecular Crystals", Benjamin, New York, 1968, p. 10.
- 149. T. Forster in "Comparative Effects of Radiation", M. Burton,
  J. Kirby-Smith, and J. Magee, Eds., John Wiley and Sons, New
  York, 1960, p. 300.
- 150. T. A. Milne and F. T. Green, J. Chem. Phys., 47, 3668 (1967).
- D. Golomb and R. E. Good, J. Chem. Phys., 49, 4176 (1968).
- 152. C. Bibart and G. Ewing, <u>ibid.</u>, <u>61</u>, 1284 (1974).
- 153. P. N. Skancke and J. E. Boggs, Chem. Phys. Lett., 21, 316 (1973).
- 154. B. Stevens, Advances in Photochemistry, 8, 161 (1971).
- 155. E. Konijnenburg, Thesis, University of Amsterdam, 1963.
- 156. T. Azumi and S. P. McGlynn, J. Chem. Phys., 41, 3131 (1964).
- 157. W. J. Hehre and W. A. Lathan, J. Chem. Phys., 56, 5255 (1972).
- 158. S. Huzinaga and C. Arnau, J. Chem. Phys., 53, 348 (1970).
- 159. M. Y. Kraft and V. P. Parini, Doklady, 77, 57 (1951).
- 160. W. L. Roth, T. W. DeWitt, and A. J. Smith, J. Amer. Chem. Soc., <u>69</u>, 2881 (1947).



## APPENDIX A

TRANSIENT EMITTING SPECIES IN PHOSPHORUS CHEMILUMINESCENCE

R. J. Van Zee and A. U. Khan, J. Chem. Phys., In Press

TRANSIENT EMITTING SPECIES IN PHOSPHORUS CHEMILUMINESCENCE

Richard J. Van Zee and Ahsan U. Khan Departments of Chemistry and Biophysics Michigan State University East Lansing, Michigan 48824

The phosphorescence of phosphorus oxidation is the oldest and the best known chemiluminescing reaction, but a definitive spectroscopic study of this classic system has been lacking. In this paper we report the results of an investigation of the oxidation of  $P_4$  vapor under atmospheric conditions, with added H<sub>2</sub>O or D<sub>2</sub>O vapor. In spectral studies of small horizontal rectangular cross-sections of the phosphorus flame, the relative ratios of emission from the transient species remained the same regardless of the cross-section chosen, which permits accurate spectral analysis of the chemiluminescence. We have analyzed the visible and ultraviolet spectrum of the reaction, consisting of discrete band structure in the 228.8-272.1 nm region and a broad continuum onsetting at 335 nm and extending to 800 nm and longer, upon which are superimposed a number of weak bands from 450-650 nm. Discrete band emissions enabled the identification of the bands at 228.8-272.1 nm with the PO  $\gamma$ -system transitions, PO( $A^2\Sigma^+$ )  $\rightarrow$  PO( $X^2\Pi$ ). Spectral changes arising from the substitution of  $D_2^0$  vapor for  $H_2^0$  vapor in the reaction led to the assignment of the weak bands at 450-650 nm to HPO (or DPO),  $\tilde{A}(^{1}A'') \rightarrow \tilde{X}(^{1}A')$ . The main band emission in the visible region, the broad continuum which cannot be identified with any simple electronic transition, exhibits the kinetic and spectral characteristics of an excimer, an excited state dimer with only one member of the molecular pair being electronically excited. In the case of phosphorus chemiluminescence the dimer is (PO\*...PO) and the equilibrium reaction for its formation is  $(P0*...P0) \stackrel{+}{\rightarrow} PO(^{4}\Pi) + PO(X^{2}\Pi) \stackrel{+}{\rightarrow} PO(B^{2}\Sigma^{+}) +$ PO( $X^{2}\Pi$ ). The existence of the (PO) $_{2}^{*}$  excimer has been confirmed by affecting the dynamics of this equilibrium through dilution with buffer gas and through thermal dissociation of the excimer, resulting in the appearance of the formerly quenched (0,0) transition of the PO  $\beta$ -emission in the spectrum. Our investigation has eliminated the possibility that the visible continuum

arises from either  $PO_2$  or HOPO. Enough information has been extracted from temperature dependent studies to construct the approximate shapes of the potential energy surfaces of the ground  $(\Delta \overline{\nu}_g = 35 \pm 200 \text{ cm}^{-1})$  and the first excited states  $(\Delta \overline{\nu}_{ex} = 846 \pm 200 \text{ cm}^{-1})$  of the  $(PO)_2^*$  excimer.

The classic case of phosphorescence of solid phosphorus has been studied previously in the vapor phase and as a surface oxidation chemiluminescence reaction. A modern spectroscopic study of this historically best known chemiluminescence system has been lacking. In this paper we have investigated the chemiluminescence system of  $P_4$  vapor in the oxidation reaction in the presence of air, with added  $H_2O$  or  $D_2O$  vapor. Small polyatomic molecular species are readily identified from discrete band emission. The main band emission in the visible region, which cannot be identified with any simple electronic transition, is the focus of attention in this paper.

#### I. HISTORICAL PERSPECTIVE

The generally recognized discoverer of phosphorus glow is Henning Brand, who originally devised a process for isolating pure phosphorus in 1669. 
Because of the secrecy surrounding Brand's isolation process, scientific investigation of the phenomenon really began with Robert Boyle, the most notable of the early workers, who independently discovered and published a process for isolating pure phosphorus. He established the requirement of air for the generation of chemiluminescence, and observed an erratic dependence of the chemiluminescence intensity on the concentration of air. DeFourcroy extended this observation and determined the upper and lower bounds of oxygen pressure for chemiluminescence. In the late ninteenth century Dixon and Baker, working independently, discovered that water was necessary in the luminescence reaction; rigorously dried phosphorus and oxygen are stable in the absence of water vapor, even when heated to 290°C. The first suggestion as to the identify of the emitting species originated in 1890 with Thorpe and Tutton, who, from studies of phosphorus trioxide oxidation, proposed P<sub>2</sub>O<sub>5</sub>

as the major emitter. In 1924 Downey discovered that, in addition to the visible glow, the reaction emits a sufficient amount of short wavelength radiation to produce ionized particles and ozone in the reaction sphere.4 A year later Emeleus found that similar visible and uv emission arises from burning phosphorus hydride (PH<sub>3</sub>) in air and in oxygen.<sup>5</sup> In 1928 Bowen determined the quantum yield of the reaction to be at least one visible photon per 2000 P<sub>4</sub> molecules oxidized, a surprisingly low value. 6 Miller in 1929 established that the intermediate oxides of phosphorus are not the emitting species; in fact,  $P_2O_3$  is an inhibitor of phosphorus chemiluminescence.<sup>7</sup> Kinetic studies by Semenoff in 1928 established that a chain reaction occurs and that there is an upper and lower bound of oxygen pressure in sustaining the reaction. 8 From the spectral correspondence to phosphorus chemiluminescence at atmospheric pressure of phosphorus glow from a Geissler tube (electric discharge), Ghosh and Ball in 1931 suggested that the emitting species was PO.9 Ghosh and Ball's work influenced subsequent researchers to concentrate on electric discharge studies rather than studying the reaction under atmospheric conditions. 10-22

The PO emission as proposed by Ghosh and Ball can account for the ultraviolet emission from phosphorus chemiluminescence, but it cannot directly explain the visible emission, consisting of a continuum upon which are superimposed a number of weak bands in the green. Some attempts have been made to attribute the continuum to polyatomic molecules such as  $PO_2^{23}$  and  $HOPO.^{24}$ 

In a previous communication we have suggested that <u>i</u>)  $(P0)_{2}^{*}$  excimers formed between a ground state PO molecule and an electronically excited PO molecule are responsible for the continuum, and that <u>ii</u>) the discrete structure superimposed on the continuum arises from HPO. In this paper we examine the existence of the  $(P0)_{2}^{*}$  excimer based on an investigation of the

effects of temperature variation and dilutant gas on the chemiluminescence spectrum. A moisture dependence study and substitution of  $D_2O$  vapor for  $H_2O$  vapor in the reaction further confirm our identification of the transient emitting species in the phosphorus green flame as PO, HPO and  $(PO)_2^*$  excimer, and conclusively demonstrate that the continuum emission cannot arise from any protonated species such as HOPO. Thermal studies also rule out the possibility of  $PO_2$  being involved in the continuum emission in any major way.

II. EXPERIMENTAL CONDITIONS

### II. EXPERIMENTAL CONDITIONS

The white phosphorus used in these experiments was obtained from Baker, the nitrogen from Airco, deuterium oxide from Columbia Company (99.5% purity). Low resolution emission spectra were recorded with a 0.3 meter McPherson Model 218 Monochromator using an EMI 9558 QB Photomultiplier, an Eldorado Model 201 Universal Photometer and a Sargent Model TR Recorder. Spectra were also taken with a Heath EU-7000 .5 meter Monochromator with an RCA 1P28 Photomultiplier, a Heath Photometer and a Sargent Model SR Recorder. Figure legends indicate the exact instrumentation used in recording the spectrum depicted.

Medium resolution spectra were taken with similar instrumentation, scanning at slower speeds and narrower slit widths. In this paper the overall spectral characteristics are discussed with reference to low resolution spectra for emphasis, but spectral assignments and activation energy studies were made with reference to medium resolution spectra.

## Room Temperature Spectra

The phosphorus was placed in a 50 ml glass flask immersed in a water bath  $(57^{\circ}\text{C})$ . Nitrogen saturated with water or deuterium oxide at room temperature passed through the flask and, carrying with it  $P_4$  vapor, was led into a 3 mm glass tube. Chemiluminescence occurred at the end of the 3 mm tube, with air being used as the source of molecular oxygen.

## Temperature Dependent Spectra

The phosphorus and nitrogen were treated as described in the previous paragraph. The vapor stream then contained nitrogen gas, saturated with  $H_2O$  (or  $D_2O$ ) vapor at room temperature and with  $P_4$  vapor at  $60^{\circ}C$ . Two methods

were used to heat the vapor stream. Method (a) the quartz tube containing the pre-mixed stream was heated electrically by nichrom wire sandwiched between layers of asbestos tape wrapped around the tube. The temperature of the flame at the end of the quartz tube was measured by a thermocouple, and spectra were taken of the flame. Method (b) the pre-mixed flow of phosphorus, nitrogen and  $H_2O$  ( $D_2O$ ) vapor prepared as indicated above was led through a 3 mm quartz tube heated electrically as in method (a). The composite system was inserted into a wider quartz tube surrounded by asbestos. The quartz reaction chamber was heated electrically by nichrom wire sandwiched between the asbestos layers. A window in the asbestos cover near the end of the internal quartz tube allowed the spectrum to be taken while the chamber was kept heated to a constant temperature. The temperature was monitored by a thermocouple seated near the base of the flame.

# Concentration Dependent Spectra

A 50 ml flask containing phosphorus was heated in a constant temperature water bath at 60°C. Nitrogen saturated with water vapor at room temperature passed through this flask at a constant flow rate. The nitrogen stream, carrying with it P<sub>4</sub> vapor and H<sub>2</sub>O vapor, then entered the dilution chamber, a 50 ml glass flask. A second source of nitrogen at a constant flow rate was connected to the dilution chamber, enabling dilution of the reactants while maintaining a constant flow of phosphorus vapor into the dilution chamber. The diluted stream entered a 3 mm quartz tube, heated electrically as in method (a) above. Chemiluminescence occurred at the end of the 3 mm tube, and the spectrum was recorded.

## Dried Sample

To study the effect of drying the sample, the phosphorus used was previously distilled over  $P_2O_5$  in a closed system in the absence of air, then the flask containing the distilled phosphorus was heated electrically to about  $60\,^{\circ}\text{C}$ . Nitrogen from a cylinder was bubbled through concentrated sulfuric acid, then through a U-tube containing phosphorus pentoxide. The nitrogen stream then entered the flask containing the distilled phosphorus and passed into the reaction chamber, carrying with it  $P_4$  vapor. Molecular oxygen from a cylinder was bubbled through concentrated sulfuric acid and then through a U-tube containing phosphorus pentoxide before entering the reaction chamber, a long quartz tube where the nitrogen and oxygen streams were allowed to mix freely. Chemiluminescence occurred at the end of the nitrogen outlet, a 3 mm glass tube within the reaction chamber.

### Cross-section of the Flame

To study the homogeneity of the flame with respect to ratios of the emitting species, a system similar to that in the section on Temperature Dependent Spectra, Method (a), was used, except that the heated tube was 7 mm in diameter. Several horizontal cross-sections of area 2 x 3 mm of the resulting conical flame, 40 mm in length and 7 mm wide at the base, were spectrally analyzed. This was done at room temperature and at 320°C.

Roc

of ing

sib sio

con

tio

med

ind

ing ban

of

sys ato

455

are

spec find

Or t

1

crea

### III. RESULTS AND DISCUSSION

# Room Temperature Spectra

The work of Dixon and Baker established that at least a catalytic amount of water vapor was essential to the chemiluminescence reaction accompanying phosphorus oxidation by molecular oxygen and suggested to us the possibility that substitution of  $D_2O$  vapor for  $H_2O$  vapor might effect the emission. Figure 1 is a low resolution spectrum of phosphorus glow under ambient conditions (room temperature, atmospheric pressure and saturation with water vapor). Figure 2 was taken under the same conditions except for the substitution of  $D_2O$  vapor for  $H_2O$  vapor. Actual spectral assignments were made from medium resolution studies of the same systems.

The discrete band structure superimposed on the continuum in the 450-650 nm region in Figure 1 shows a clearly recognizable isotopic shift in Figure 2, indicating deuterium incorporation in the emitting species. There is a striking enhancement of emission intensity and the appearance of a number of new bands in this region. Table I is a comparison from medium resolution spectra of the four most intense bands in the 450-650 nm region of the  $D_2O$  and  $H_2O$  systems with similar bands found by Lam Thanh and Peyron in the reaction of atomic hydrogen atomic oxygen and phosphorus in gas discharge. These bands are assigned as  $\tilde{A}(^1A'') \rightarrow \tilde{X}(^1A')$  in HPO and DPO. 28

The only transition so far identified in HPO and DPO is  $\hat{A} \rightarrow \hat{X}$  around 465-680 nm. Under gas discharge conditions deuterium substitution in this species is difficult to effect, in contrast to the ease of substitution we find under our experimental conditions. No detailed information is available on the electronic structure of the transient species HPO. However, the increase in structure and marked intensity enhancement in the emission from

in

DPO, compared to that of HPO, suggests a predissociation in the excited states of HPO reminiscent of that found by Clement and Ramsey for HNO. <sup>31</sup> Clement and Ramsey established a predissociation in these species (48.6 kcal/mole for HNO and 49.1 kcal/mole for DNO) and observed that the 12 emission bands associated with HNO in the region 600-900 nm increased to 18 bands in the DNO spectrum, with an accompanying increase in intensity. This increase in structure and intensity in such small radicals as HPO and HNO indicates a pronounced general effect of deuterium substitution on the radiationless transition processes, consistent with current theories of radiationless transitions. <sup>32</sup>

The discrete bands in Figures 1 and 2 at 228.8-272.1 nm correspond to PO bands investigated by Ghosh and Ball, and the assignment for these bands is PO  $\gamma$ -system,  $A^2\Sigma^+ \rightarrow X^2\Pi$ . At higher sensitivity and resolution, some of the very weak bands in the 325.0-337.0 nm region can be assigned to PO  $\beta$ -system,  $B^2\Sigma^+ \rightarrow X^2\Pi$ . In studies of the glow associated with phosphorus and atomic oxygen in an electric discharge, the most intense emission arises from the PO  $\beta$ -system;  $^{18},^{24}$  whereas, in our studies at atmospheric pressure most of the emission is from the continuum, and the PO  $\beta$ -system emission is barely discernible. As expected, neither the PO  $\beta$  or  $\gamma$  emissions show frequency shifts indicating deuterium incorporation. The frequency distribution of the continuum is also unaffected by deuterium substitution, although the area under the spectral curve of the continuum is decreased.

The overall spectral characteristics, a quenched monomer (FO  $\beta$ -system) adjacent to a red-shifted, diffuse emission band, are strongly suggestive of excimer formation. An excimer is an excited state dimer in which one member of the molecular pair is electronically excited, and the other is in its ground electronic state. Under the influence of coulombic and exchange interaction between the monomers, the excited state of the excimer complex

is stabilized to a greater extent than is the ground state. As a consequence, the emission spectrum of an excimer is in general red-shifted in comparison to the monomer emission. The usual methods for excimer identification are not applicable to our investigation since we have no rigorous control over the concentration of the excited species in the chemiluminescent reaction. As a consequence, we were obliged to devise four diagnostic tests for the identification of the  $(PO)_2^*$  excimer which are applicable to our experimental system:

- 1. Thermal dissociation of the excimer should occur with a concommittant increase in the intensity of the monomer emission in the spectrum.
- 2. The dynamics of the excimer equilibrium with the monomer should be affected by dilution with inert gas.
- 3. The dynamics of the excimer equilibrium with the monomer should be affected by changes in the total pressure of the system.
- 4. Since the ground state of the excimer is dissociative, there should be an absence of direct absorption from the excimer ground state to its excited state.

In identifying an excimer in the phosphorus flame, spectroscopic evidence of criteria 1) and 2) is of central importance. Criterion 3) is a somewhat weaker argument, and 4), being a negative criterion, is least evidential. In planning our experimental attack, we have emphasized criteria 1) and 2). There is circumstantial evidence for 3) in the literature. 18,24 Our attempts to establish criterion 4) were consistent with the expected results; i.e.,

ç

F)

di

co

5.77

st

նև

fo

pro

ass atn

e<u>x</u>(

Mon

we were unable to identify any absorption band associated with the visible continuum observed in the emission spectrum. This cannot be taken as definitive, however.

To elucidate the nature of  $(PO)_{2}^{*}$  excimer formation and its consequent spectral properties, we begin by presenting a potential energy diagram for PO (Figure 3) originally published by Verma, 20 and somewhat modified by us for clarity in the present discussion. Once PO is generated in an electronically excited state, the energy then degrades to the lowest excited electronic state, the forbidden <sup>4</sup> II state, possibly through a mechanism of dipole-dipole interaction between two PO molecules similar to that in NO as proposed by Gordon and Chiu. Radiative transitions from collision complexes or excimer complexes involving higher excited states of PO are in direct competition with radiationless degredation to lower electronic states, and the probability of direct emission from such collision complexes is small, resulting in an accumulation of energy in the <sup>4</sup>II state which is metastable and is the lowest excited electronic state of PO. Because of the metastability of the  $^4\,\mathrm{II}$  state, excimer formation between a PO molecule in the  $^4\,\mathrm{II}$ state and a ground state PO molecule is a probable event, particularly under our experimental conditions of high concentration and high pressure. Excimer formation is less likely under gas discharge conditions where much lower pressures and concentrations are involved. In fact in gas discharge studies there are only indirect manifestations of weak emissions which could be associated with the visible continuum seen in phosphorus chemiluminescence at atmospheric pressure (criterion 3). 18,24 Because of their low binding energy, excimers in general are labile to thermal dissociation to generate the monomer in an excited state. In the case of  $(PO)_{2}^{*}$  the dissociation would

be  $(PO)_2^* \neq PO(^4\Pi) + PO(X^2\Pi)$ . Since the radiative transition  $^4\Pi + X^2\Pi$  is spin forbidden and the  $^4\Pi$  and  $B^2\Sigma^+$  states are close enough energetically for thermal population to occur, we expect the (0,0) transition of the PO  $\beta$ -system to appear on thermal dissociation of the excimer (criterion 1). The equilibrium reaction would be  $(PO)_2^* \neq PO(^4\Pi) + PO(X^2\Pi) \neq PO(B^2\Sigma^+) + PO(X^2\Pi)$ . We also expect an effect of the concentration of buffer gas on the intensity of the PO  $\beta$  emission above temperatures where the excimer equilibrium favors dissociation to the monomers (criterion 2).

# Temperature Dependent Studies

Figures 4 and 5 are temperature dependent studies of the chemiluminescence from  $P_4$  vapor at atmospheric pressure, saturated with  $H_2O$  vapor or  $D_2O$  vapor. In Figure 4 with increasing temperature, there is an appearance and a marked increase of emission from the (0,0) transition of the PO  $\beta$ -system at 320 nm. This is as predicted from criterion 1 since the excimer dissociates with increasing temperature. In Figure 4 there is also an overall decrease of total luminosity and an apparent decrease in the intensity of emission from the HPO and PO  $\gamma$ -systems.

Figure 5 is a similar temperature study using  $D_2O$  vapor in place of  $H_2O$  vapor. Again with rising temperature, emission from the (0,0) transition of the PO  $\beta$ -system becomes increasingly pronounced. As in the room temperature spectra, the DPO bands of Figure 5 are stronger and more structured than the HPO bands of Figure 4. At 335°C we find a new band system around 300 nm which may be either a  $P_2$  or an OD transition. Further analysis of these bands is in progress.

In view of the complexities of a dynamic system subject to multiple branch chain reactions,  $^{8}$  it is not surprising that the overall luminosity

of the system decreases with increasing temperature. However, for an approximate kinetic analysis, we have normalized the data with respect to total luminosity, in order to find the variation in relative species concentration at each temperature. Normalization enables us to obtain the binding energy of the excimer by an Arrhenius plot  $(I/I_0 = Ae^{-\Delta E/kT})$  where  $\Delta E$  is the stabilization energy, the energy difference between the first excited state of the excimer and the  $B^2\Sigma^+$  electronic state of PO (v' = 0).

In Figure 6a is a plot of log I vs 1/T where I is the total area under the spectral curve of the PO  $\beta$  (0,0) emission, taken from medium resolution spectra. Triangular points are from the reaction using H<sub>2</sub>O vapor and circled points from the reaction using D<sub>2</sub>O vapor. A least square fit method using the KINET program was employed in analyzing the data. 35 The line drawn by the computer gives an activation barrier of  $\Delta E = 846\pm200$  cm<sup>-1</sup> (in drawing the line, points originating from the reaction with H<sub>2</sub>O vapor and with D<sub>2</sub>O vapor were considered jointly). Scattering of data points occurs at the two temperature extremes. At low temperature PO B emission is extremely weak, and at high temperature the temperature stability of the chemiluminescence flame is difficult to maintain, resulting in higher uncertainty at these temperatures. Figure 6b is a similar plot using the PO y-system bands. There is an initial increase of  $\gamma$ -system intensity with increasing temperature up to about  $370\,^{\circ}K$ . Above 370°K the emission is thermally quenched with  $\Delta E = 650\pm26$  cm<sup>-1</sup>. Figure 6c shows the HPO and DPO emission intensity variation with temperature,  $\Delta E = 107 \pm 47 \text{ cm}^{-1}$ .

Using the results of Figure 6a, we have constructed an approximate potential energy diagram (Figure 7) for the  $(PO)_2^*$  excimer. The relative energies of the PO monomer states are shown on the right hand side of the

figure. The excited state stabilization of the excimer with respect to the monomer states,  $\Delta \overline{\nu}_{\rm ex}$  is  $\Delta E$  calculated from Figure 6a. To get an approximate value for  $\Delta \overline{\nu}_{\rm g}$ , the ground state stabilization of the excimer with respect to the monomer states, we need  $\overline{\nu}_{\rm oo}$  (excimer), the onset of the continuum emission at the shortest wavelength at 0°K. Estimating this value to be 335 nm (29,850 cm<sup>-1</sup>) from the spectral behavior, and since  $\overline{\nu}_{\rm oo}$  (PO  $\beta$  system) = 30,731 cm<sup>-1</sup>,  $\Delta \overline{\nu}_{\rm g} = \overline{\nu}_{\rm oo}$  (PO  $\beta$ -system) -  $\overline{\nu}_{\rm oo}$  (excimer) -  $\Delta \overline{\nu}_{\rm ex} = 35^{\pm}200$  cm<sup>-1</sup>. Within our experimental limits, the ground state of the excimer is clearly dissociative. It is interesting to note that Dinerman and Ewing have found a ground state stabilization of about 200 cm<sup>-1</sup> for the dimer (NO...NO).

## Dilution Studies

A further confirmation of the excimer nature of the continuum emission is given by Figure 8, in which the phosphorus glow at about  $300^{\circ}$ C was studied as a function of dilutant gas (nitrogen). Spectrum (a) has a higher flow rate of nitrogen and evinces a marked enhancement of emission from the (0,0) FO  $\beta$ -system transition. This is an unequivocal confirmation of criterion 2. The rest of the spectrum is relatively unaffected by dilution.

By analogy with NO<sub>2</sub> where the recombination reaction NO + 0 + NO<sub>2</sub><sup>\*</sup> gives rise to a diffuse chemiluminescence, it has been suggested that the visible continuum in phosphorus chemiluminescence arises from a similar reaction PO + 0  $\rightarrow$  PO<sub>2</sub><sup>\*</sup>. However, it should be pointed out that the NO<sub>2</sub> chemiluminescence is a recombination or associative chemiluminescence, and no emission from the excited state of NO is observed in the dissociation reaction. The fact that we observe the (0,0) transition from the PO  $\beta$ -system on thermal dissociation of the species responsible for the continuum and that this emission is also subject to an increased intensity with increasing buffer gas would clearly eliminate the possibility that the recombination reaction PO + O  $\rightarrow$  PO<sub>2</sub><sup>\*</sup> is responsible for the continuum.

E a

> H 0

> > t t

14

S S

s t

In th

## Dried Sample

The continuum emission in phosphorus chemiluminescence has also been attributed to HOPO by analogy with HONO, which exhibits predissociative behavior in the near uv region. 24 The emission spectrum (Figure 9) obtained using previously dried reactants shows a pronounced relative increase in the intensity of the continuum emission with respect to the HPO emission, which argues against the involvement of HOPO or any other protonated species. The HPO bands of Figure 9 are very weak, and it is clear that most of the intensity of the visible emission originates from the continuum. Under very stringent drying conditions, Dixon and Baker failed to see, by visual observation, any chemiluminescence when dried phosphorus was placed in contact with dried molecular oxygen. 8 In our system we evidently have sufficient water vapor to sustain the reaction. A critical examination of the work of Dixon and Baker is currently underway.

## Cross-section of the Flame

The cool chemiluminescent phosphorus glow is a diffusion limited flame  $^{37}$  with luminescent reactions taking place at the interface of  $P_4$  vapor and atmospheric oxygen. As is the case with a diffusion flame, all short lived species are present in every macroscopic cross-section. All the emitting species involved are expected to have very short lifetimes because they undergo allowed transitions,  $^2\Sigma^+ \rightarrow ^2\Pi$  or  $^1A'' \rightarrow ^1A'$ . In these studies the relative ratios of emission of PO- $\gamma$ , PO- $\beta$ , HPO (DPO) and (PO) $^*_2$  remained the same in any small horizontal rectangular section of the flame. This was true from the base to the tip of the flame at both temperatures monitored. In terms of the ratios of the emitting species in the visible and ultraviolet, this means that the position of the flame is not important relative to the

slit of the monochromator. The only difference in going from one horizontal section to the next was in absolute emission intensity. In the dark portion of the plume very near the tip of the flame we have observed some new, much weaker emission in the 700-800 nm region, and an analysis of this emission will be reported later.

### IV. SOME MECHANISTIC CONSIDERATIONS

The reaction of molecular oxygen, phosphorus and water vapor under atmospheric conditions is a gas phase reaction of  $P_4$  giving the final product  $P_4O_{10}$ . Bowen and Pells established that, as a lower limit in the chemiluminescence reaction, at least one visible photon is produced per 2000  $P_4$  oxidized molecules. In this investigation we have identified some of the transient emitting species, electronically excited PO and HPO molecules. It is not clear whether all the PO molecules are created in the excited state and subject to a potent quenching process, or if only a small fraction of the reaction proceeds via electronically excited PO, as would seem to be suggested from the low quantum yield. The reaction is highly exothermic, yet does not produce local heating, as is evident from the cool flame; hence, electronic excitation may be the major energy channel.

From gas discharge studies of atomic oxygen and atomic phosphorus, Walsh, by analogy to NO, proposed the following mechanism for the generation of PO excited states:

$$P(^{4}S) + O(^{3}P) + PO(X^{2}\Pi) = PO(X^{2}\Pi) + PO(A^{2}\Sigma^{+} \text{ or } B^{2}\Pi).$$

Due to energetic considerations, he predicts a sharp cut-off of PO emission above the  $B^2\Sigma^+$  state (v' = 10) which is consistent with gas discharge results. However, at atmospheric pressure we see indications of emission associated with highly excited  $C(^2\Sigma^-)$  and  $C'(^2\Lambda)$  electronic states (see Figure 10 and Table II). Thermodynamically the creation of these states is possible since for the reaction  $P_4(g) + SO_2(g) \rightarrow P_4O_{10}(s)$   $\Delta H = 730$  kcal/mole. The relative intensities of emissions from PO  $\beta$ - and  $\gamma$ -systems under gas discharge conditions

change greatly at atmospheric pressure. For these reasons, it is unlikely, therefore, that the generation of excited PO\* proceeds by the same mechanism in both cases.

Once generated in an electronically excited state, PO is the central species in the luminescence process. The major radiative modes of decay are the following:

- 1.  $\gamma$ -band:  $PO(A^2\Sigma^+) + PO(X^2II) + h\nu$ .
- 2.  $\beta$ -band:  $PO(B^2\Sigma^+) \rightarrow PO(X^2\Pi) + h_V$ .
- 3. Visible Excimer Emission:

$$PO(B^{2}\Sigma^{+}) + PO(X^{2}\Pi) \neq PO(^{4}\Pi) + PO(X^{2}\Pi) \neq (PO)^{*}_{2}$$
  
 $(PO)^{*}_{2} + 2PO(X^{2}\Pi) + h_{V}.$ 

At atmospheric pressure HPO (DPO) emission arises from the transition

4. 
$$A(^{1}A'') \rightarrow X(^{1}A') + h_{V}$$
.

The generation of HPO in the phosphorus chemiluminescence reaction may proceed by a mechanism similar to the sequence proposed by Ibaraki,  $\underline{\text{et al.}}$ , 39 for the generation of HNO from a cross molecular beam study of the chemiluminescence of H + NO:

$$H + N_2O_2 \rightarrow HNO^* + NO$$
  
 $HNO^* \rightarrow HNO + hv.$ 

It is worthwhile to note that although in discussing the oxides of phosphorus we have several times reasoned by analogy with the behavior of the oxides of nitrogen, the two cases are analogous only to a limited extent.

The detailed electronic structure of PO must differ from NO in the dimension and charge distribution of the orbitals and, more importantly in this discussion,

in spin-orbit coupling parameters which determine the ease with which the  ${}^4\Pi$  state of PO or NO would be populated from the  ${}^2\Sigma^+$  state. These parameters would play a critical role in the formation of an excimer from either species. It has been suggested that the continuum emission in phosphorus chemiluminescence originates from PO<sub>2</sub> by analogy with NO<sub>2</sub>. However, the appearance of PO  $\beta$ -system emission with increasing temperature (criterion 1 for excimer formation) in our thermal study is not analogous to the behavior of the NO<sub>2</sub> chemiluminescence system; i.e., thermal dissociation of NO<sub>2</sub> does not lead to the appearance of emission from the lowest allowed electronic excited state of NO, the  $\gamma$ -system.

#### V. SUMMARY

In this paper we have analyzed the visible and ultraviolet spectrum of the oxidation of  $\mathbf{P}_4$  vapor in the presence of moist air at atmospheric pressure. In spectral studies of small horizontal rectangular cross-sections of the phosphorus flame, the relative ratios of emission from the transient species remained the same regardless of the cross-section chosen, which permits accurate spectral analysis of the chemiluminescence. By investigating the effects of temperature variation, dilutant gas and deuterium substitution, we have demonstrated that the major emitting species in the cool phosphorus green flame is (PO) \* excimer and have identified HPO bands in the chemiluminescence for the first time. Our investigation has eliminated the possibility that the visible continuum arises from either PO2 or HOPO. Some weak transitions from the  $C(^2\Sigma^-)$  and  $C'(^2\Delta)$  states have also been observed, indicating that the mechanism of the reaction at atmospheric pressure differs from that in the reaction of atomic phosphorus and atomic oxygen in gas discharge experiments. From thermal studies estimates of the binding energies of the excimer in its first excited state (846±200 cm<sup>-1</sup>) and in the ground state (35±200 cm<sup>-1</sup>) have been calculated. Enough information has been extracted to construct the approximate shapes of the potential energy surfaces of the  $(PO)_{2}^{*}$  excimer.

Further investigation at higher resolution is necessary so that the intensity variations of each vibronic state can be followed more closely. Of particular interest is a high resolution study using deuterium substitution of the conjoint variations of the HPO system and the PO  $\beta$ - and  $\gamma$ -systems. To date there has been no spectral attempt to investigate the vacuum uv emission. Quantum yield measurements of the reaction need to be repeated. Several of these projects are underway in our laboratory.

#### REFERENCES

- 1. E. N. Harvey, "A History of Luminescence", The American Philosophical Society, Philadelphia, PA., 1957. (For a discussion of the early history, this is a comprehensive and excellent review.)
- 2. H. B. Baker, J. Chem. Soc., 47, 340 (1885); Phil. Trans. 179A, 571 (1888).
- 3. T. E. Thorpe and A. E. Tutton, J. Chem. Soc. (Trans.), <u>57</u>, 545 (1890); <u>59</u>, 1019 (1891).
- 4. W. E. Downey, J. Chem. Soc., 125, 347 (1924).
- 5. J. Emeleus, J. Chem. Soc., 127, 1362 (1925).
- 6. E. J. Bowen and E. G. Pells, J. Chem. Soc., 1096 (1927).
- 7. C. C. Miller, J. Chem. Soc., 1823 (1929).
- 8. N. Semenov, Z. Physik., 46, 109 (1928).
- 9. P. N. Ghosh and G. N. Ball, Z. Physik., 71, 362 (1931).
- 10. K. Dressler, Helv. Phys. Acta., 28, 563 (1958).
- 11. K. K. Durga and P. T. Rao, Indian J. Phys., 32, 223 (1958).
- 12. N. L. Singh, Can. J. Phys., 37, 136 (1959).
- 13. H. Guenebaut, C. Couet and Houlon, C. R. Acad. Sc., (Paris) <u>258</u>, 3457 (1964); ibid., 258, 6370 (1964).
- 14. B. Coquart, C. Couet, N. Tuan Anh, and H. Guenebaut, J. Chim. Phys. Physicochim. Biol., 64, 1197 (1967).
- 15. M. N. Dixit and N. A. Narashimham, Proc. Indian Acad. Sci., 68, 1 (1968).
- R. D. Verma and M. N. Dixit, Can. J. Phys., 46, 2079 (1968).
- 17. R. D. Verma, Can. J. Phys., 48, 2391 (1970).
- 18. R. D. Verma and H. P. Broida, Can. J. Phys., 48, 2991 (1970).
- 19. R. D. Verma, Can. J. Phys., 49, 279 (1971).
- R. D. Verma, M. N. Dixit, S. S. Jois, S. Nagaraj, and S. R. Singhal,
   Can. J. Phys., 49, 3180 (1971).
- 21. R. D. Verma and S. S. Jois, Can. J. Phys., 51, 322 (1973).
- 22. R. D. Verma and S. R. Singhal, Can. J. Phys., 53, 411 (1975).

- 23. H. Cordes and W. Witschel, Z. Physik. Chem., 46, 35 (1965).
- 24. P. B. Davies and B. A. Thrush, Proc. Roy. Soc. A., 302, 243 (1968).
- 25. R. J. VanZee and A. U. Khan, J. Amer. Chem. Soc., 96, 6805 (1974).
- 26. M. Lam Thanh and M. Peyron, J. Chim. Phys. Physicochim. Biol., <u>59</u>, 688 (1962).
- 27. Ibid., 60, 1289 (1963).
- 28. Ibid., 61, 1531 (1964).
- 29. Ibid., 63, 266 (1966).
- 30. See G. Herzberg, "Molecular Spectra and Molecular Structure, III. Electronic Spectra and Electronic Structure of Polyatomic Molecules", D. VanNostrand, New York, NY, 1966.
- 31. M. J. Y. Clement and D. A. Ramsay, Can. J. Phys., 39, 205 (1961).
- 32. See N.Mataga and T. Kubota, "Molecular Interactions and Electronic Spectra", Marcel Dekker, Inc., New York, 1970.
- 33. See J. B. Birks, "Photophysics", Wiley-Interscience, New York, NY, 1970.
- 34. R. G. Gordon and Ying-Nan Chiu, J. Chem. Phys., 55, 1469 (1971).
- 35. J. L. Dye and V. A. Nicely, J. Chem. Ed., 48, 433 (1971).
- 36. C. E. Dinerman and G. E. Ewing, J. Chem. Phys., 53, 626 (1970).
- 37. See A. G. Gaydon and H. G. Wolfhard, "Flames", Chapman and Hall Ltd., London, 1970, p. 141.
- 38. A. D. Walsh in "The Threshold of Space", M. Zelikoff, Ed. Pergamon Press, London, 1957, p. 165.
- 39. T. Ibaraki, K. Kodera, and I. Kusunoki, J. Phy. Chem., 79, 95 (1975).

TABLE I

Electronic Transition (in cm <sup>-1</sup> ) Lam Thanh, et al.				This Work	
( v' 1 v' 2 v' 3)	(v" <sub>1</sub> v" <sub>2</sub> v" <sub>3</sub> )	HPO	DPO	НРО	DPO
(000)	<b>+</b> (000)	19,047	19,117	19,030	19,100
(000)	<b>→</b> (001)	18,062	18,367	18,050	18,360
(000)	<b>+</b> (010)	17,860	17,931	17,850	17,930
(000)	<b>→</b> (002)	17,091	17,646	17,100	17,630

TABLE II

Assigned Transition 18	$\lambda_{air}^{}$ (Å) 18	This Work
v' - v''		
$c^2\Sigma^ x^2\Pi$		
$\frac{c^2 \Sigma^ \chi^2 II}{(n+6)^* - 1}$	1997.5	1996
(n+6) - 1	2006.2	2007
(n+9) - 3	2022.2	2021
(n+7) - 3	2072.6	2071
(n+7) - 3	2078.4	2077
(n+7) - 4	2130.9	2130
(n+1) - 1	2148.4	2147
(n+1) - 1, (n+4) - 3	2160.2	2160
(n+9) - 6	2164.9	2164
(n+4) - 3	2170.1	2168
(n+9) - 6	2175.7	2174
(n+3) - 3	2205.0	2205
(n+1) - 3	2266.3	2263
(n+1) - 3	2277.3	2275
$C'^2\Delta - X^2II$		
3 - 1	2229.8	2227
6 - 3	2238.0	2238
1 - 0, 6 - 3	2247.3	2246

n is an unknown number.

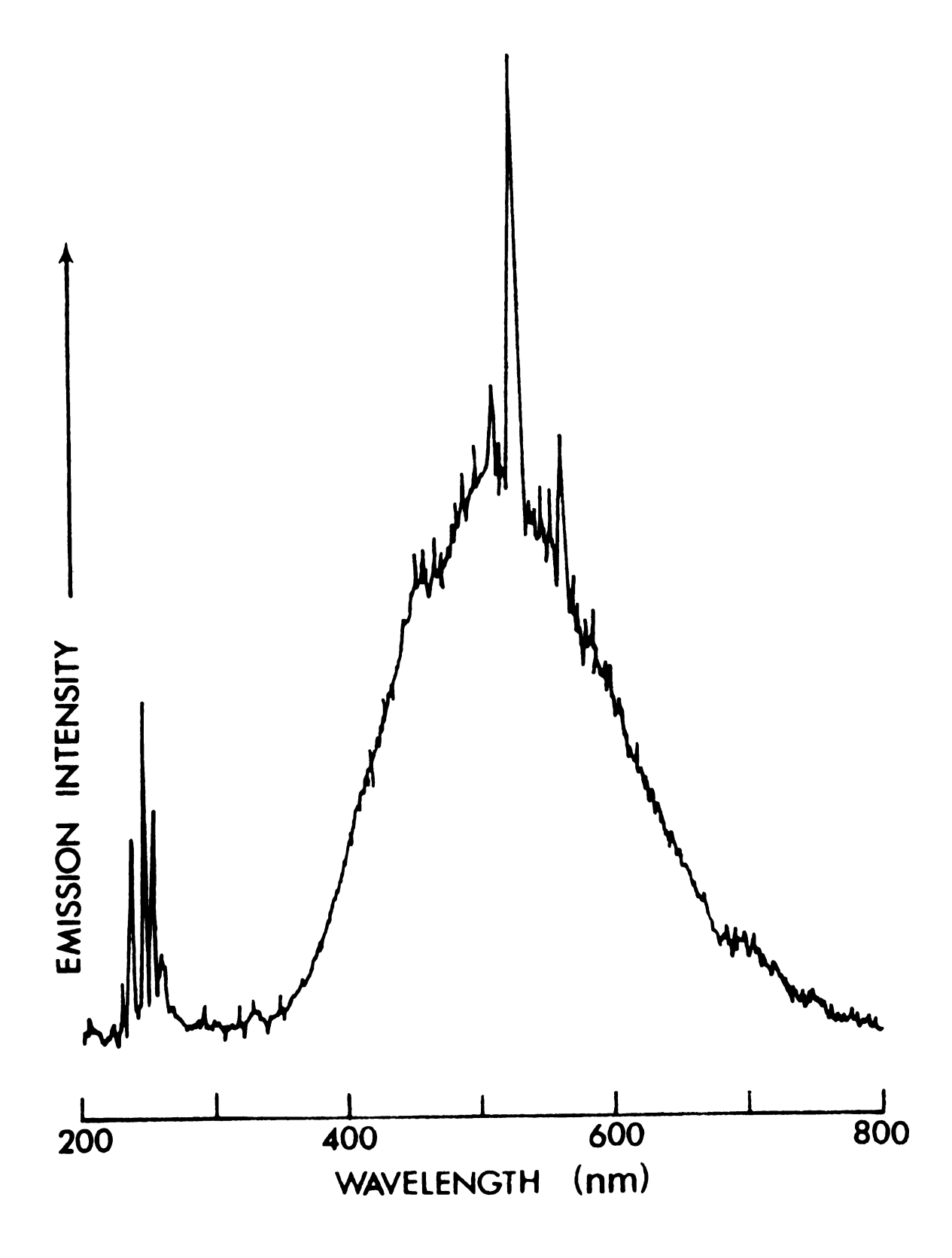
### FIGURE CAPTIONS

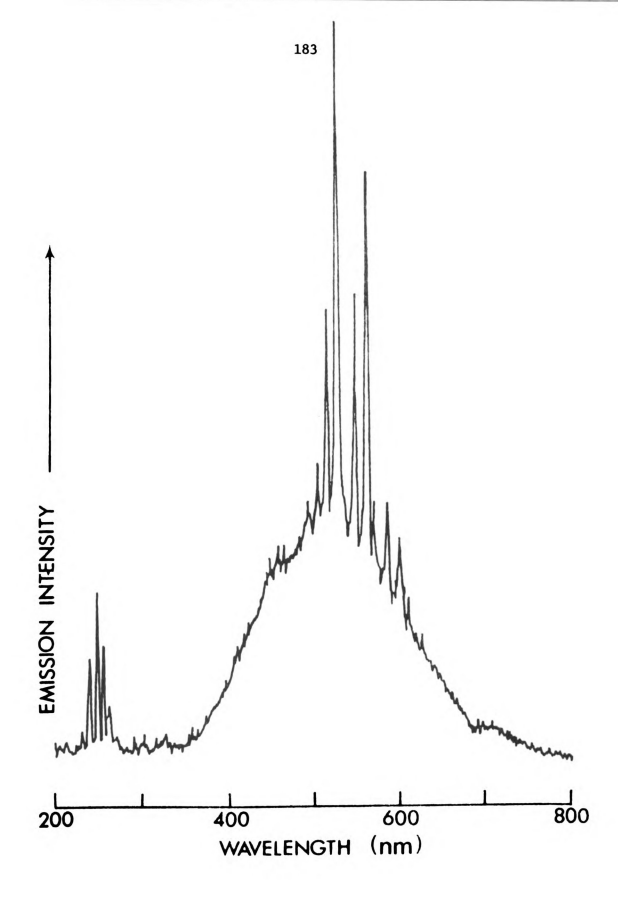
- Fig. 1 Chemiluminescence spectrum of the room temperature reaction, on contact with air, of P<sub>4</sub> vapor and H<sub>2</sub>O vapor carried by a nitrogen stream. Taken with a McPherson monochromator and an EMI 9558QB photomultiplier. The discreet bands at 228.8-272.1 nm correspond to PO-γ bands, those at 450-650 correspond to HPO emission.
- Fig. 2 Chemiluminescence spectrum of the room temperature reaction, on contact with air, of P<sub>4</sub> vapor and D<sub>2</sub>O vapor carried by a nitrogen stream. Taken with the same equipment as Fig. 1. The discreet bands at 450-650 nm correspond to DPO emission.
- Fig. 3 Potential energy diagram for the PO molecule taken from Verma, et al., 20 slightly modified.
- Fig. 4 Temperature dependent chemiluminescence spectra for the reaction, on contact with air in a heated chamber, of  $P_4$  vapor and  $H_2O$  vapor carried by a heated nitrogen stream (method (b) in the text). Taken with a Heath monochromator and RCA 1P28 photomultiplier. Emission from the(0,0) transition of the PO  $\beta$ -system in the region 320-340 nm increases dramatically with increasing temperature. Temperature is in  $^{\circ}C$ . The discreet bands at 325.0-337.0 nm correspond to PO- $\beta$  bands.
- Fig. 5 Temperature dependent chemiluminescence spectra for the reaction, on contact with air in a heated chamber, of P<sub>4</sub> vapor and D<sub>2</sub>O vapor carried by a heated nitrogen stream (method (b) in the text). Taken with the same equipment as Fig. 4.
- Fig. 6 Plots of log (intensity) versus 1/T for a) PO  $\beta$ -system (0,0) emission; b) PO  $\gamma$ -system and c) HPO(DPO)  $^{1}\tilde{A}'' \rightarrow ^{1}\tilde{A}'$  system. Intensity values were derived from temperature dependent chemiluminescence spectra for the reaction on contact with air of  $P_4$  vapor and  $H_2O$

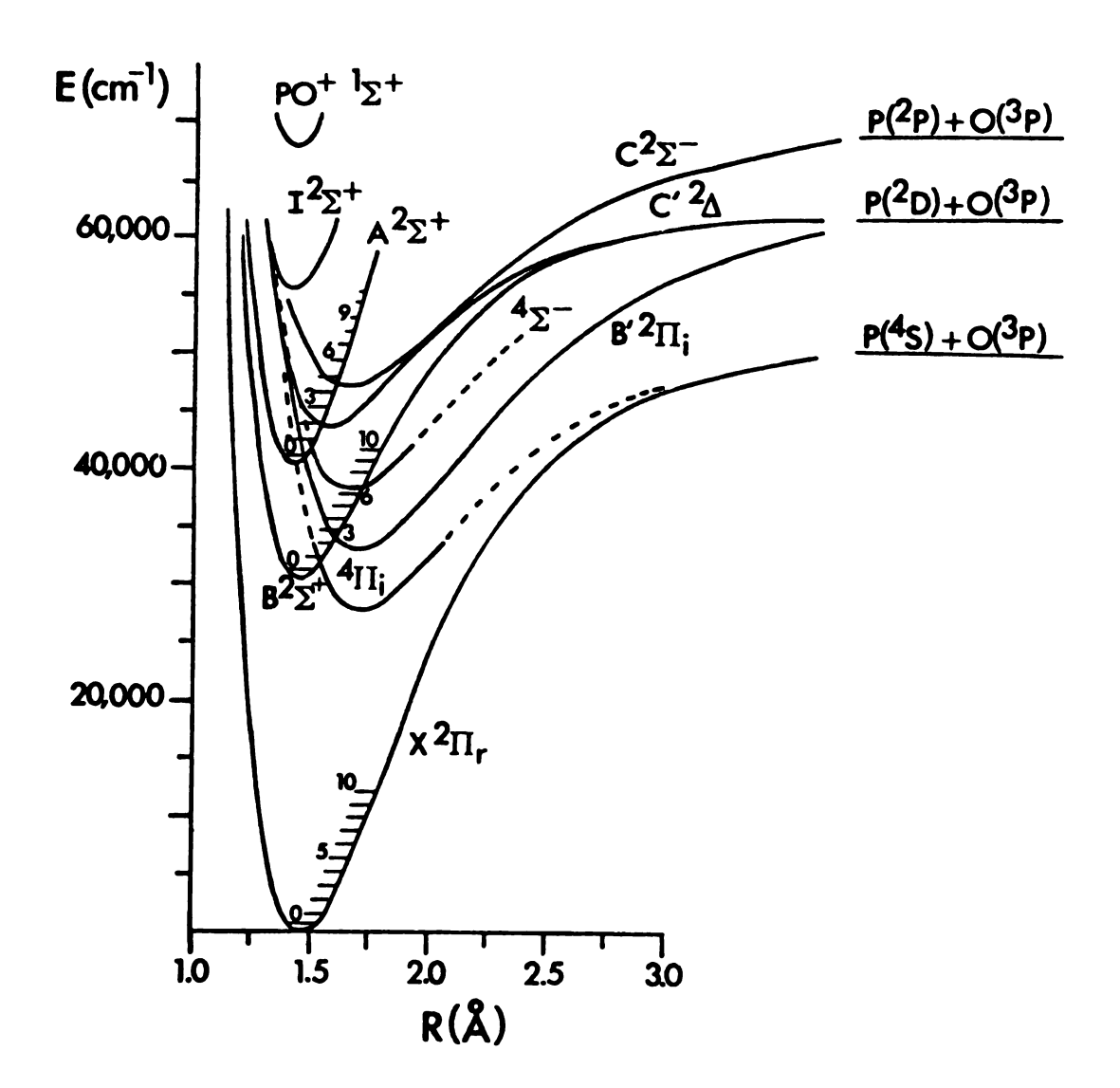
vapor (triangular points) or D<sub>2</sub>O vapor (circled points) carried in a heated nitrogen stream (method (a) in the text). Taken with a Heath monochromator and RCA 1P28 photomultiplier. Data were normalized with respect to total luminosity.

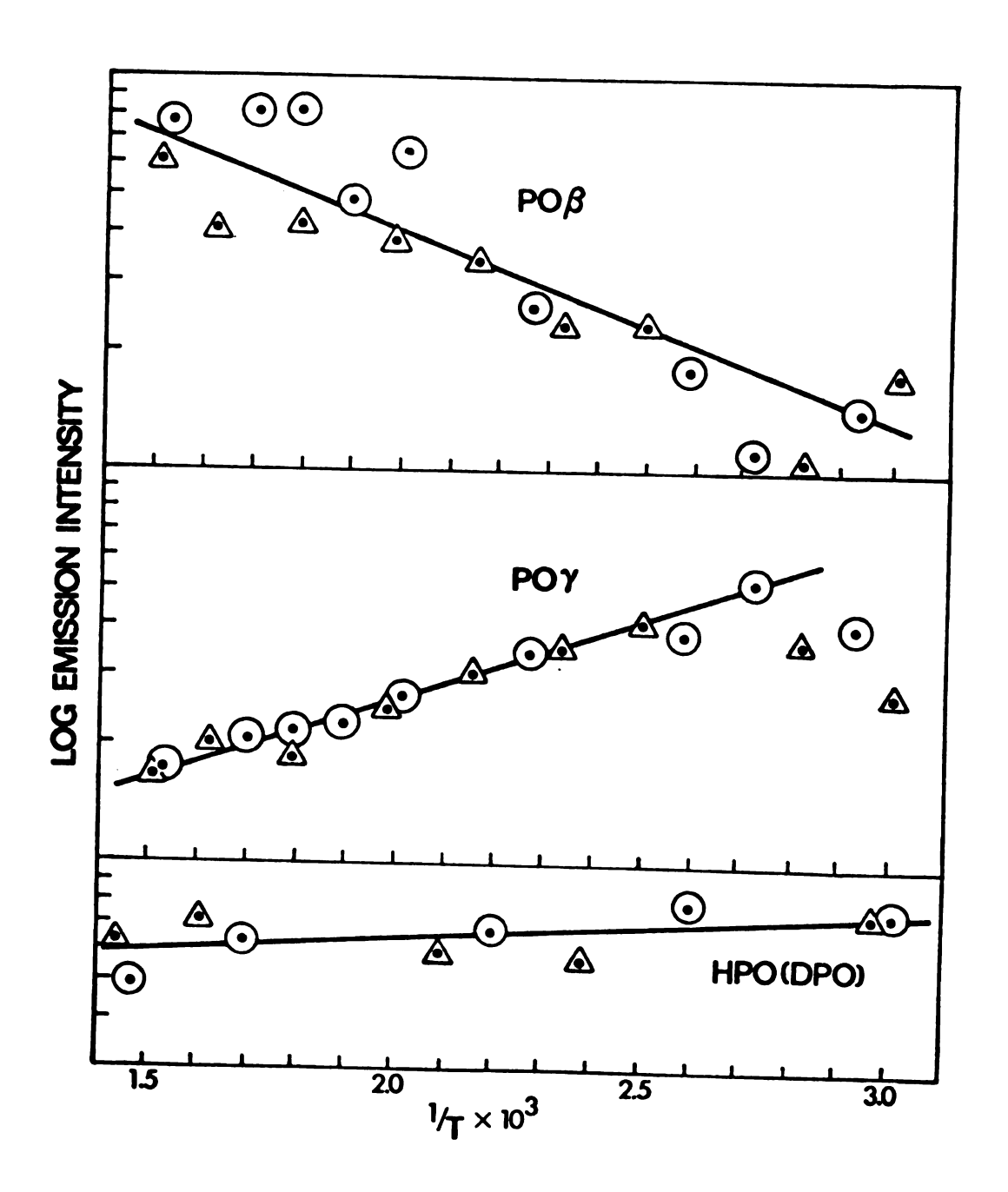
- Fig. 7 Potential energy diagram for the (PO)\* excimer showing the dissociative ground state and the stabilized excited state of the excimer. The relative energies of the PO monomer states are shown on the right hand side.
- Fig. 8 Chemiluminescence spectra of the reaction, on contact with air, of P<sub>4</sub> vapor and H<sub>2</sub>O vapor carried by a heated ( 300°C by method (a)) nitrogen stream. Spectrum (a) is the diluted stream, (b) is without dilution. Both spectra were taken with a Heath monochromator and RCA 1P28 photomultiplier.
- Fig. 9 Dry chemiluminescence spectrum of the room temperature reaction, on contact with oxygen, of P<sub>4</sub> vapor carried by a nitrogen stream.

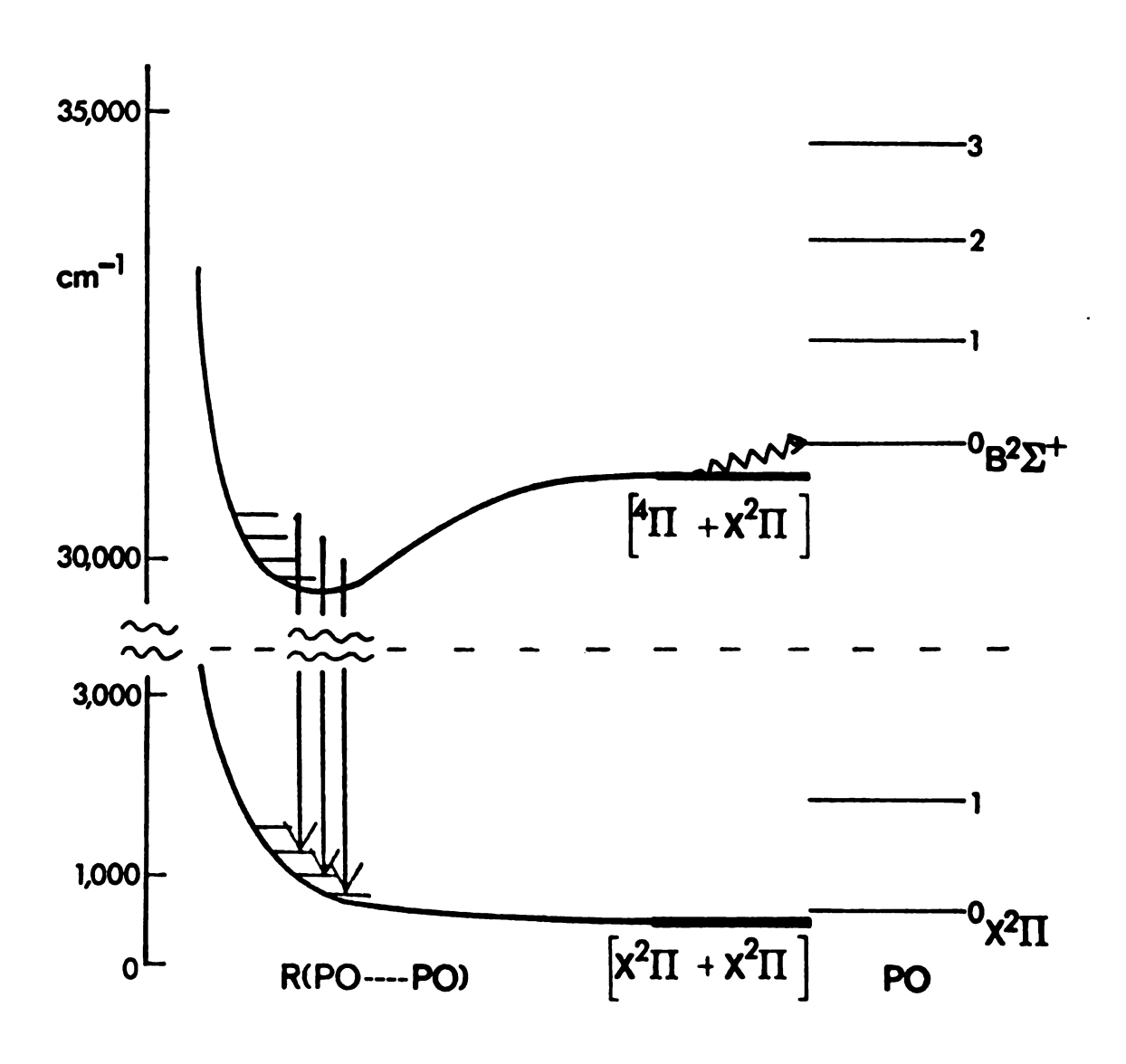
  All reactants and the carrier gas were previously dried. Taken with a McPherson monochromator and EMI 9558QB photomultiplier.
- Fig. 10 Gas phase room temperature phosphorus chemiluminescence showing weak high energy emission from the  $C(^2\Sigma^-)$  and  $C'(^2\Delta)$  electronic states of PO. See Table II for a comparison with known transitions. Other lines have not yet been identified. Taken with a McPherson monochromator and RCA 1P28 photomultiplier.

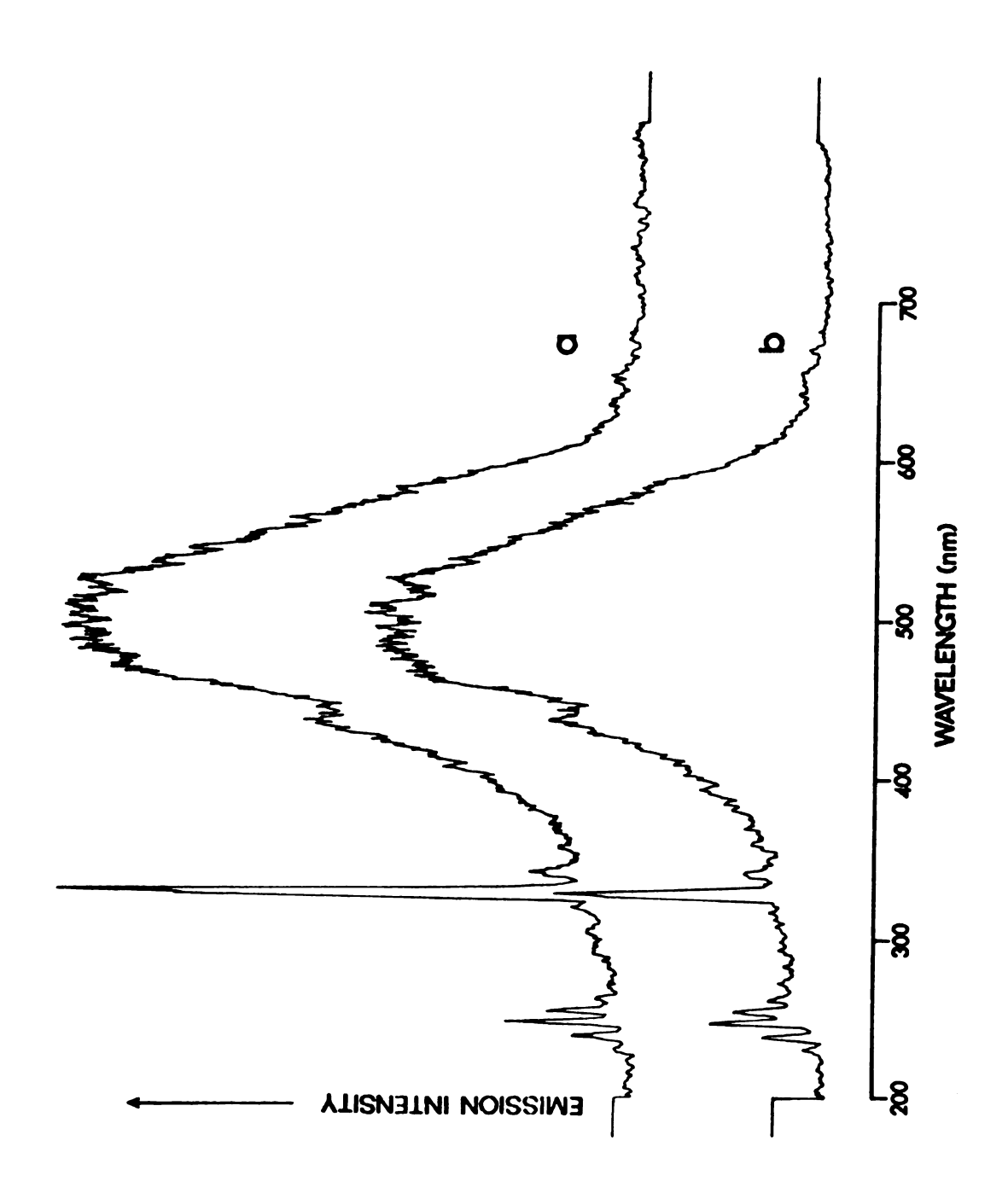


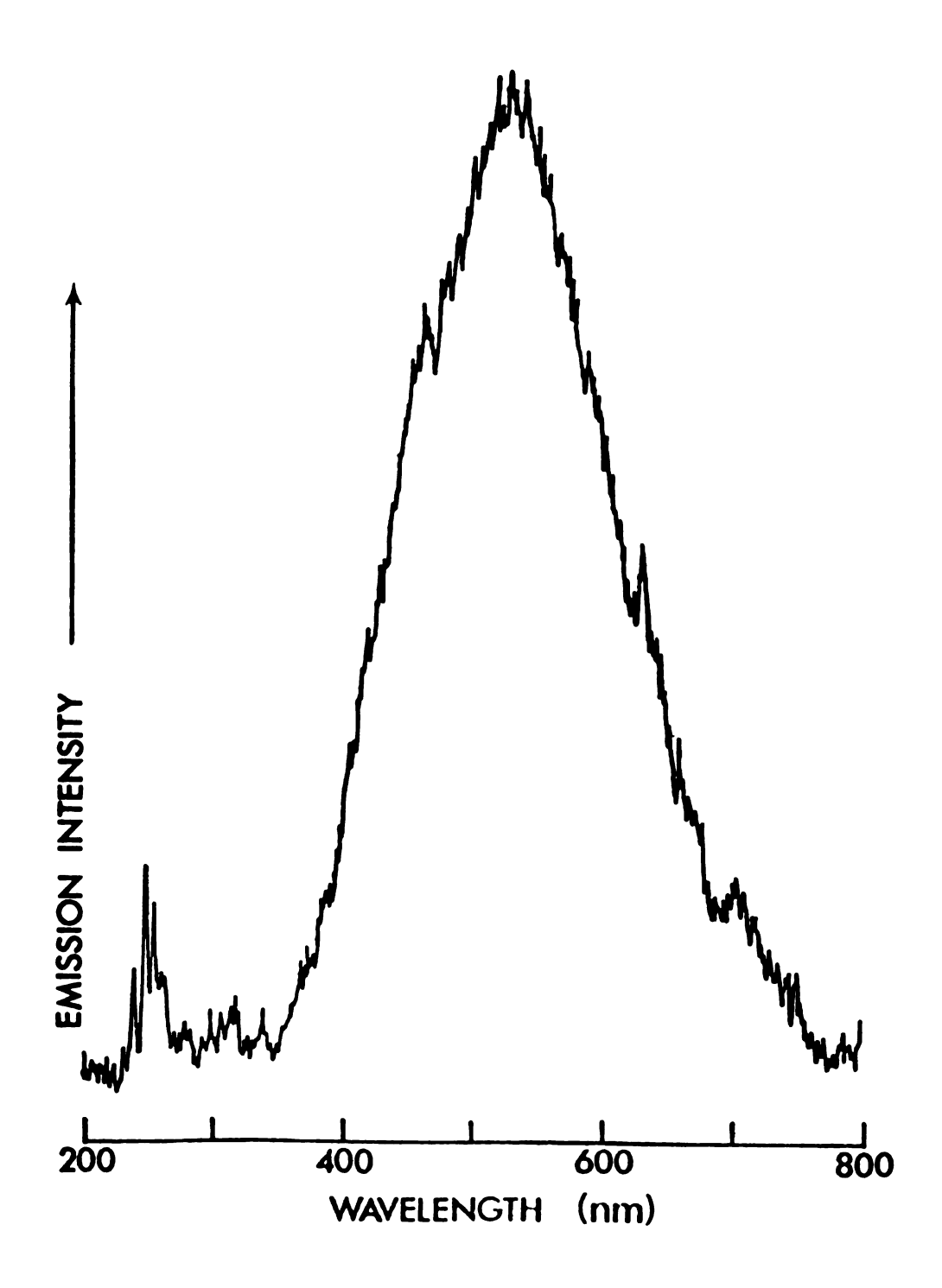


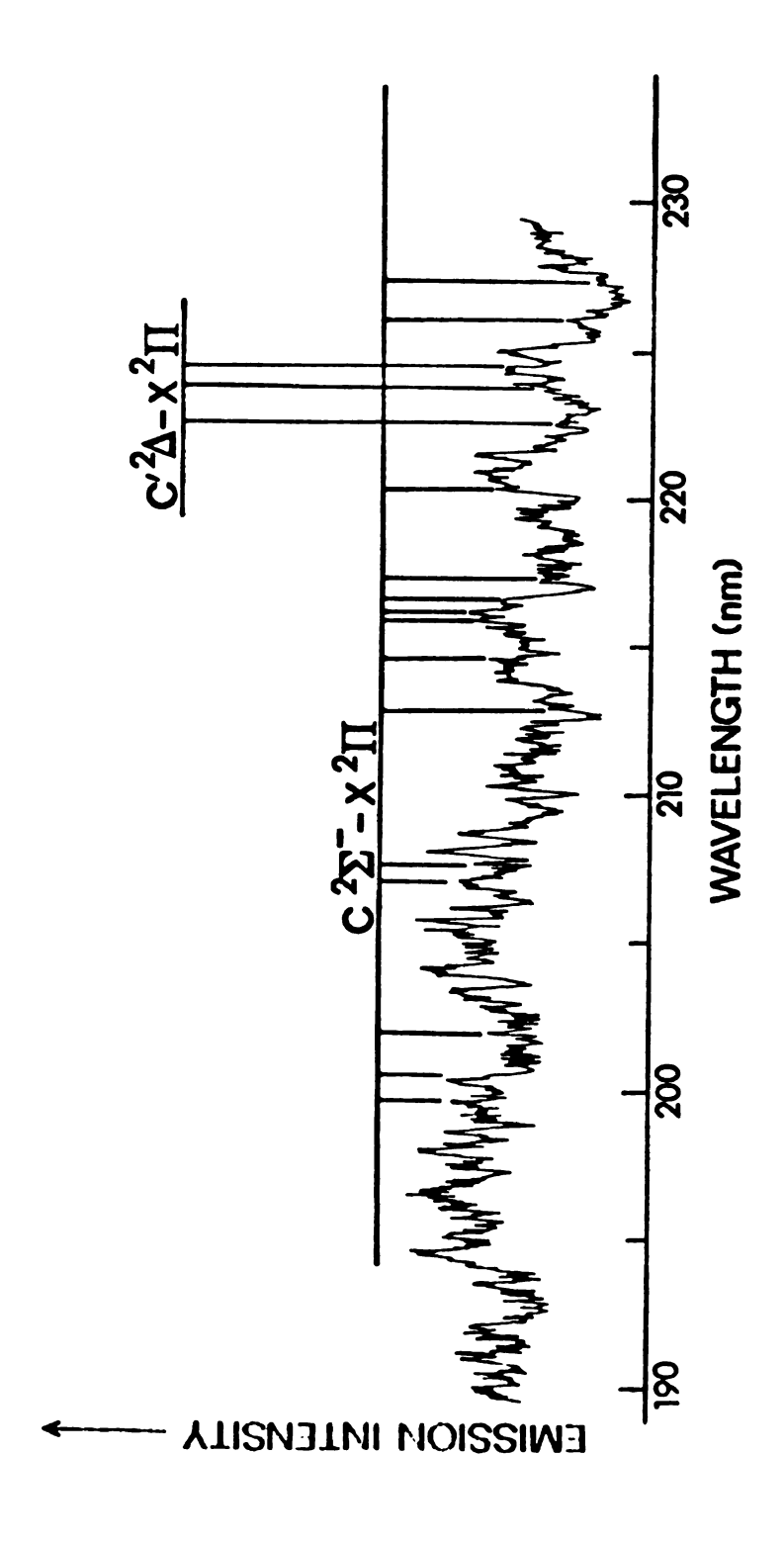












# APPENDIX B

THE ELECTRONIC ORIGIN OF THE COOL GREEN PHOSPHORUS FLAME

R. J. Van Zee and A. U. Khan, Chem. Phys. Lett.,  $\underline{36}$ , 123 (1975)

# Reprinted from:

# CHEMICAL PHYSICS LETTERS

Volume 36, No. 1, 15 October 1975

# THE ELECTRONIC ORIGIN OF THE COOL GREEN PHOSPHORUS FLAME

Richard J. VANZEE and Ahsan U. KHAN

Departments of Chemistry and Biophysics, Michigan State University, East Lansing, Michigan 48824, USA

pp. 123 - 125



#### THE ELECTRONIC ORIGIN OF THE COOL GREEN PHOSPHORUS FLAME

Richard J. VANZEE and Ahsan U. KHAN

Departments of Chemistry and Biophysics, Michigan State University, East Lansing, Michigan 48824, USA

Received 26 June 1975

The major electronic origin of the cool green phosphorus flame is an excited state dimer (PO) $\frac{1}{2}$  of phosphorus monoxide. A spectroscopic investigation of the gas phase oxidation of P<sub>4</sub> vapor in moist air has established that the visible continuum which is the main spectral feature of phosphorus chemiluminescence originates from a (PO) $\frac{1}{2}$  excimer complex. When complex formation is inhibited by increasing the reaction temperature and by diluting the reactants with buffer gas, a new emission from the electronically excited monomer appears. This emission can be assigned to the PO  $\beta$ -system and its appearance is kinetically and spectrally consistent with the following equilibria for the excimer: (PO) $\frac{1}{2} \stackrel{?}{\rightleftharpoons} PO(X^2\Pi) + PO(^4\Pi)$   $\stackrel{?}{\rightleftharpoons} PO(B^2\Sigma^+) + PO(X^2\Pi)$ .

The beginning of the modern chemistry of chemiluminescence can be traced to Henning Brand, who in 1669 subjected urine to a series of chemical treatments and isolated a mysterious compound that glowed on exposure to air [1]\*. This mysterious glow, which is greenish in color and cool to the touch, has resisted all attempts at identification over the last three hundred years. In this communication we report a spectroscopic investigation that strongly suggests that the green glow originating from the gas phase oxidation of P<sub>4</sub> vapor in moist air is due to a  $(PO)_2^*$  excimer complex. In this complex one of the PO molecules is electronically excited, most probably to the lowest metastable electronic <sup>4</sup> II state, and the other is in the ground <sup>2</sup> II state. The excimer complex is responsible for the main spectral feature of the chemiluminescence, a broad band emission beginning at 335 nm and extending into the infrared. With either thermal dissociation of the complex or dilution of the P<sub>4</sub> vapor stream at higher temperatures with inert gas, a new spectral feature appears, emission from the PO  $\beta$ -system [2]. Radiative transition from the  ${}^4\Pi$  state to the ground  ${}^2\Pi$  state of PO is spin forbidden and the <sup>4</sup> II state is close enough energetically for thermal population of the  $B^2\Sigma^+$  states

of the PO  $\beta$ -system to occur; so that the appearance of PO  $\beta$ -system emission under these conditions is spectrally and kinetically consistent with the following equilibria for the excimer:

$$(PO)_{2}^{*} \neq PO(^{4}\Pi) + PO(X^{2}\Pi) \neq PO(B^{2}\Sigma^{+}) + PO(X^{2}\Pi).$$

The white phosphorus used was obtained from Baker and the nitrogen from Airco. Spectra were recorded with a Heath EU-7000 0.5 m monochromator with an RCA 1P28 photomultiplier and Sargent Model SR recorder. For the temperature dependent studies, a nitrogen stream saturated with water vapor at room temperature and with P4 vapor at 60°C passed through a 3 mm quartz tube heated electrically by nichrom wire sandwiched between layers of asbestos tape. The composite system was inserted into a wider quartz tube also heated electrically by nichrom wire sandwiched between layers of asbestos tape. Spectra were recorded through a window in the asbestos cover, and the temperature was monitored by a thermocouple seated near the base of the flame at the end of the internal quartz tube. For the concentration dependent spectra, a nitrogen stream saturated with water vapor at room temperature and with P<sub>4</sub> vapor at 60°C passed into a 50 ml glass flask. A second source of nitrogen at the same pressure was connected to the flask, and the diluted stream passed into a 3 mm quartz tube

<sup>\*</sup> For a discussion of the early history, this is a comprehensive and excellent review.

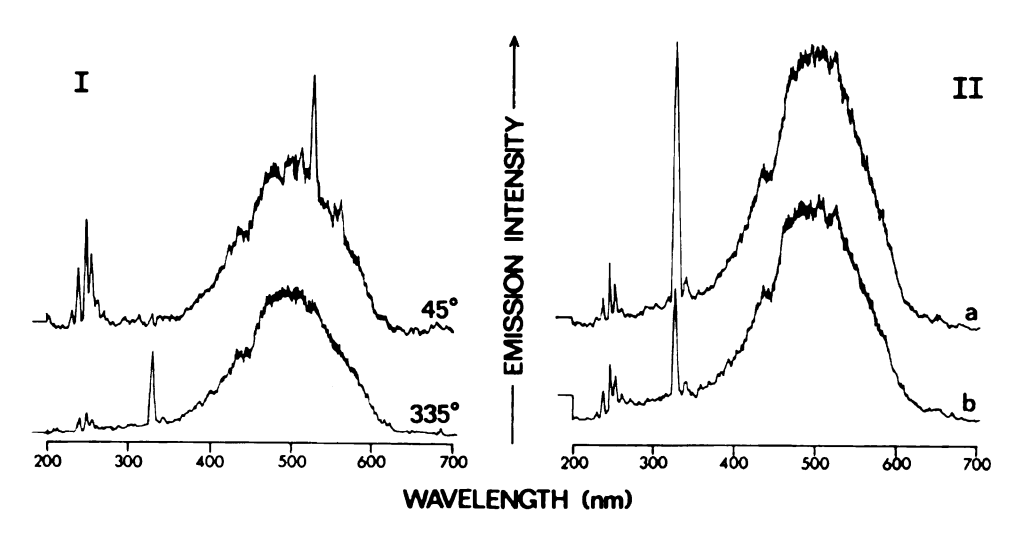


Fig. 1. Phosphorus chemiluminescence emission. Section I is a temperature variation study at 35°C and at 325°C. The visible continuum beginning at 335 nm originates from the  $(PO)_2^*$  excimer. The fine band emission from 228.8–272.1 nm is the PO  $\gamma$ -system, PO(A  $^2\Sigma^+$ )  $\rightarrow$  PO(X  $^2\Pi$ ); and the discrete emission at 320 nm is the (0,0) transition of the PO  $\beta$ -system, PO(B  $^2\Sigma^+$ )  $\rightarrow$  PO(X  $^2\Pi$ ). Superimposed on the continuum at 450–650 nm are fine band emissions of HPO,  $\widetilde{A}(^1A'')$   $\rightarrow \widetilde{X}(^1A')$ , previously identified from deuterium incorporation studies [6]. Section II is a comparison of spectra from the diluted (a) and non-diluted (b) phosphorus flame at 300°C. Nitrogen was the dilutant gas. It should be noted that a direct quantitative comparison of the emission intensity from one spectrum to another is not strictly valid because of the variable nature of the flame; rather the relative emission intensities of the various components within a single spectrum should be considered. For thermal activation studies, the spectra were normalized with respect to total luminosity.

heated electrically by nichrom wire sandwiched between layers of asbestos tape. Spectra were taken of the flame at the end of the tube, and the temperature was monitored by a thermocouple seated nearby.

Section I of fig. 1 shows the appearance of the (0,0) transition of the PO  $\beta$ -system at 335°C and at 320 nm on thermal dissociation of the excimer. Actual spectral assignments were made from medium resolution spectra scanning at slower speeds and narrower slit widths. Activation studies, based on the temperature dependent intensity of the (0,0) PO  $\beta$ -system transition using additional temperature settings, give a  $\Delta E = 846 \pm 200$  cm<sup>-1</sup> activation energy for the dissociation of the  $(PO)_2^*$  excimer. The data was normalized with respect to total luminosity at each temperature. A more detailed analysis will be published elsewhere.

In section II of fig. 1, the diluted spectrum shows a marked relative enhancement of emission from the (0,0) transition of the PO  $\beta$ -system, consistent with an equilibrium shift toward the monomer. It has been suggested that the phosphorus chemiluminescence continuum originates from PO<sub>2</sub> by analogy to

NO<sub>2</sub> where a diffuse emission results from the recombination NO + O  $\rightarrow$  NO<sub>2</sub> +  $h\nu$  [3]. However, this is unlikely since the thermal and dilution effects observed in phosphorus chemiluminescence are not analogous to the observed behavior of NO2; i.e., similar conditions do not produce emission from the NO  $\beta$ -system, the lowest NO emission system. The continuum emission in the phosphorus flame has also been attributed to HOPO by analogy with HONO, which exhibits predissociative behavior in the near UV region [4]. In a separate experiment using reactants and carrier gas rigorously dried with phosphorus pentoxide, the intensity of the continuum emission shows a pronounced increase relative to the decreased HPO emission. Hence, it is unlikely that the continuum emission involves HOPO or any other protonated species.

In gas discharge studies Verma et al. [5] have identified a  $^4\Sigma^-$  state of PO from indirect evidence in an analysis of perturbations which produce an anomalously strong (6,6) emission in the PO  $\beta$ -system. Under certain conditions we have also observed a similar anomalously strong (6,6) PO  $\beta$ -system transition in the phosphorus flame. Since the inten-

sity of PO  $\beta$ -system bands in the flame depends on the dissociation of the (PO) $_2^*$  excimer, this suggest that the  $^4\Sigma^-$  state of PO may also be involved in excimer formation, in addition to the lowest electronically excited  $^4\Pi$  state. The conditions favoring the anomalous (6,6) emission need to be more carefully defined. Further investigation into the energetics and electronic structure of the metastable phosphorus—oxygen excimer complex is in progress. Hopefully a clearer delineation of the oldest known chemiluminescence system will provide a new approach to the question of metastable phosphorus—oxygen bonding central to an understanding of many bioenergetic reactions.

#### References

- [1] E.N. Harvey, A history of luminescence (The American Philosophical Society, Philadelphia, 1957).
- [2] R.D. Verma and H.P. Broida, Can. J. Phys. 48 (1970) 2991.
- [3] H. Cordes and W. Witschel, Z. Physik. Chem. 46 (1965) 35.
- [4] P.B. Davies and B.A. Thrush, Proc. Roy. Soc. A302 (1968) 243.
- [5] R.D. Verma and S.S. Jois, Can. J. Phys. 51 (1973) 322.
- [6] R.J. VanZee and A.U. Khan, J. Am. Chem. Soc. 96 (1974) 6805.

# APPENDIX C

A STRIKING DEUTERIUM EFFECT IN PHOSPHORUS CHEMILUMINESCENCE.

IDENTIFICATION OF THE EMITTING SPECIES

R. J. Van Zee and A. U. Khan, J. Amer. Chem. Soc.,  $\underline{96}$ , 6805 (1974)

# A Striking Deuterium Effect in Phosphorus Chemiluminescence. Identification of the Emitting Species

### A Striking Deuterium Effect in Phosphorus Chemiluminescence. Identification of the Emitting Species

Sir:

Under conditions similar to naturally occurring phosphorus chemiluminescence, <sup>1</sup> a substitution of deuterium oxide for water in the reaction of phosphorus, molecular oxygen, and water was undertaken in our laboratory, and a marked frequency shift and changes in the intensity distribution were observed in the chemiluminescence spectrum. Comparative analysis of the spectra identifies the major emitters in the visible region as  $(PO)_2^*$  excimer and HPO. In the ultraviolet we confirm the finding of Rumpf<sup>2</sup> that the major emitting species is PO, and, in the assignment of PO  $\gamma$  (a) and weak PO  $\beta$  bands (b), we also concur with Walsh. <sup>3</sup>

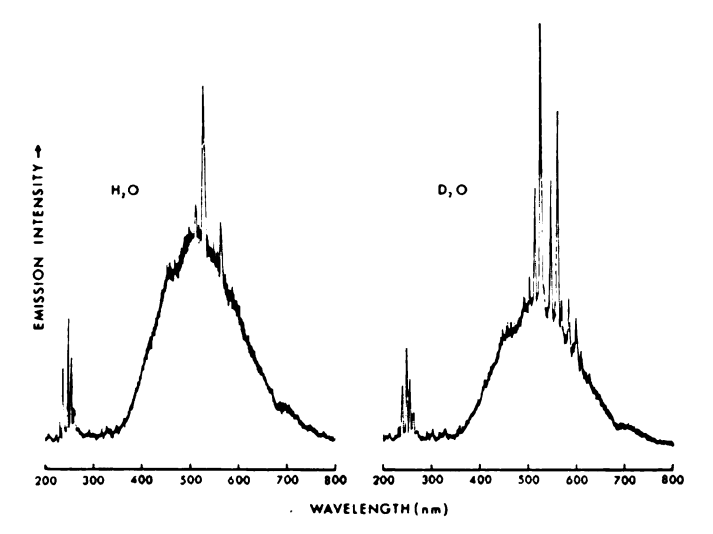


Figure 1. Chemiluminescence spectra of phosphorus. Left-hand side chemiluminescence due to the reaction of phosphorus, H<sub>2</sub>O, and O<sub>2</sub>. Right-hand side chemiluminescence due to the reaction of phosphorus, D<sub>2</sub>O, and O<sub>2</sub>.

Based on our experiments, our tentative assignments are: (a) 228.8-272.1 nm PO  $\gamma$  system (A  $^2\Sigma \rightarrow X^2\Pi$ ), (b) 325.0-337.0 nm PO  $\beta$  system (B  $^2\Sigma \rightarrow X$   $^2\Pi$ ), (c) 335.0-800 (possibly to 1250) nm; diffuse band system, excimer emission

$$PO^* + PO \longrightarrow (PO)_2^* \longrightarrow 2PO + h\nu$$

(d) 450.0-650.0 nm; discrete band system<sup>4-6</sup>

$$\tilde{A} (^{1}A'') \longrightarrow \tilde{X} (^{1}A') \longrightarrow \begin{cases} HPO \\ DPO \end{cases}$$

The phosphorus (Baker) source was a 50-ml glass flask immersed in a water bath (57°). Nitrogen (Airco) saturated with H<sub>2</sub>O or D<sub>2</sub>O (Columbia, 99.5%) at room temperature was passed through a flask into a 3-mm glass tube. Chemiluminescence occurred at the end of the tube, with air being used as the source of molecular oxygen. A 0.3-m McPherson Model 218 monochromator with an EMI 9558 QB photomultiplier, an Eldorado Model 201 universal photometer, and a Sargent Model TR recorder were used to obtain the spectra.

In Figure 1 the continuum which produces most of the visible green color starts at around 335.0 nm and extends to 800 nm. (In a different experiment performed only with  $H_2O$  and using a RCA 7102 photomultiplier and a Warner Swasey scanning monochromator coupled to a Nicolet 1074 signal averager, the continuum extends to 1250.0 nm). We are tentatively suggesting that this emission originates from  $(PO)_2^*$  excimer, based on the following considerations. (1) The Walsh excitation mechanism proposed to explain the PO  $\beta$  and  $\gamma$  band emission is

$$P(^{4}S) + O(^{3}P) + PO(X^{3}\Pi) = PO(X^{3}\Pi) + PO(A^{3}\Sigma^{+} \text{ or } B^{3}\Pi)$$

<sup>(1)</sup> See E. N. Harvey, "A History of Luminescence," The American Philosophical Society, Philadelphia, Pa., 1957.

<sup>(2)</sup> K. Rumpf, Z. Phys. Chem., Abt. B, 38, 469 (1938).

<sup>(3)</sup> A. D. Walsh in "The Threshold of Space," M. Zelikoff, Ed., Pergamon Press, London, 1957, p 165.

<sup>(4)</sup> M. Lam Thanh and M. Peyron, J. Chim. Phys. Physicochim. Biol., **60**, 1289 (1963).

<sup>(5)</sup> M. Lam Thanh and M. Peyron, J. Chim. Phys. Physicochim. Biol., 63, 266 (1966).

<sup>(6)</sup> See G. Herzberg, "Molecular Spectra and Molecular Structure, III. Electronic Spectra and Electronic Structure of Polyatomic Molecules," D. Van Nostrand, New York, N. Y., 1966.

<sup>(7)</sup> For a general discussion on excimer see J. B. Birks, "Photophysics," Wiley-Interscience, New York, N. Y., 1970.

This mechanism would perforce generate an electronically excited PO\* in the close proximity of a ground state PO, an ideal situation for excimer formation. (2) The overall spectral characteristics—a discreet band juxtaposed to a broad diffuse band on the longer wavelength side—are strongly indicative of excimer formation. Since an excimer has a bound excited electronic state and a dissociative ground state, the excimer emission is diffuse and red shifted from the monomer emission. (3) In the chemiluminescent reaction we observe an isotope effect on the kinetics of the luminescence reactions, in which emission from PO  $\gamma$  falls to 84% of its original value, and the intensity of the continuum decreases to 70%. The kinetic dependence is currently under investigation.

The discrete visible bands show the most marked deuterium effect. The few weak bands seen with H<sub>2</sub>O are increased in intensity by a factor of 5 in D<sub>2</sub>O and a number of new bands are seen. Unlike the PO bands which do not exhibit frequency shift, the most intense band at 525.5 nm (19,030 cm<sup>-1</sup>) is shifted to 523.5 nm (19,100 cm<sup>-1</sup>) and other bands are similarly shifted to the blue (see Table I). The characteristic frequency shift due to isotopic substitution indicates the species has H covalently bound (d). In an electric discharge investigation of the Ludlam<sup>8</sup> bands associated with the burning of phosphorus in hydrogen, Lam Thanh and Peyron<sup>4</sup> attributed similar bands to HPO and DPO (d). The increase in the emission intensity of DPO compared to HPO can be understood in terms of decrease in the Franck-Condon factors in substituting D<sub>2</sub>O for H<sub>2</sub>O and the consequent decrease in the radiationless transitions.9 An interpretation of this phenom-

Table I

	$\begin{array}{c} \text{HPO} \\ (\nu_1'\nu_2'\nu_3') \rightarrow \\ (\nu_1''\nu_2''\nu_2'') \end{array}$	DPO $(\nu_1'\nu_2'\nu_3') \rightarrow (\nu_1''\nu_2''\nu_3'')$
	$(000) \to (010)$	<b>(000)</b> → <b>(</b> 010)
Lam Thanh and Peyron <sup>4,5</sup>	17,860 cm <sup>-1</sup>	17,931 cm <sup>-1</sup>
	(559.91 nm)	(557.69 nm)
This work	17,850 cm <sup>-1</sup>	17,930 cm <sup>-1</sup>
	(560.2 nm)	(557.8 nm)
Most intense transition	$(000) \rightarrow (000)$	$(000) \rightarrow (000)$
Lam Thanh and Peyron <sup>4,5</sup>	19,047 cm <sup>-1</sup>	19,116 cm <sup>-1</sup>
	(525.01 nm)	(523.12 nm)
This work	$19,030 \text{ cm}^{-1}$	19,100 cm <sup>-1</sup>
	(525.5 nm)	(523.5 nm)

enon would possibly be similar to the case of predissociative HNO. 10

Currently we are investigating kinetic aspects of the excimer emission and are attempting to clarify the assignments associated with some weak lines in the ultraviolet. Since the essential features of the emitting species have now been established, it should be possible to understand the detailed nature of the oldest known chemiluminescence system.

- (8) E. B. Ludlam, J. Chem. Phys., 3, 617 (1935).
- (9) G. W. Robinson and R. P. Frosch, J. Chem. Phys., 37, 1962 (1962); 38, 1187 (1963).
- (10) M. J. Y. Clement and D. A. Ramsay, Can. J. Phys., 39, 205 (1961).

#### Richard J. Van Zee, Ahsan U. Khan\*

Departments of Chemistry and Biophysics Michigan State University East Lansing, Michigan 48824 Received June 18, 1974

to the

pling to be well to be the state of the stat

85. (. 08\* ) <sub>(.</sub> 0r. . )

e Zee Ass

MICHIGAN STATE UNIV. LIBRARIES
31293017299359